Palaeobiodiversity and Palaeoenvironments (2022) 102:629–696
https://doi.org/10.1007/s12549-022-00539-x

SENCKENBERG

ORIGINAL PAPER

Drowning, extinction, and subsequent facies development of the Devonian Hönne Valley Reef (northern Rhenish Massif, Germany)

Sören Stichling[1] · Ralph Thomas Becker[2] · Sven Hartenfels[1,4] · Zhor Sarah Aboussalam[2] · Andreas May[3]

Received: 25 November 2021 / Revised: 24 May 2022 / Accepted: 3 June 2022 / Published online: 17 September 2022

Abstract

The Hagen-Balve Reef is one of the largest Devonian carbonate complexes in the Rhenish Massif exposed in many former or active, economically significant quarries, especially in the Hönne Valley region at its eastern end. The timing and patterns of reef drowning, final extinction, and the middle Frasnian to middle Famennian post-reefal facies history, including details of the global Kellwasser Crisis, were studied based on two boreholes (HON_1101 and B102) and one outcrop at the Beul near Eisborn. More than 100 conodont samples provided a fine biostratigraphic framework and included new forms left in open nomenclature. The ca. upper 80 m of the new Asbeck Member of the Hagen-Balve Formation consists of relatively monotonous lagoonal successions assigned to four microfacies types. The local diversity of reef builders, mostly stromatoporoids, is low. Fenestral microbialites indicate very shallow and rather hostile back-reef settings. Near the Middle/Upper Devonian boundary, the eustatic pulses of the global Frasnes Events led to a significant backstepping of the reef margin, with reef core/outer slope facies overlying lagoonal facies. This flooding drastically reduced the carbonate accumulation rate and enabled the invasion of drowned back-reef areas by open-water organisms, such as polygnathid conodonts. Within this Eisborn Member, five microfacies types and numerous subtypes are distinguished including low-diversity "coral gardens" and a final, top lower Frasnian parabiostrome dominated by tabulate and colonial rugose corals. There was no cap stage ("Iberg Facies"). Two phases of the Basal Frasnes Event are marked by dark, organic rich limestones with subordinate reef builders. Based on conodont fauna from overlying nodular limestones of the new, (hemi-)pelagic Beul Formation, the final Hönne Valley reef extinction was caused by the eustatic Middlesex Event at the lower/middle Frasnian boundary. Within the Beul Formation, eight subphotic submarine rise microfacies types are distinguished. After a lower middle Frasnian phase of extreme condensation, rich conodont faunas enable the recognition of most upper Frasnian to middle Famennian zones. The global *semichatovae* Event led to a regionally unique intercalation by four phases of organic-rich, laminated black shales and intervening thin limestones in core HON_1101. The Lower Kellwasser Event is represented in HON_1101 by atypical, moderately C_{org}-rich, recrystallized, peloidal ostracod-mollusk pack-grainstones. The Upper Kellwasser level begins with an ostracod bloom, followed either by recrystallized mollusk wacke-packstones (HON_1101) or laminated, argillaceous mudstones (B102). The first indicates a rarely documented shallow subphotic, better oxygenated setting than typical Upper Kellwasser facies. As elsewhere, the top-Frasnian conodont extinction was severe. The lower/middle Famennian carbonate microfacies of the Beul Formation is relatively monotonous and typical for an oxic, pelagic submarine rise. The youngest recorded nodular limestones fall in the *Palmatolepis marginifera utahensis* Zone. Regionally uniform lydites of the Hardt Formation show that the local palaeotopography was levelled before the base of the

This article is a contribution to the special issue "The Rhenish Massif: More than 150 years of research in a Variscan mountain chain"

✉ Ralph Thomas Becker
rbecker@uni-muenster.de

Sören Stichling
soeren.stichling@gd.nrw.de

Sven Hartenfels
sven.hartenfels@gd.nrw.de

Zhor Sarah Aboussalam
taghanic@uni-muenster.de

[1] Geologischer Dienst Nordrhein-Westfalen – Landesbetrieb – De-Greiff-Str. 195, 47803 Krefeld, Germany

[2] Institut für Geologie und Paläontologie, Westfälische Wilhelms-Universität Münster, Corrensstr. 24, 48149 Münster, Germany

[3] Friedrich-List-Straße 66, 59425 Unna, Germany

[4] Institut für Geologie und Mineralogie, Universität zu Köln, Zülpicher Str. 49a, 50674 Köln, Germany

Viséan. The Hönne Valley case study and comparisons with western parts of the Hagen-Balve Reef and other Rhenish reefs underline the significance of Givetian to middle Frasnian eustatic and anoxic events as causes for reef extinctions.

Keywords Rhenish Massif · Devonian · Reefs · Conodonts · Microfacies · Global events

Introduction

On a global scale, the Givetian and Frasnian were the time of maximum Phanerozoic reef growth (e.g. Kiessling et al. 1999; Flügel and Kiessling 2002; Copper 2002a; Copper and Scotese 2003). In this context, the Givetian–Frasnian Hönne Valley Reef, as the northeastern part of the elongated Hagen-Balve Reef Complex, is one of the best-known examples in the northern Rhenish Massif. The Hagen-Balve Reef Belt is exposed in many outcrops along the northern, eastern, and southeastern margin of the 1st order Remscheid-Altena Anticline between Hagen in the West and Balve in the East (compare Becker et al. 2016c; Fig. 1).

The complete disappearance of metazoan reefs at the end of the Frasnian, during the global Kellwasser Crisis, was dramatic (e.g. Copper 2002b) but is not well understood (Racki 2005). It is intriguing that the reef majority did not reach the end-Frasnian with its anoxic to hypoxic Upper Kellwasser level. This is especially true for the Rhenish Massif (e.g. Eder and Franke 1982; Stritzke 1989; Aboussalam and Becker 2016; Brinkmann and Stoppel, in press) or westwards, for the Ardennes Shelf (e.g. Denayer and Poty 2010; Mottequin et al. 2015; Mottequin and Poty 2016). The terminal Frasnian transgression and spread of hypoxia killed in Central Europe obviously only small biostromes and the last remaining carbonate platforms. The latter differed from the main Givetian/Frasnian reefs since they were predominantly formed by calcimicrobes and harbored only subordinate last stromatoporoids, rugose and tabulate corals (e.g. Elbingerode Reef, Fuchs 1990; Wülfrath Reef, Becker et al. 2016b; Hartenfels et al. 2017; upper Frasnian biostrome south of Heiligenhaus, Becker et al. 2016b; Hartenfels et al. 2018). In this context, there is a surprising lack of modern research on Rhenish Devonian reef extinctions, with very few high-resolution data concerning the precise timing of extinctions and of possible stepwise drowning episodes, the palaeoecology of terminal reef stages, and facies-based reconstructions of triggering factors. An exception is the rarely quoted Ph.D. study for reefal limestones of the Lahn Syncline by Oetken (1997). Eder and Franke (1982) claimed that local factors caused variable pre-Kellwasser extinctions. Is this generally true or did the now well-established sequence of 2nd to 4th order global events (summarised by Becker et al. 2016a, 2020) play a major role? The latter interpretation has been preferred for reefal episodes of the Aachen region (Aboussalam and Becker 2016) and of the Velbert Anticline (Wülfrath, e.g. Becker et al. 2016b; Hofermühle; Becker et al. 2016b). These questions are significant for a deeper understanding of global reef megacycles (Hladil 1986) and a refined view on global fluctuations of reef abundance in time and space (e.g. Kiessling 2008).

In the frame of a cooperation project, the Lhoist Germany Rheinkalk GmbH provided drill cores and access to their quarries in the Hönne Valley region. This enabled us to analyse the regional microfacies developments and biostratigraphy of the upper parts of the Devonian carbonate succession, from the final reef stage (the up to 200 m thick "Upper Micrite Formation", compare Eiserlo 1987) through the open platform Eisborn Member of Becker et al. (2016b) to post-reefal nodular limestones. Applying the wide definition of the term reef by Flügel and Kiessling (2002), we focused on the following approaches:

1. Detailed, bed-by-bed logging of macroscopic lithology and macrofauna in drill cores HON_1101 and B102, with a focus on the reef builders of the last reef stage.
2. Microfacies documentation and analysis of all carbonate types, with emphasis on the, so far, poorly known final reef drowning stages.
3. Continuous conodont sampling and biostratigraphic dating, applying the most recent conodont scales, recognising new and rare forms, and with a focus on the hardly known faunas from final reef stages.
4. Lithological and biostratigraphical correlation between the two cores and the re-sampled Beul outcrop of Nowak (2010) and Becker et al. (2016c).
5. Reconstruction of palaeoecological trends and the precise timing of the stepwise regional reef extinction and post-reefal history in the context of known global events.

Our study yielded the most detailed data set for the extinction of any German Devonian reef. On a global scale, there are few other examples, where microfacies successions of a drowning Givetian carbonate platform have been documented with a similarly precise biostratigraphic scale. This will enable future comparisons and provide a base for the recognition of potential patterns that cannot be concluded from the study of a single reef. A refined knowledge of Middle Palaeozoic reef extinctions holds clues for a better general understanding how reefs reacted and developed in times of biotic crises.

Abbreviations

Conodont genera: *Ad.* = *Ancyrodella*, *Ag.* = *Ancyrognathus*, *Bel.* = *Belodella*, *Br.* = *Branmehla*, *Ct.* = *Ctenopolygnathus*, *I.* = *Icriodus*, *L.* = *Linguipolygnathus*, *Mes.* = *Mesotaxis*, *"Oz."*

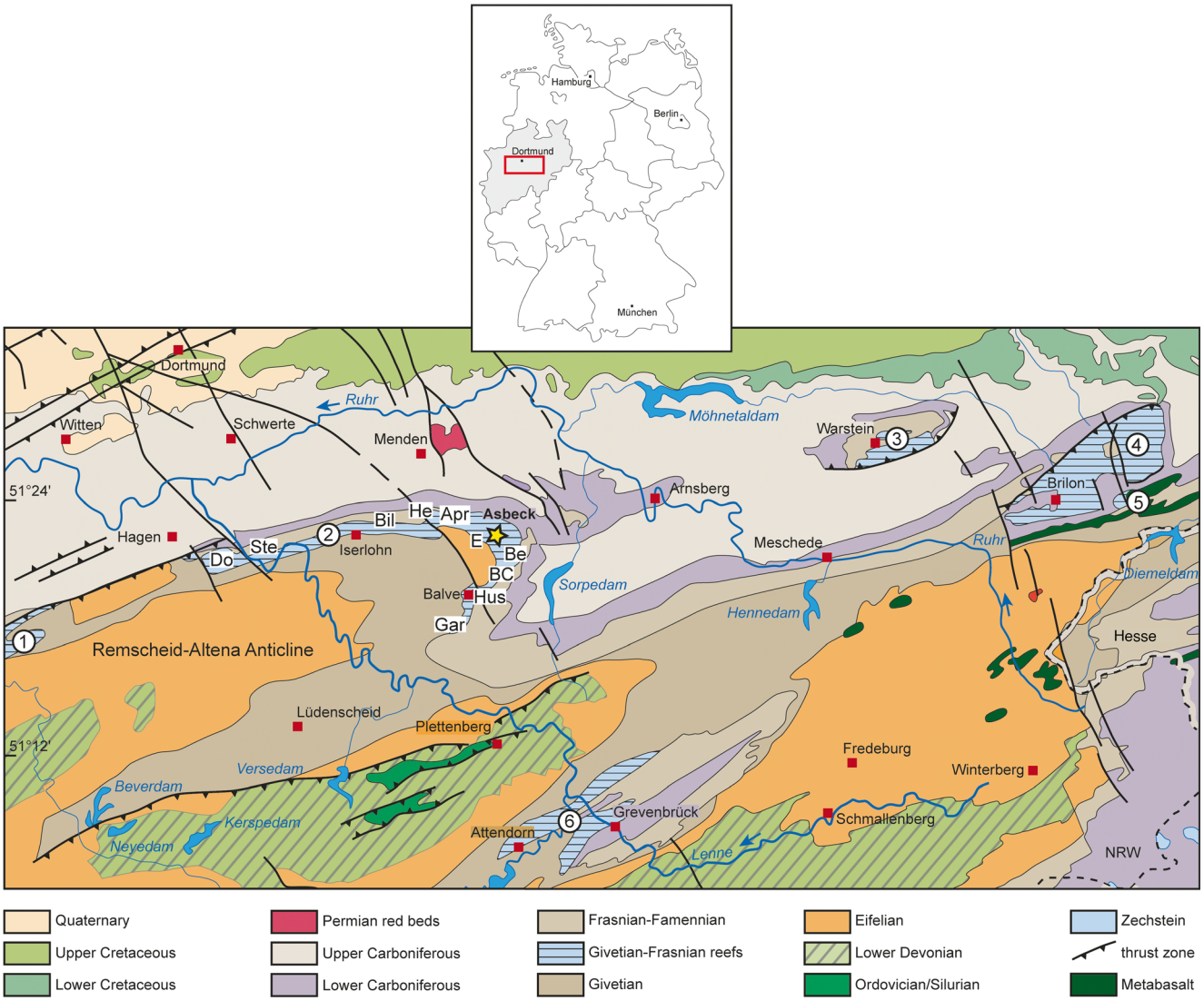

Fig. 1 Distribution of Givetian/Frasnian reef complexes in the northern Rhenish Massif, showing the position of the Hönne Valley (yellow star) north of Balve. *1* Wuppertal Reef (eastern part), *2* Hagen-Balve Reef, *3* Warstein Reef, *4* Brilon Reef, *5* Messinghausen Atoll, *6* Attendorn-Elspe Reef; *Do* Donnerkuhle Quarry at Hagen-Eppenhausen; *Ste* Steltenberg Quarry in Hagen-Hohenlimburg, *Bil* Bilveringsen, *He* Hemer, *Apr* Hemer-Apricke, *E* Emil Quarry, just west of the Hönne Valley, *Be* Beckum, *BC* Balve Cave (Helle Quarry), *Hus* Husenberg at the eastern margin of Balve, *Gar* Garbeck (re-drawn from Ribbert et al. 2017, pl. 1)

= *"Ozarkodina"*, *Pa.* = *Palmatolepis*, *Po.* = *Polygnathus*, *Sk.* = *Skeletognathus*, *Z.* = *Zieglerina*.

Coral and stromatoporoid genera: *Alv.* = *Alveolites*, *Am.* = *Amphipora*, *Hex.* = *Hexagonaria*, *K.* = *Keega*, *St.* = *Stachyodes*, *Th.* = *Thamnopora*.

Repository

All specimens are stored in the Geomuseum of the Westfälische Wilhelms University Münster (GMM), conodont originals under B9A.14, brachiopods under B5B.17, ammonoids under B6C.56. Slides with the majority of other conodonts and thin-sections with reef faunas are stored according to their localities, bed numbers, or core depth.

Regional geological setting

The lower Givetian of the Remscheid-Altena Anticline, located east of the Rhine river, belonged to the southeastern shelf of Laurussia (Old Red Continent), which was characterised by the deposition of prodeltaic siliciclastics (Honsel Formations, compare Hartkopf-Fröder and Weber 2016, fig. 2). Only small biostromes formed in protected positions or on small topographic highs (e.g. May 1983, 1992, 1994b, 2003). These lasted only for brief episodes and were buried by shifting silt- and sandstone wedges. Higher in the lower Givetian succession, the detrital discharge decreased strongly, probably because of increasing aridity in the Old Red source area (Becker et al. 2016c) or by transgressive pulses. Consequently, reef growth was established

widely in the Rhenish Massif, ranging from small, isolated biostromes to laterally extensive and hundreds of metres thick bioherms that are of economic significance (e.g. Jux 1960a, 1960b; Krebs 1971, 1974; Burchette 1981). East of the Rhine river, well-known examples are the reefs of Hofermühle, Wülfrath, Neandertal, Wuppertal, Hagen-Balve, Attendorn, Warstein, and Brilon (Fig. 1). Traditionally, very different reefal carbonates, including marginal slope debris, were summarised under the term "Massenkalk", which referred to the hardness and often poor stratification of the rocks. The rock name was adopted as a common formation name on many geological maps, even if there was clearly no continuity between the individual reefs and irrespective of different facies developments and age. Although the term "Massenkalk" is still used, e.g. by workers of limestone quarries and industrial plants, it is more correct to call such reefal deposits carbonate complexes (Krebs 1974) or, after Burchette (1981), reef complexes, as most build-ups are partly stratified. Regionally, different formation names (e.g. Hartkopf-Fröder and Weber 2016, Bergisch Gladbach-Paffrath Syncline: Büchel Formation; Becker et al. 2016b, Wülfrath: Wülfrath Formation; Becker et al. 2016c, Hagen to Hönne Valley: Hagen-Balve Formation) have been introduced but this process of lithostratigraphical revisions has not yet been completed.

The studied reefal limestones of the Hönne Valley region belong to the Hagen-Balve Reef Complex (Fig. 1) and Hagen-Balve Formation. Following the Variscan strike direction, it stretches for more than 20 km along the northern limb and NE-diving axial ramp of the Remscheid-Altena Anticline (Fig. 1). The reef belt has been exploited economically in numerous quarries along its entire range but active quarrying concentrates at the western (Donnerkuhle Quarry at Hagen-Eppenhausen, Steltenberg Quarry at Hagen-Hohenlimburg; Fig. 1), and eastern (Hemer-Becke and Hönne Valley) ends. The elongated structure probably represents the eroded remnants of a fringing reef north of a structural high in the core of the anticline (Paproth 1986). A maximum thickness of nearly 1000 m of Givetian shallow water carbonates accumulated in the Hönne Valley region. This enormous carbonate succession proves a period of stable conditions, in which reef growth and subsidence were in balance. As mentioned by Becker et al. (2016c), the old geological map by Paeckelmann (1938) displays a complex pattern of numerous faults. However, recent mapping by Münster (e.g. Kruse 2013; Richter 2013) and Cologne (Bahr 2021) students clearly suggest a smaller fault number.

The Hönne Valley Reef: an overview

Research history

Detailed geological research started in the Hönne Valley in the early 20th century with the pioneer work of Denckmann and Lotz (1900) and Denckmann (1901a, 1903, 1905) in the frame of the initial geological mapping by the Prussian Geological Survey. Paeckelmann (1924, 1938) continued the mapping and added details concerning faunas, lithostratigraphy, and local facies developments. For example, he separated the true reef limestones from marginal slope deposits and lower slope to off-reef, dark, organic-rich Flinz facies. He also described the condensed, post-reefal carbonates and adjacent basinal shales. The lithostratigraphic scheme developed by the time does not agree with modern standard terminology but has hardly been revised since. Therefore, we introduce two new formations and two new members.

Jux (1960a, 1960b) studied Hönne Valley quarries in his general, descriptive review of Rhenish Devonian reefs. As a supposed typical example, he logged the now abandoned Emil Quarry west of the valley (Fig. 1) and documented the different, thin-bedded "Massenkalk" facies further to the south, near Garbeck and at the famous Balve Cave (Fig. 1). Subsequently, Eder (1970, 1971) analysed this Givetian Garbeck Limestone and recognised it as the marginal slope deposits of the southern Hönne Valley Reef. In the huge Asbeck Quarry (Fig. 2), Schudack (1993) logged the middle Givetian inner platform succession and recognised cyclic reef growth, which was explained by relative sea-level change due to regional tectonic movements since the lack of biostratigraphical data prevented a correlation with eustatic changes. Strutz (2004) analysed a drill core (HON 01/02) of the Beul area with special emphasis on the microfacies of the upper lagoonal part of the Asbeck succession. He recognised the potential of thin bentonites for regional correlation. Polenz (2008) published a popular scientific booklet with geological, historical, and recent ecological

Fig. 2 Aerial view (from Google Earth) of the northern Hönne Valley region (Oberrödinghausen in the NW to Eisborn in the E), with the roadcut section at the eastern slope of the B515 (yellow asterisk), huge, active Asbeck Quarry (filled with the "blue lagoon"), Horst Quarry (*H*) just to the south, and with the position of the two logged boreholes (*1* B102, *2* HON_1101) and of the Beul outcrop (*3*)

data of the Hönne Valley area. The unpublished B.Sc. Thesis of Nowak (2010) dealt with the youngest reef deposits at the Beul, whilst the B.Sc. Thesis of Stichling (2011) was devoted to the microfacies and stratigraphy of the adjacent drill core B102. Some of the results are presented herein. Becker et al. (2016c) provided an overview of the reef development in the Hönne Valley, with a more complete compilation of former research, first data on the initial phase at Binolen, the main reef phase of Emil Quarry (Fig. 1), and the final phase on the Beul outcrop, including its carbon isotope stratigraphy. Preliminary data of our joint project with the Lhoist Germany Rheinkalk GmbH were presented during the IGCP 596-SDS Symposium in Bruxelles and the post-meeting excursion (Stichling et al. 2015; Becker et al. 2016c), Closing Meeting of IGCP 591 at Ghent (Stichling et al. 2016), and at the ICOS IV in Valencia (Stichling et al. 2017).

Lithostratigraphy

The Hönne Valley sedimentary history and palaeogeography were complex due to the interplay of laterally variable carbonate facies/accumulation, synsedimentary tectonics (fluctuating subsidence), and volcanism. This resulted in a small-scale palaeotopography with either local or more widespread lithological units. The thick reefal succession is underlain by the lower Givetian **Upper Honsel Formation**, which represents an offshore, fine siliciclastic prodelta depositional system (Çinar 1978). Embedded are small-sized lenses of biostromal limestones with reef corals (e.g. May and Marks 2014). They represent initial reef phases that failed due to renewed high clastic influxes.

The thick succession of reef carbonates started with a sharp boundary after the shedding of silt and fine sand ended completely (Becker et al. 2016c). This **Hagen-Balve Formation** is subdivided vertically and laterally into different members (Fig. 3). At the base, the **Binolen Member,** described by Löw et al. (2022), comprises the initial, dark limestones with corals, stromatoporoids, brachiopods, and abundant crinoid debris. It represents the Schwelm Facies sensu Krebs (1974). Dated by brachiopods and conodonts, biostrome growth began in higher parts of the lower Givetian.

The succession turns into the main reef stage, the biohermal Dorp Facies, which characterises the new **Asbeck Member**. It is named after its type locality, the Asbeck Quarry (Fig. 2). The base is exposed at Binolen (Löw et al. 2022, this issue) and defined by the first appearance of back reef limestones, which reflect the change from an open platform into a bioherm with a protected inner lagoon. From the Asbeck Quarry, Schudack (1993) described more than 600 m of cyclic lagoonal and reef core facies and distinguished six major facies associations: reef-core, sublagoonal, lagoonal, restricted lagoonal, intertidal, and supratidal environments. His five "formation" names do not agree with the standard lithostratigraphic nomenclature. They are treated by us as subunits (submembers) of the Asbeck Member. The first and oldest stage, the "Lower Micrite Formation", is characterised by micritic limestones and fenestral fabrics; it falls in the lower/middle Givetian due to the presence of *Stringocephalus*. The "Lower Stromatoporoid-Limestone Formation" represents the second stage with extensive reef growth by massive stromatoporoids. It is followed by a mixed phase that exhibits micritic lagoonal deposits as well as reefal carbonates dominated by large stromatoporoids, the so-called "Micrite-Stromatoporoid-Formation". The overlying unit is, again, a stromatoporoid reefal stage, the "Upper Stromatoporoid-Limestone Formation". Micritic lagoonal carbonates dominate the last phase, the "Upper Micrite Formation". The top of the reef is not exposed in the Asbeck Quarry.

The term "Eskesberg Facies" was introduced by Krebs (1974) for well-bedded, organic rich, and dark back reef facies. These are well-exposed in the northern wall of the abandoned Emil Quarry west of the Hönne Valley (see Becker et al. 2016c). They deposited during deepening phases in concert with decreasing bottom turbulence while organic productivity was high. In the Asbeck Quarry, a corresponding thick black marl interrupts as a marker interval the backreef limestones. The lagoonal Asbeck Member at Emil is well stratified, differentiated (Jux 1960a), and subdivided by a marker bentonite (Becker et al. 2016c, figs. 8–9). The source of the volcaniclastics lay in the south, in the Balve area, where thick volcanic sequences occur. The Emil succession is dated as lower/middle Givetian by storm layers enriched in mostly fragmented, thick-shelled *Stringocephalus* (e.g. Becker et al. 2016c, fig. 10).

The **Eisborn Member,** introduced by Becker et al. (2016c), is characterised by a strongly reduced carbonate accumulation and an influx of open shelf organisms, such as conodonts, brachiopods, and trilobites. The type-section is a small natural cliff in the forest at the Beul (Locality 3 in Fig. 2). Denckmann (1903) and Paeckelmann (1924, 1938) described from the top of the reef succession locally fossiliferous crinoidal limestones containing brachiopods. Such proximal slope deposits resemble the well-bedded **Schleddenhof Member** of the western parts of the Hagen-Balve Reef Complex (Fig. 3), especially from Iserlohn-Letmathe (Beckmann 1961) and from the famous brachiopod locality at Iserlohn-Bilveringsen (e.g. Torley 1908, 1934; Fig. 1).

Outcrops to the south, from near the Balve Cave to Garbeck (Fig. 1), exhibit the mentioned Garbeck Limestone that was studied intensively by Eder (1970, 1971); it is re-named as **Garbeck Member** of the Hagen-Balve Formation. It represents an intergradation and transition from reefal to marginal slope sediments including proximal debris flows with corals and stromatoporoids, crinoid limestones, and organic-rich turbidites as well as dark-grey shales/marls. Conodont re-sampling yielded only sparse faunas from 3–4 kg samples. Records of *L. weddigei* from the upper 8–10 m confirmed a lower/middle Givetian age, in accord

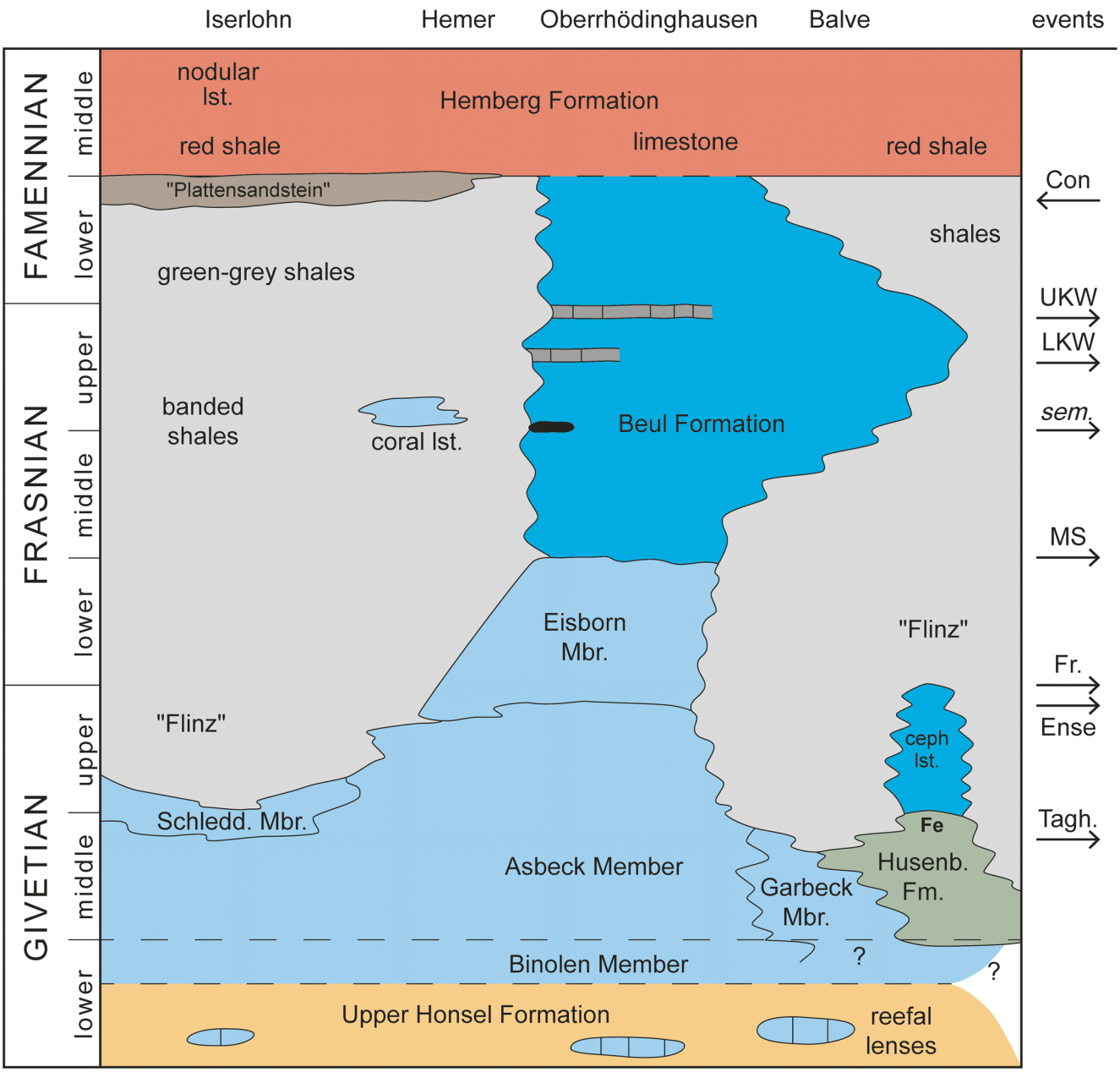

Fig. 3 Schematic overview of Givetian to middle Famennian lithostratigraphy along the central to eastern parts of the Hagen-Balve Reef Complex (Iserlohn to Balve areas; locality positions shown in Figs. 1–2) and global event succession (*arrow to the right* transgressive, *arrow to the left* regressive). *Fe* hematitic iron ore, *ceph. lst*. cephalopod limestone without formation name, *Tagh* Taghanic Crisis, *Ense* Ense Event, *Fr* Basal Frasnes Event, *sem*. *semichatovae* Event, *LKW* Lower Kellwasser Event, *MS* Middlesex Event, *UKW* Upper Kellwasser Event, *Con* (regressive) Condroz Events. Note that most basinal successions still lack modern lithostratigraphic terms. The "Flinz" includes both dark-grey shales and turbiditic limestones derived from the contemporaneous or drowned reef

with *Stringocephalus* occurrences (Paeckelmann 1938) and previous conodont data (Eder 1971; Dornsiepen 1973). The Garbeck Member accumulated synchronously with the Asbeck Member on the southern reef slope.

At Balve (Fig. 1), marginal slope limestones grade into contemporaneous volcaniclastics, tuffites, and overlying iron ore bodies. The proposed new **Husenberg Formation** is named after the Husenberg, the type locality forming the eastern end of the Balve village. The lower and upper boundaries of the formation are defined by the onset and disappearance of volcanic rocks. Locally, there are intercalated middle Givetian debris limestones (Paeckelmann 1938; Dornsiepen 1973), resulting in a total thickness of up to 290 m (Paeckelmann 1938). As mentioned before, the pyroclastic complex is the source for thin bentonites intercalated in the reef platform succession in the north.

Both the Garbeck Member and Husenberg Formation are variably overlain by thick upper Givetian pelagic shales with intercalated detrital limestones ("Flinz Facies"; e.g. Dornsiepen

1973; Clausen 1989) grading into Frasnian "Bänderschiefer" (Paeckelmann 1924; banded shale in Fig. 3), nodular shales, or condensed nodular limestone (e.g. at the Husenberg east of Balve, Paeckelmann 1938; Dobrzinski 2001; Fig. 3). The basinal facies has not yet received valid lithostratigraphic terms. Middle/upper Givetian cephalopod limestones with marker goniatites occur only rarely and in combination with volcanogenic hematite ore (Husenberg, Limmerstein: Paeckelmann 1924, 1938). They suggest deposition on persisting small submarine rises after volcanic activity had ended. Dornsiepen (1973) stated that the most southern, partly very coarse reefal debris of the Balve-Langenholthausen area was not derived from the main Hönne Valley Reef but from small, isolated volcanic reef mounds. They require further investigations.

A steep reef slope, with dark turbiditic limestones and shales ("Flinz Facies") existed also just west of the Hönne Valley. In the Emil Quarry, Jux (1960a) noted black Flinz beds that followed above a 3 m thick upper slope reef breccia. Unfortunately, this important level has been mined away. A similar succession continues westwards towards Hemer-Apricke (Spiske 2003; Fig. 3).

The Asbeck and Horst quarries (Fig. 2) sit on the axial ramp of the Remscheid-Altena Anticline and represent the central area of the Hönne Valley Reef, which turned after its drowning into a large, subphotic submarine rise. This resulted in the accumulation of grey to reddish (hemi-)pelagic limestones with goniatites embracing the two black Kellwasser levels (Paeckelmann 1924) that has no valid lithostratigraphical name. The previously used terms Adorf Limestone and "Nehden-Schichten" (e.g. Paeckelmann 1938) refer to units of the eastern Sauerland that differ partly in facies and stratigraphical range. More importantly, there was no depositional continuity between the eastern pelagic limestones and shales and those of the Hönne region. The type Adorf Limestone (= Adorf Formation) was restricted to small volcanic submarine rises (e.g. Saupe and Becker 2022, this issue), the distinctive goniatite shales of the type Nehden Formation accumulated only in isolated drowned lagoons of the Brilon Reef (Becker 1993; Becker et al. 2016d). The term *Cheiloceras* Limestone, used in the Hönne Valley region by Paeckelmann (1938), does not conform with modern lithostratigraphical standards and could be confused with the *Cheiloceras* Limestone of the Aachen region, which has a very restricted stratigraphic position (e.g. Schmidt 1951). Therefore, we propose the new term **Beul Formation**, defined by the onset of condensed, light-grey nodular or flaser-bedded limestones with pelagic fauna, intercalated by subordinate marls, black shales or limestones, such as the famous Kellwasser Beds. The Upper Kellwasser level provides a lithostratigraphic boundary to separate Lower and Upper Members. The type-section is the natural cliff above our Locality 3 at the Beul, with further outcrops to the north (Schäfer 1978; Hacke 1999). The maximum thickness is ca. 35–40 m.

Laterally, on both limbs of the Remscheid-Altena Anticline, the Beul Formation grades into basinal Frasnian banded or grey-green shales, followed by lower Famennian black shales and sandstones ("Plattensandstein"; Fig. 3), which all lack valid formation names. Paeckelmann (1924, 1938) described the intermediate Frasnian facies, with a mixture of basinal shales, fine-grained grey limestones, and dark, turbiditic Flinz limestones.

Above the Beul Formation, the change to reddish nodular beds ("Fossley" or "Kramenzelkalk") marks the base of the middle Famennian **Hemberg Formation**, which has a wide distribution along the northern flank of the Remscheid-Altena Anticline (e.g. Becker 1992; Hartenfels and Becker 2016a) and beyond (e.g. Becker et al. 2016c). Upper Famennian to lower Tournaisian nodular limestones and the middle Tournaisian Lower Alum Shale deposited only on parts of the submarine high (Paeckelmann 1938; Kruse 2013; discussion in Söte et al. 2017; Hartenfels et al. 2022, this issue.). The final drowning of the pelagic platform occurred around the Tournaisian/Viséan boundary, when the uniform lydite facies of the Hardt Formation covered the whole region. At least since the Upper Carboniferous, the area of the Remscheid-Altena Anticline was continuously a terrestrial high. Therefore, younger pre-Quarternary sediments are restricted in the Hönne Valley to Permian redbeds (Menden Conglomerate), Cretaceous karst fillings, and Tertiary weathering products (Polenz 2008).

Studied localities and drill cores

Drill core HON_1101 (coordinates: x = ^{34}21.227, y = ^{56}95.936m, map sheet 4613 Balve) was sunk by the Lhoist Germany Rheinkalk GmbH and reached a depth of nearly 160 metres. The borehole is located northeast of the Asbeck Quarry (Fig. 2). As Holocene sediments are either thin or absent, most core material consists of thick reefal limestone (upper ca. 70 m of Asbeck Member, interrupted in the upper part by a 6.7 m thick fault zone), overlain by coarse debris correlating with the Eisborn Member (ca. 12 m), (hemi-)pelagic Frasnian to Famennian limestones (Beul Formation, ca. 19.5 m middle/upper Frasnian, ca. 15 m lower/middle Famennian), followed by ca. 5.5 m of the locally argillaceous Hemberg Formation (Fig. 4). The core was sunk in the frame of an exploration campaign for the local mining and was archived for possible future analysis.

Drill core B102 (coordinates: x = ^{34}21.192, y = ^{56}95.769, map sheet 4613 Balve) was sunk for exploration of the limestone resources in the northeastern Beul area (Fig. 2). It also penetrated the upper part of the Asbeck Member and its overlying Upper Devonian (hemi-)pelagic sediments containing the thin Upper Kellwasser level. The final depth was at 106 m (Bed -97, Stichling 2011). The coarse debris interval correlated with the lateral Eisborn Member is only ca. 3 m thick (beds -25 to -27) and overlain by 17 m limestones of the Beul Formation (ca. 12.6 m Frasnian, ca. 4.5 m lower Famennian), and, after a long time of non-deposition, by Viséan cherts (Fig. 5).

Within a forest at the northeastern end of the Asbeck Quarry, the Beul outcrop forms a small cliff and the highest topographic elevation in the adjacent area (Fig. 2). It is located at the eastern end of the Beul hill (x = ^{34}21.470, y = ^{56}95.590, map sheet 4613 Balve), approximately 800 m to the northwest of the centre of the village Eisborn. Hacke (1999) recorded it as his outcrop AB6. Access is possible by following in Eisborn the road "Zum Blechen" to the west, leading after some curves eventually to a track branching, where the main downslope track should be taken. The latter is barred at the entrance of the quarry area. Since this is an area of active mining, a permission by the Lhoist Germany Rheinkalk GmbH is mandatory. Nowadays, it is the only location in the Hönne Valley region, where the drowning stage (Eisborn Member) and following (hemi-)pelagic nodular limestone succession (Beul Formation) can be investigated. An adjacent second cliff noted by Hacke (1999) as Outcrop AB5 exposes higher parts of the Beul Formation. Based on the B.Sc. Thesis of Nowak (2010), a summary of the succession and remarks on the younger Famennian strata were published by Becker et al. (2016c).

Methods

Between 2014 and summer 2022, repeated fieldwork provided more than 30 conodont and 53 microfacies samples from the Beul outcrop. During the logging of cores HON_1101 and B102, macrofauna and lithofacies were recorded continuously, with a focus on vertical facies changes. Our study concentrated on the final phase of local reef development, from the upper part of the Asbeck Member, through the Eisborn Member and overlying Beul Formation. The main part of the Asbeck Member has been sufficiently studied by Schudack (1993) and Strutz (2004).

All lithological types were sampled for thin-sections, using sizes of 75 x 100 mm or 100 x 150 mm. Overall 77 conodont samples were taken from both cores and 124 microfacies thin-sections were produced from core halves. The microfacies analysis was conducted by using transmitted light microscopes (Leica MZ 6, Leica MZ 12.5, fully motorized Keyence VHX). Facies interpretations follow the Dunham classification for carbonate rocks (Dunham 1962; Embry and Klovan 1971), the characterisation of Facies Zones (FZ) after Wilson (1975), the Standard Microfacies Types (SM) sensu Flügel (1978, 2004), and updates by Hartenfels (2011). These formed the frame for comparisons with Devonian microfacies analyses of other authors.

Conodont samples taken from the core material weighted 300 to 400 g, whereas Beul samples weighted at least 3 kg, since their overall yield was low. The limestones were dissolved by using a 10 % solution of formic acid, with washed residues separated into 0.100–0.315, 0.315–0.630, and > 0.630 mm fractions. The residues of the finest fraction were subject to heavy liquid separation using diluted sodium polytungstate ($3Na_2WO_4 \times 9WO_3 \times H_2O$, 2.76–2.78 g ml^{-1}). The samples yielded between 0 and more than 1.000 platform elements per kg, with peak abundances in Famennian nodular limestones. Because many multi-element reconstructions are still doubtful, mostly the Pa element taxonomy has been utilised, with the exception of *Pa. winchelli* (= *subrecta*) and *Pa. bogartensis* (= *rotunda*) in the Frasnian. Ramiform elements were picked but not identified; only supposed Pb elements with platforms (*Nothognathella*) were recorded. Biostratigraphic dating applied the revised zonations of Aboussalam (2003), Aboussalam and Becker (2007), and Narkiewicz and Bultynck (2010) for the Givetian, the Montagne Noire (MN) zonation sensu Klapper (1989), with updates in Girard et al. (2005), Becker et al. (2016a, 2020), and Pisarzowska et al. (2020) for the Frasnian. Spalletta et al. (2017) revised the terminology of Famennian zones, but we refer also to the traditional zonation of Ziegler and Sandberg (1984, 1990) and subdivisions proposed by Schülke (1995). Representative conodonts were photographed with a SEM at Münster.

Fig. 4 Complete section log of drill core HON_1101, showing lithostratigraphic boundaries, stage/substage intervals, the level of conodont samples, reef fauna, and the microfacies succession. For legend see Fig. 5. Bed -32 is an interval without core recovery ▶

Microfacies analysis

Three facies sets are distinguished that represent the Asbeck Member (MF-A), Eisborn Member (MF-B), and the Beul Formation (MF-C). A coarse detrital facies aligned with Set A is intermediate to Set B. It represents the reefal backstepping correlating in time with the initial lagoon drowning. The distribution of MF-types in the Rhenish Massif and, partly, beyond is given in order to place the Hönne Valley microfacies into a wider context, especially since there is no published review on Givetian/Frasnian MF-type distributions that could be quoted.

MF-A: Asbeck Member (Dorp Facies types)

MF-A1: Micritic, dendroid stromatoporoid float-rudstone (Fig. 6a–e)

Examples: HON_1101, Bed -24 (98.20–98.42 m), Bed -25 (102.80–103.00 m), Bed -27 (104.55–104.69 and 105.38–105.65 m), Bed -31 (123.61–124.85 and 132.00–132.56 m), Bed -39 (164.83–165.00 m); B102, Bed -33 (36.00–35.49 m and 35.36–35.49 m), Bed -38 (41.35–41.55 m), Bed -56 (56.70–56.84 m), top Bed -57 (57.17–57.35 m).
Description: Macroscopically, there are medium grey limestones with abundant stromatoporoids, dominated by well-

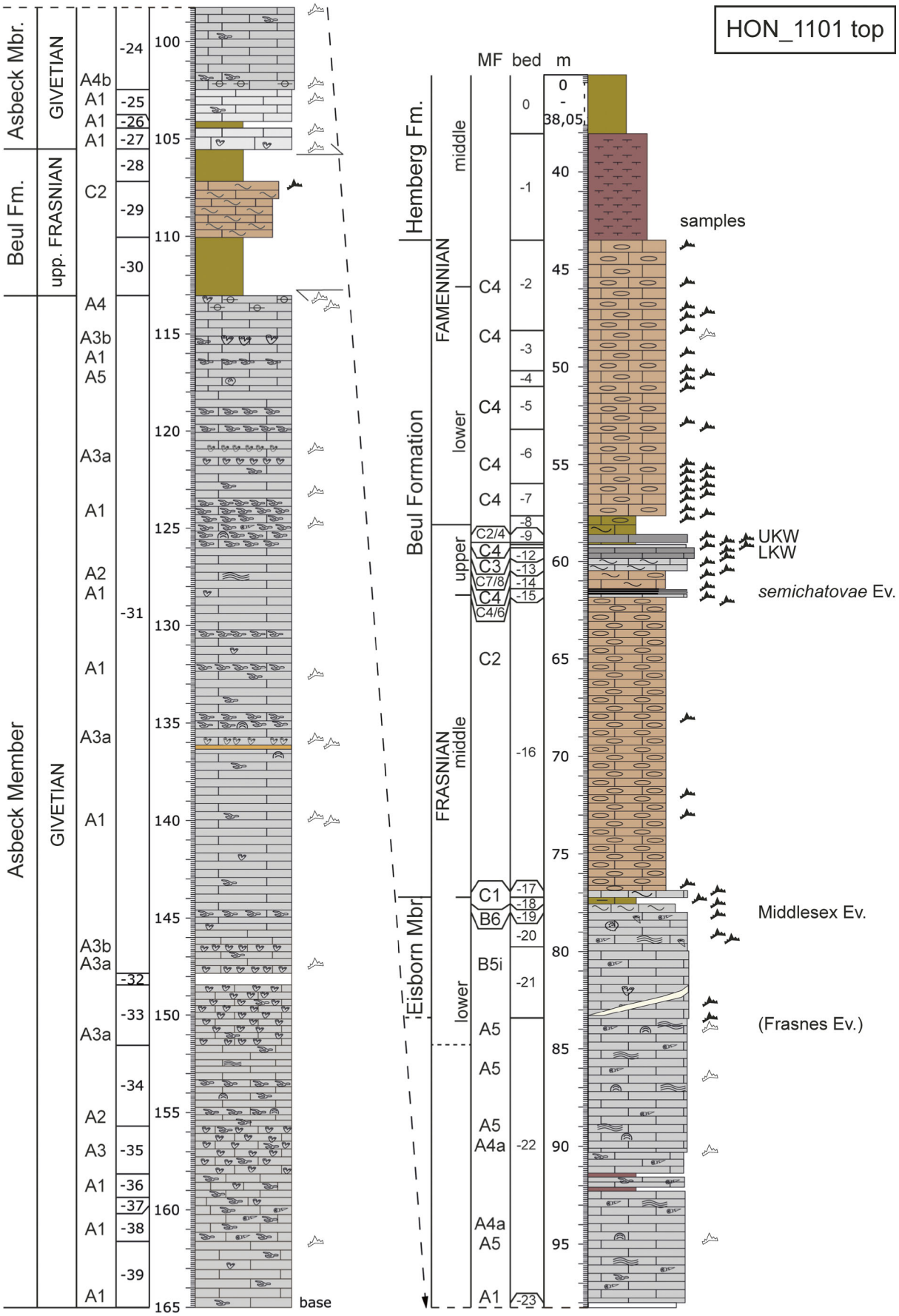
HON_1101 top
Asbeck Mbr.
Beul Fm.
Asbeck Member
GIVETIAN
upp. FRASNIAN
GIVETIAN
A4b
A1
A1
A1
A4
A3b
A1
A5
A3a
A1
A2
A1
A1
A3a
A1
A3b
A3a
A3a
A2
A3
A1
A1
A1
-24
-25
-26
-27
-28
C2
-29
-30
-31
-32
-33
-34
-35
-36
-37
-38
-39
100
105
110
115
120
125
130
135
140
145
150
155
160
165
base
MF
bed
m
Hemberg Fm.
Beul Formation
Eisborn Mbr
middle
FAMENNIAN
lower
upper
FRASNIAN
middle
lower
C4
C4
C4
C4
C4
C2/4
C4
C3
C7/8
C4
C4/6
C2
C1
B6
B5i
A5
A5
A5
A4a
A4a
A5
A1
0
-1
-2
-3
-4
-5
-6
-7
-8
-9
-12
-13
-14
-15
-16
-17
-18
-19
-20
-21
-22
-23
0
38,05
40
45
50
55
60
65
70
75
80
85
90
95
samples
UKW
LKW
semichatovae Ev.
Middlesex Ev.
(Frasnes Ev.)

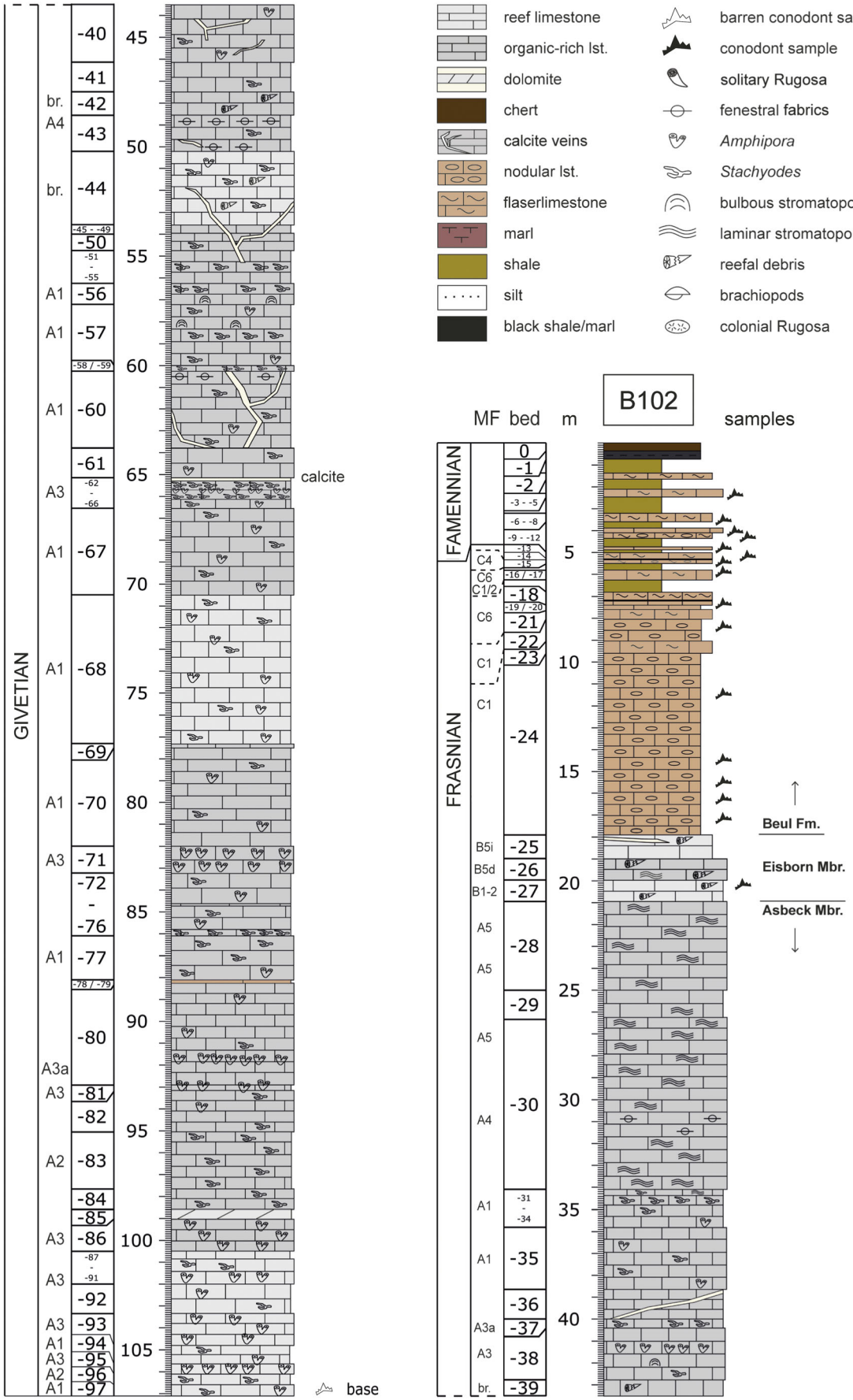
reef limestone
organic-rich lst.
dolomite
chert
calcite veins
nodular lst.
flaserlimestone
marl
shale
silt
black shale/marl
barren conodont sample
conodont sample
solitary Rugosa
fenestral fabrics
Amphipora
Stachyodes
bulbous stromatoporids
laminar stromatoporids
reefal debris
brachiopods
colonial Rugosa
GIVETIAN
calcite
base
B102
MF bed
m
samples
FAMENNIAN
FRASNIAN
Beul Fm.
Eisborn Mbr.
Asbeck Mbr.

◀ **Fig. 5** Complete section log of drill core B102, showing lithostratigraphic boundaries, stage/substage intervals, the level of conodont samples, reef fauna, and the microfacies (MF) succession (*br* breccia levels)

preserved, dendroid forms, such as *Stachyodes* (Fig. 6a–c, e) and delicate *Amphipora* (Fig. 6b–c, e). They are associated with mostly small, bulbous stromatoporoids (*Stromatopora* sp., *Stachyodes (Sphaerostroma) crassa,* Fig. 6b, e). However, rare larger ones (*Actinostroma*, Fig. 6d) as well as monogeneric *Stachyodes* assemblages (Fig. 6a) can be found. Subordinate faunal elements are ostracods, calcispheres/parathuramminid foraminifers (Fig. 6c), rare gastropods, brachiopods, and thin shell filaments. The lack of tabulate and rugose corals is distinctive. Parautochthonous bioclasts occur within a micritic, peloidal (e.g. Fig. 6a, e), partly micrite winnowed, sparitic matrix (e.g. Fig. 6b), indicating a bioturbated float-rudstone. In specific beds, floatstones dominate (Fig. 6a–c), with some intergrading into rudstones (Fig. 6e) and towards MF-A3 (Fig. 6b, lower right). Clay seams and microstylolites are common. As a result of compaction and pressure solution, bioclasts partly dissolved (Fig. 6e). Geopetal structures occur, too (e.g. Fig. 6c). Tectonic stress is documented by thick calcite veins (Fig. 5d).

A variant, **MF-A1***, is characterised in parts of core B102 (e.g. Bed -68, ca. 70.50–77.30 m, Bed -87, 100.50–100.86 m, Bed -89, 101.10–101.38 m) by a very low content of branching stromatoporoids; it is intermediate towards wackestones with reef builders.

Interpretation: MF-A1 is wide-spread in the upper Asbeck Member both in HON_1101 and B102. Following Krebs (1974), *Stachyodes* prefers niches between more massive, bulbous reef builders. In back reef environments, it is characteristic for moderately agitated settings (Eichholt and Becker 2016). In contrast to the more delicate *Amphipora* branches, *Stachyodes* was stronger and, therefore, more tolerant to currents and wave activity, which is noticeable by occasional micrite winnowing. The co-occurrence of *Amphipora* and calcispheres/parathuramminid foraminifers speaks for deposition in a relatively calm lagoonal environment (Flügel 2004). The branching stromatoporoids may have formed small patch reefs within the back-reef. Units with poor macrofauna (MF-A1*) accumulated far from these and received mostly finer detritus. According to the modell sensu Wilson (1975), MF-A1 can be integrated in FZ 7 and SMF 7 sensu Flügel (2004).

Distribution: Comparable stromatoporoid float-rudstones have been widely described from Rhenish reefs. Krebs (1974), May (1987), Fuchs (1990), Malmsheimer et al. (1991), Schudack (1993), and Becker et al. (2016c) reported this facies type from the Dornap, Hagen-Balve, and Brilon reef complexes. Weller (1991) described a similar facies type from the Elbingerode Reef Complex of the Harz Mountains. A *Stachyodes* dominated variety is mentioned by Faber (1980) from the Eifel Mountains. Further occurrences are given by Flick and Schmidt (1987) from small atolls in the southern part of the Rhenish Massif. Krebs (1974) described a dark, bulbous stromatoporoid-*Amphipora* facies, which, in contrast to MF-A1, contains echinoderms, thamnoporids, and alveolitids. Outside the Rhenish Massif, there are similarities with the "stromatoporoid float-/rud-/boundstone" found in patch reefs of the Oued Cherrat Zone of the Moroccan Meseta (Eichholt and Becker 2016, their MF A5).

MF-A2: Detrital stromatoporoid grain-rudstone (Fig. 6f)

Examples: HON_1101, Sample-31c (127.79–127.89 m), Bed -34 (155.05–155.30 m).

Description: The medium grey limestone contains a high number of broken stromatoporoids, mostly dendroid *Stachyodes* and *Amphipora*; laminar and bulbous forms occur, too. The assemblage is completed by disarticulated, thick-shelled brachiopods (Fig. 6f), minor echinoderm debris (probably crinoids), calcispheres/parathuramminid foraminifers, and ostracods. In accordance with MF-A1, tabulate and rugose corals are absent. Bioclasts are subrounded and their size, especially in the case of laminar stromatoporoids, can reach more than 10 cm in exceptional cases. The poorly preserved and unsorted skeletal remains and associated, small-sized micritic lithoclasts are embedded within a peloidal grainstone matrix with microsparitic cement. Some bioclasts show marginally an initial micritisation. Microstylolites are partly strongly developed.

Interpretation: MF A-2 was deposited in a back reef setting adjacent to patch reefs and represents a high energy environment laterally to MF-A1. A prominent feature is the mixture of organisms, which originally belonged to different reefal zones. Transport may have occurred by waves, storm events, or in channels (compare the turbulent back-reef Zone IVb of Machel and Hunter 1994). Considering the close relationship to MF-A1, MF-A2 falls in the FZ7 sensu Wilson (1975).

Distribution: Similar facies types are known from the Rhenish Massif in the "detrital-stromatoporoid-coral-algae facies" sensu Krebs (1974). MF-A2 is also documented from the Elbingerode Reef Complex, Harz Mountains (Weller 1991). In the western continuation of the Rhenish Shelf, in SW Devon, Garland et al. (1996) described a corresponding MF5 (*Stachyodes* rud- and grainstones) as "high-energy accumulation of back reef talus". Eichholt and Becker (2016) distinguished a similar "detrital, bioclastic grainstone/rudstone (back reef breccia)" in the Moroccan Meseta and discussed its affiliation with SMF 5 sensu Flügel (2004).

MF-A3: Amphipora float-rudstone

Description: Macroscopically, this facies type occurs as a medium grey limestone with abundant, delicate *Amphipora*

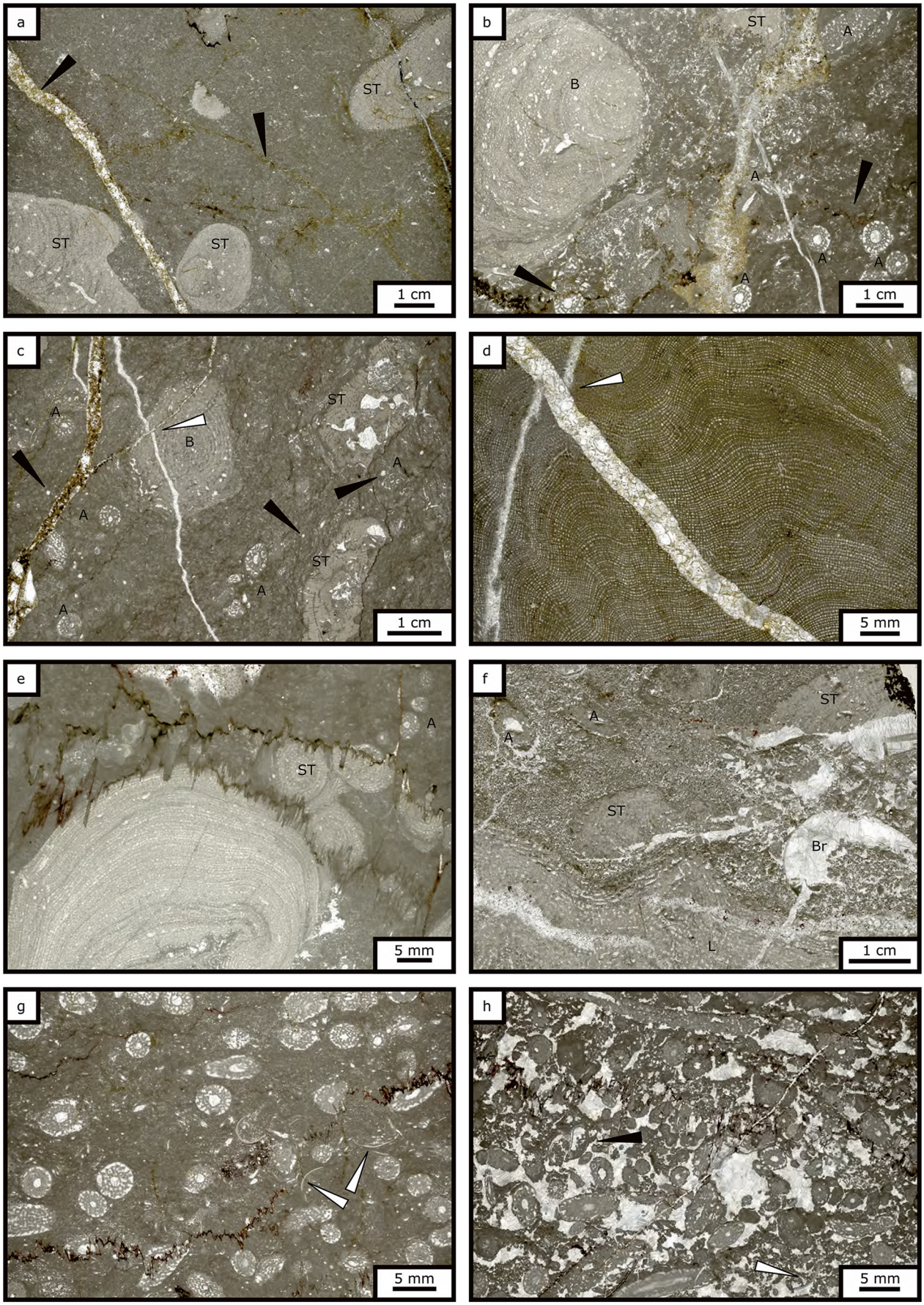
a
ST
ST
ST
1 cm
b
ST
A
B
A
A
A
A
1 cm
c
A
B
ST
A
A
ST
A
A
1 cm
d
5 mm
e
A
ST
5 mm
f
ST
A
A
ST
Br
L
1 cm
g
5 mm
h
5 mm

◀ **Fig. 6** Microfacies types from cores of the Asbeck Member. **a–e** MF-A1, Micritic, dendroid stromatoporoid float-rudstone **a** *Stachyodes (St.) costulata* (*ST*) branches floating in a fine, micrite saturated matrix; with calcite veins (*black arrow*) and some dolomitization (HON_1101, 102.80–103.00 m, Bed -25) **b** Rare bulbous stromatoporoid (*B Stromatopora* sp.) and associated delicate *Amphipora* branches (*A Am.* ex gr. *laxeperforata*) floating in a bioturbated matrix with partly washed out micrite and stylolite seams (*black arrows*) (HON_1101, 165.83–165.00 m, Bed -39) **c** *Amphipora* branches (*A Am.* ex gr. *laxeperforata*), small bulbous stromatoporoid (*B St. (Sphaerostroma) crassa*), *Stachyodes (St.) costulata* (*ST*) with cavities, partly filled with peloids, and small "calcispheres" (*black arrows*) in a dense, bioturbated matrix; two generations of calcite/dolomite veins (*white arrow*) demonstrate polyphase, post-depositional fracturing (HON_1101, 124.61–124.85m, Bed -31) **d** Detail of a bulbous stromatoporoid (*Actinostroma clathrata*) with two vein generations (*white arrow*) (HON_1101, 105.38–105.65 m, Bed -27) **e** Bulbous stromatoporoid (*B Stromatopora* sp.) in growth position, overlain by *St. (Sphaerostroma) crassa* (*ST*) and *Amphipora* (*A*) branches floating in a dense micritic matrix; multiple stylolite seams cut off fossils and indicate a significant diagenetic loss of original carbonate (B102, 41.35–41.55m, Bed -38) **f** MF-A2, detrital stromatoporoid grain-rudstone with laminar stromatoporoids (*L Parallelopora* sp.), *Amphipora* (*A Am.* ex gr. *laxeperforata*), *Stachyodes* (*ST*), and crushed brachiopods (*Br*) embedded within a peloidal pack-grainstone matrix (HON_1101, 155.05–155.30 m, Bed -34) **g** MF-A3a, *Amphipora* float-bafflestone, *Am.* ex gr. *laxeperforata* branches embedded in micritic to fine detrital (wackestone) matrix with shell filaments (pelecypods, *white arrows*) and stylolitic dissolution seams (HON_1101, 91.77–91.92 m, Bed -25) **h** MF-A3b, *Amphipora* rudstone with with *Am.* ex gr. *laxeperforata, Stachyodes (St.)* sp., microspar matrix, subordinate small gastropods (*black arrow*), and pelecypods (*white arrow*); micrite has mostly been been washed out (HON_1101, 146.64–146.78 m, Bed -31)

branches. Associated are subordinate *Stachyodes* and bulbous to laminar stromatoporoids, fragmented shells, gastropods, ostracods, and calcispheres/parathuramminid foraminifers (Fig. 6g). In thin-sections that are normal to the branch axes, it is difficult to separate parautochthonous *Amphipora* float- and autochthonous bafflestones. Clay seams formed by pressure solution and compaction are common. There are two MF-A3 subtypes:

MF-A3a: Amphipora Floatstone (Fig. 6e (upper right corner), 6g)

Examples: HON_1101, Bed -31 (120.76–121.00 and 135.86–136.10 m), Bed -33 (151.41–151.55 m); B102, Bed -38 (41.35–41.55 m), Bed -80 (91.77–91.92 m).

This subtype is characterised by a micritic, peloidal, and bioturbated matrix with moderate amounts of biodetritus.

MF-A3b: Amphipora Rudstone (Fig. 6h)

Examples: HON_1101, Bed -31 (115.27–115.42 and 146.64–146.78 m).

In contrast to MF-A3a, the matrix is dominated by peloids and sparite, as micrite has been washed out; the amount of *Amphipora* branches is higher. Combined oblique and longitudinal sections confirm that the branches mostly are fragmented.

Interpretation: The environment was a mostly quiet, restricted, and shallow lagoon (Flügel and Hötzl 1976), where *Amphipora* found ideal conditions for growth (see Krebs 1974). The *Amphipora* float-rudstones are probably the result of episodic storm events. Fragmented branches were transported over short distances, especially in MF-A3b, where water agitation also caused winnowing of the matrix.

Distribution: Related facies types are widely known from the Rhenish Massif (e.g. Bergisch Gladbach: Jux 1960a, 1964; Bohatý and Herbig 2010; Hartkopf-Fröder and Weber 2016; Agger Valley: Jux 1960a; Dornap Reef: Jux 1960a; Hagen-Balve Reef Complex: Jux 1960a; May 1987; Schudack 1993; Becker et al. 2016c; Brilon Reef Complex: Malmsheimer et al. 1991; Kürschner et al. 1999) and Harz Mountains (Elbingerode Reef Complex: Weller 1991). Machel and Hunter (1994) assigned *Amphipora* float- and grainstones to their moderately turbulent back-reef Zone IIIb. In SW Devon, MF-A3 was described by Garland et al. (1996) as their MF6. From the Moroccan Meseta, a related facies type was documented by Eichholt and Becker (2016) as "*Amphipora* float-/rud-/boundstone". It corresponds to FZ 7 sensu Wilson (1975), a restricted-marine platform environment, and to SMF 7 sensu Flügel (2004).

MF-A4: Fenestral pack-grain-bindstone

Description: MF-A4 occurs macroscopically as medium grey limestone with a low fossil content. It is distinguished by dominant fenestral fabrics, ranging from subrounded to elongate, irregular and laminar spar-filled primary cavities ("birdseyes", Ham 1952). The matrix consists mostly of well rounded, equal-sized peloids (Fig. 7c). In a few cases, the intergranular spaces are filled with microspar. Rare faunal elements are *Amphipora*, *Stachyodes*, other stromatoporoids (bulbous and laminar forms), dendroid corals, parathuramminids, gastropods, ostracods, and indeterminate fragmented shells. Pressure solution led to the common formation of stylolites; calcite veins reflect diagenetic and tectonic stress. Two MF-A4 subtypes are distinguished.

MF-A4a: Peloidal and fenestral pack-grainstone (Fig. 7a, c)

Examples: HON_1101, Bed -22 (90.05–90.15 and 94.60–94.80 m), Bed -31 (113.05–113.22 m); B102, Bed -30 (30.97–31.12 m).

Subtype MF-A4a is characterised by numerous, isolated, up to 2.5 cm long, sparitic birdseye structures. Some voids are filled with dark sediment at their bases. Occasionally (Fig. 7c), there are thin, laminated microbial micrite layers marking minor discontinuity surfaces.

MF-A4b: Laminated, fenestral bindstone (Fig. 7b)

Examples: HON_1101, Bed -24 (102.00–102.20 m), Bed -31 (113.50–113.60 m).

An incipient, biogenic zebra structure sensu Weller (1989) is formed by layers of small, but variably sized fenestrae, which may form horizontal ribbons. They alternate with peloidal pack- or grainstones layers. Parathuramminid foraminifers and microbial micrite layers are present.

In core B102, in the middle part of Bed -30 (30.85–30.97 m), fenestral and peloidal grainstones with some amphiporids (MF-A4a) show a strong increase of laminar and branching stromatoporoids. This fenestral stromatoporoid floatstones with peloidal grainstone matrix, including some gastropods, is intermediate between MF-A4 and A2 and not separated as a microfacies type.

Interpretation: Transitions between both subtypes are common, which differ by the variable preservation (complete or disarticulated) of originally organic, microbial mats that were filled by orthosparite very early in diagenesis. Subordinate birdseyes with internal sediment are transitional towards *Stromatactis* that characterise mudmounds (e.g. Bathurst 1959, 1980) or drowned Rhenish reef platforms (Schlupkothen Facies, Krebs 1974; Becker et al. 2016b). Peloid formation is a result of clotted micrite reworking due to permanent currents (Fåhræus et al. 1974; Flügel 2004). The combination of peloids and fenestral fabrics is a typical feature of mudmounds and reef lagoons. Mestermann (1995) distinguished six types of fenestrae in the Brilon Reef lagoon, four of which are present in our cores; the two vertical types are missing. Zhou and Pratt (2019) differentiated peloid types in a Frasnian fenestral mudmound of Canada. In our case, both rounded bacterial peloids and subangular intraclastic peloids (= mud peloids sensu Flügel 2004) are present and intergrade.

Mixed peloidal-fenestral fabrics indicate intertidal conditions, a shallow lagoon with a permanent influence of waves and currents. The habitat was hostile to the majority of reefal organisms. The alternation of mudstones and peloidal pack-grainstones is typical for peritidal to even supratidal environments. The poor preservation of the subordinate bioclasts indicates re-deposition. This facies is comparable with FZ 8 of Wilson (1975) and SMF 21 sensu Flügel (2004), Facies 2 sensu Schudack (1993, laminite facies), and Zone 1b, fenestral laminites, of Machel and Hunter (1994).

Distribution: Related facies haven been described from Hagen-Hohenlimburg by Koch-Früchtl and Früchtl (1993) and from the Brilon Reef Complex (May 1987; Mestermann 1995). Krebs (1974) described a fenestral facies from the Langenaubach Reef Complex of the southern Rhenish Massif and suggested an intertidal palaeoenvironment with slightly increased salinity. Salinity fluctuations would exclude stenohaline organisms. In SW Devon, MF-A4a was described by Garland et al. (1996) as MF9 (restricted, shallow subtidal to intertidal), MF-A4b as MF12 (restricted intertidal to supratidal ponds).

MF-A5: Crinoidal stromatoporoid-coral rudstone (Fig. 7d–e, g)

Examples: HON_1101, Bed -22 (90.05–90.15, 83.30–83.50, 86.30–86.45, and 94.80–94.98 m); B102, Bed -25 (18.63–18.97 m), Bed -28 (23.07–23.25 and 24.20–24.38 m).

Fig. 7 Microfacies types from cores of the Asbeck and Eisborn members. **a–c** MF-A4, fenestral pack-grain-bindstone **a** MF-A4a, peloidal and fenestral packstone with pelmicritic matrix and abundant isometric to elongated, not oriented birdseyes, Types 3.2 and 3.3 of Mestermann (1995) (HON_1101, 94.00–94.80 m, Bed -22) **b** MF-A4b, laminated fenestral bindstone with alternating peloidal and birdseye layers (Type 3.1 of Mestermann 1995) and some parathuramminid foraminifers (*black arrow*) (HON_1101, 113.50–113.60 m, Bed -31) **c** MF-A4a, peloidal and fenestral pack-grainstone with variably sized birdseye and *Amphipora* branches (*A*) in a micritic to pelmicritic matrix with some *Stromatactis*-like birdseyes show filling with dark micrite at the base (*black arrows*) (B102, 30.97–31.12m, Bed -30) **d** MF-A5, rudstone with heavily broken stromatoporoids, including *Stachyodes (St.) costulata* (*ST*), crinoid debris (*C*), fragmented thamnoporid (*white arrow*), *Alveolites (Crassialveolites)* sp. (lower left), and bioclast interspaces filled by finer debris or sparite (HON_1101, 94.80–94.98 m, Bed -22) **e** MF-A5, rudstone with dominant crinoid debris (*C*), fragmented *Stachyodes* (*ST*), and grainstone matrix with peloids and sparite (B102, 24.20–24.38 m, Bed -28) **f** MF-B6, pack-rudstone formed by unsorted, fragmented branches of the auloporid *Roemerolites* sp. and with stylolithic dissolution surfaces; slightly darker packstone with small-sized, undefined bioclasts at the base (HON_1101, 78.00–78.15m, Bed -20) **g** MF-B5i, rudstone with bulbous (left, not clearly identifiable), laminar (*Schistodictyon* sp., lower centre, *Salairella buecheliensis*, right), and dendroid (*Stachyodes*) stromatoporoids, rare thamnoporid fragments, subordinate crinoid debris, and grainstone matrix of peloids, fine bioclasts, and sparite (HON_1101, 83.30–83.51 m, top Bed -22) **h** MF-B5i, Alveolitid-dominated rudstone (*Av Alv. (Alv.)* ex gr. *edwardsi*) with overgrown thamnoporid (*Th.* ex gr. *polyforata*) and diagenetic dissolution seams that intrude significantly into bioclasts (HON_1101, 79.12–79.32 m, Bed -20, Eisborn Member)

Description: Macroscopically, there are medium grey, fossiliferous limestones. In thin-section, poorly preserved, broken, angular stromatoporoid fragments, partly with micritic seams, are the most abundant organisms. Broken branches of *Stachyodes*, rare *Amphipora* and thamnoporids, laminar alveolitids, and solitary Rugosa are associated. Bioclasts can reach a size up to several cm (Fig. 7d). Abundant fragmented crinoids and rare calcispheres occur in interspaces. The matrix consists of peloids, coarse sparite (Fig. 7e), or small-sized detritus formed by unidentifiable bioclasts and peloids. The sorting of the components is poor. Crinoid remains are partly surrounded by syntaxial overgrowth (see Fig. 7e).

Interpretation: MF-A5 includes a higher diversity of organisms than the previous MFs. We assume a more open environment, from the reef core to the outer reef edge, as the bioclast source. Their brecciated, non-sorted arrangement, poor preservation, the lack of micrite, and the mixture of fauna typical for different settings, points to high-energy deposition by storms and waves. In comparison to the directly underlying back-reef facies types, the arrival of material from the seaward side indicates reef (inner platform) backstepping but channels through the reef core may have facilitated the material transport. MF-A5 can be assigned to FZ 4 (slope) to 5 (platform margin) sensu Wilson (1975). In the scheme of Flügel (2004), it can be classified as SMF 6 and resembles the detrital stromatoporoid-echinoderm facies of Krebs (1974).

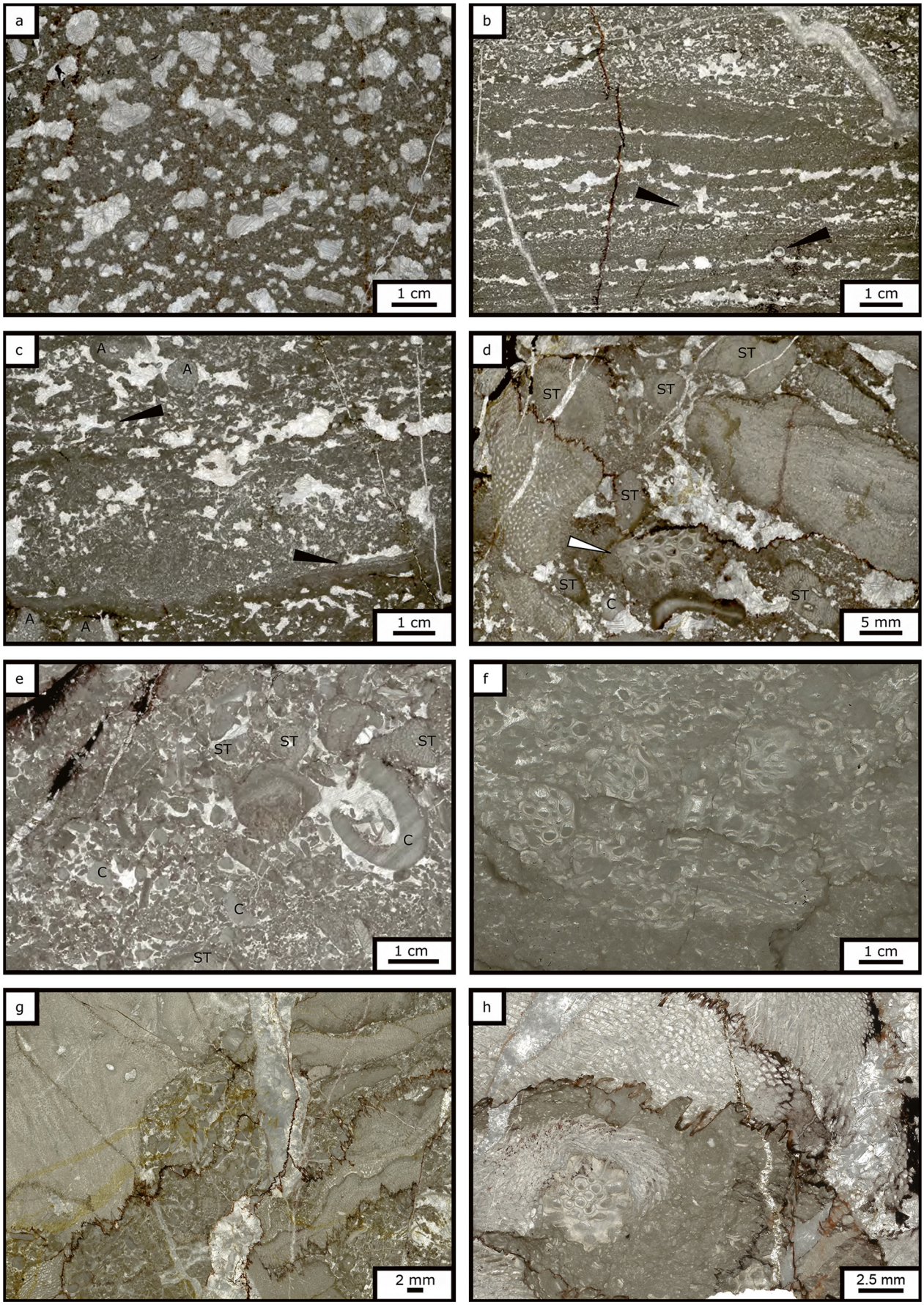
a
1 cm
b
1 cm
c
A
A
A
A
1 cm
d
ST
ST
ST
ST
ST
C
ST
5 mm
e
ST
ST
ST
C
C
C
ST
1 cm
f
1 cm
g
2 mm
h
2.5 mm

Distribution: This facies type is common in the Rhenish Massif (e.g. Krebs 1974). Machel and Hunter (1994) assigned it to the transition from the reef core to the fore-reef (their zones IV/V to IIIf). In the Moroccan Meseta, Eichholt and Becker (2016) described detrital coral-stromatoporoid floatrudstones as fore reef breccias; MF-A5 is similar to their subtype A.

MF-B: Eisborn Member (biostromal facies types)

The characteristic feature of the Eisborn Member is the combined presence of subordinate open-water biota (conodonts, brachiopods, trilobites), bioturbation, dominance of fine debris (mud- to pack- and grainstones), and of isolated, variably sized fragments of reef builders (dominant tabulate or rugose corals, some stromatoporoids), giving various types of floatstones. They represent "reef gardens" characterised by widely spaced reef builders grading into biostromes (rudboundstones of HON_1101 and of the backside of the Beul outcrop). The faunal spectrum (Table 1) is restricted. Comparisons can be made with initial reef phases (Schwelm Facies, e.g. Koch-Früchtl and Früchtl 1993; Löw et al. 2022, this issue) and Rhenish reefs that remained in the biostrome phase, since both show open water influence. Examples come from the Eifel Mountains (Faber 1980) and small reefs intercalated within siliciclastic units of the Sauerland. The latter have been well-studied for their faunas (e.g. May 1983, 1994b, 2003; May and Marks 2014) but not for their microfacies spectrum. Comparable conodont-bearing reef limestones were also described by Oetken (1997) from the Lahn Syncline in the southern Rhenish Massif. Distinctive for the Eisborn Member is the low diversity of microfauna in conodont samples and the absence of microbialites or of coarse slope debris that characterise in other German reef complexes the Iberg/Schlupkothen facies. In the Elbingerode Reef Complex of the Harz Mountains, Weller (1991) assigned some comparable facies types to a "demergence stage".

MF-B1: Peloidal and bioclastic mud-wackestone (with reefal debris) (Fig. 8a)

Examples: Beul, Bed B1 (sample from 110 cm above base), Bed B2, middle of Bed B4, Sample D-3, Bed E3; B102, lower part of Bed -27.

Description: Macroscopically, there are light- to middle-grey, fine-grained, thick- or thin-bedded, solid limestones with isolated large corals, such as thamnoporids, alveolitids (middle part of Bed B1), *Hexagonaria*-type colonial Rugosa (top of Bed B1), and stromatoporoids (upper part of Bed B4: *Stachyodes (Keega) australe, ?Euamphipora, ?Clathrocoilona*). In thin-sections, MF-B1 is characterised by a bioturbated micritic matrix that can be recrystallized (microsparitic, within Bed B1) and with a

Table 1 Corals, stromatoporoids, and other reefal fauna from the Beul section (1–13e = B1–B13e)

taxon/bed no.	1	4b	5	6	7	8	9	10a/b	10c	11	12a	13a	13b	13d	13e	C	B–D	D	E	bio
Alveolites sp.	x					x				x	x	x			x					x
Thamnopora sp.		x	x	x	x	x	x			x	x			x	x		x	x	x	x
Stayodes (Keega) australe		x					x				x	x						x		x
?Euamphipora sp.		x																		
?Clathrocoilona sp.		x																		
Thamnophyllum ex gr. *caespitosum*					x															
Flabellia sp.					x															
Thamnopora ex gr. *polyforata*							x						x		x		x	x	x	x
Stromatoporella sp.										x										
Syringopora sp.										x										
Alveolites (Alv.) edwardsi										x		x								
Platyaxum (Rosoeporella) ex gr. *gradatum*											x						x	x		
Disphyllum breviseptatum														x			x	x		x
Disphyllum rugosum															x	x	x			x
Hexagonaria aff. *davidsoni*															x					
Thamnopora ex gr. *micropora*															x					
Stachyodes (Stachyodes) sp.																x				x
Haplothecia schlotheimi																				x
Alveolites (Crassialveolites) sp.																				x
Alv. (Alveolites) sub. *suborbicularis*																				x

variable amount of peloids. Small bioclasts consist of echinoderm debris (crinoids, echinid spines), abundant shell filaments, brachiopod fragments, ostracods, thamnoporid fragments, rare calcispheres (middle part of Bed B1), and foraminifers (rare *Nanicella*, Bed E3). Diagenetic overprint led to stylolites, flaser-bedding, and calcite-healed, partly reddish fractures (Bed B3). MF-B1 grades into MF-B2 (within beds B1, B2, D, and E3), MF-B3 (Bed B4), MF-B5a (upper part of Bed B4), and MF-B5f (within Bed B2).

Interpretation: The dominance of moderately fine reef debris in combination with the occasional larger clasts of reef builders and open-water organisms suggests the setting of a drowned back reef that received with minor currents or during storms the distal talus of the submerged reef margin or from flooded patch reefs. Episodic bottom currents reworked clotted micrite as peloids. Deposition took place well below the fair-weather wave base.

Distribution: Equivalents of MF-B1 were included by Koch-Früchtl and Früchtl (1993) in their MF-Typ 4 ("microbioclastic-peloidal wackestone with packstone parts") but the latter occurred in the still open, initial reef phase at Hagen-Hohenlimburg (Steltenberg Reef, Fig. 1), not in the final drowning phase. MF-B1 can also be compared with the peloid-bearing Microfacies I1 ("micritic-arenitic crinoid facies" with reef builder debris) of Rieck and Stritzke (1999) from the atoll of the Messinghausen Anticline. MF-B1 differs from the peloid-rich back-reef Facies Zone IIB ("sparsely fossiliferous packstones and wackestone") of Machel and Hunter (1994) in the presence of open-water biota.

MF-B2: Peloidal grainstone (Fig. 8b)

Examples: Beul, beds B1 (samples from the base and from 110 cm above base) and B2 (partly); B102, higher parts of Bed -27.

Description: Macroscopically, it is a light-grey, massive, fine-grained, and macrofossil-poor limestone. In thin-sections, peloids dominate and are embedded in a sparitic matrix. Bioclasts consist of echinoderm or tabulate coral debris (B102, Bed -27) and ostracods, which are partly coated (Beul, Bed 1). Diagenetic overprint led to stylolites. MF-B2 grades into MF-B5g (Sample top reef 1D).

Interpretation: MF-B2 differs from MF-B1 in displaying evidence for more constant bottom water agitation, leading to a more complete reworking of micrite to peloids ("pseudopeloids"). It is a drowned variant of the lagoonal SMF 16 of Flügel (2004).

Distribution: Equivalents of MF-B2 are known from fore-reef settings of Eifel biostromes (Faber 1980) but rarely occur in bioherm/lagoon settings. Exceptions were found in reefs of the Harz Mountains (Franke 1973; Weller 1991) and the Moroccan Meseta (Eichholt and Becker 2016).

MF-B3: Bioclastic wacke-packstone (with reefal debris) (Fig. 8c)

Examples: Beul, beds B3, B4 (basal and middle parts), B13c, Sample lower D-3; B102, upper part of Bed -26 (ca. 19.00–19.50 m), basal 4 cm of Bed -25 (18.96–19.00 m).

Description: Macroscopically, this is a light- to middle-grey, thin- and flaser-bedded, fine-grained limestone that is poor in macrofauna. In thin-section, there are abundant bioclasts, mostly fine debris of tabulate corals, brachiopods, and echinoderms (including large echinid spines, abundant crinoids in Bed B13c), some ostracods, and rare coiled foraminifers (*Nanicella*, Bed B3) and calcispheres (base of Bed B4), surrounded by bioturbated micritic to microsparitic (base of Bed B4) matrix. Diagenetic pressure solution caused flaser-bedding (beds B3, D) and there are thin veins filled by reddish calcite. MF-B3 grades into MF-B4 and MF-B5a (within beds B4 and E1).

Interpretation: In relation to MF-B1, the higher amount of bioclasts, while the micrite has not been washed out, is somewhat contradictive. There must have been weaker bottom currents but a higher influx of reef debris originating probably from episodic storms. In modern reef environments, fragmentation of reef builders is caused to a large extent by recurrent hurricanes (e.g. Scoffin 1993). Coarse material may remain on the platform while much debris is transported towards the outer slope and lagoon, where it is deposited as tempestites with characteristic features, such as cross-bedding and grading (Aigner 1985). In the Hagen-Balve Reef Complex, typical tempestites are only known from outer slope settings (Eder 1971), not from lagoons (see Schudack 1993).

Distribution: From the initial phase of the Hagen-Balve Reef, Koch-Früchtl and Früchtl (1993) described a variant rich in siliciclastic detritus (MF-Typ 1); there is no previous documentation from terminal reef stages. MF-B3 differs from the back-reef Zone IIB of Machel and Hunter (1994) in the presence of open water biota.

MF-B4: Organic-rich, bioclastic wacke-packstone (with reefal debris) (Fig. 8d–e)

Examples: Beul, beds B5, B6, B7, B8a, B8b, B10a, B10b, samples B10c-1, B11-1, B12b.

Description: Macroscopically, there are thin-bedded, dark- to middle-grey, bituminous, fine-grained limestones with few macrofossils (e.g. *Thamnophyllum* in Bed B7, thamnoporids, alveolitids, large stromatoporoid of Bed B10c, *Stromatoporella* in Bed B11). In thin-section, the bioturbated matrix is micritic, without or with only a few peloids. The C_{org} content varies, as indicated by variably middle- or dark-grey thin-sections. Fine-grained intervals tend to be darker than the packstones. The abundant bioclasts consist of dominant fine debris of echinoderms (crinoids, echinid spines) and shells (bivalves,

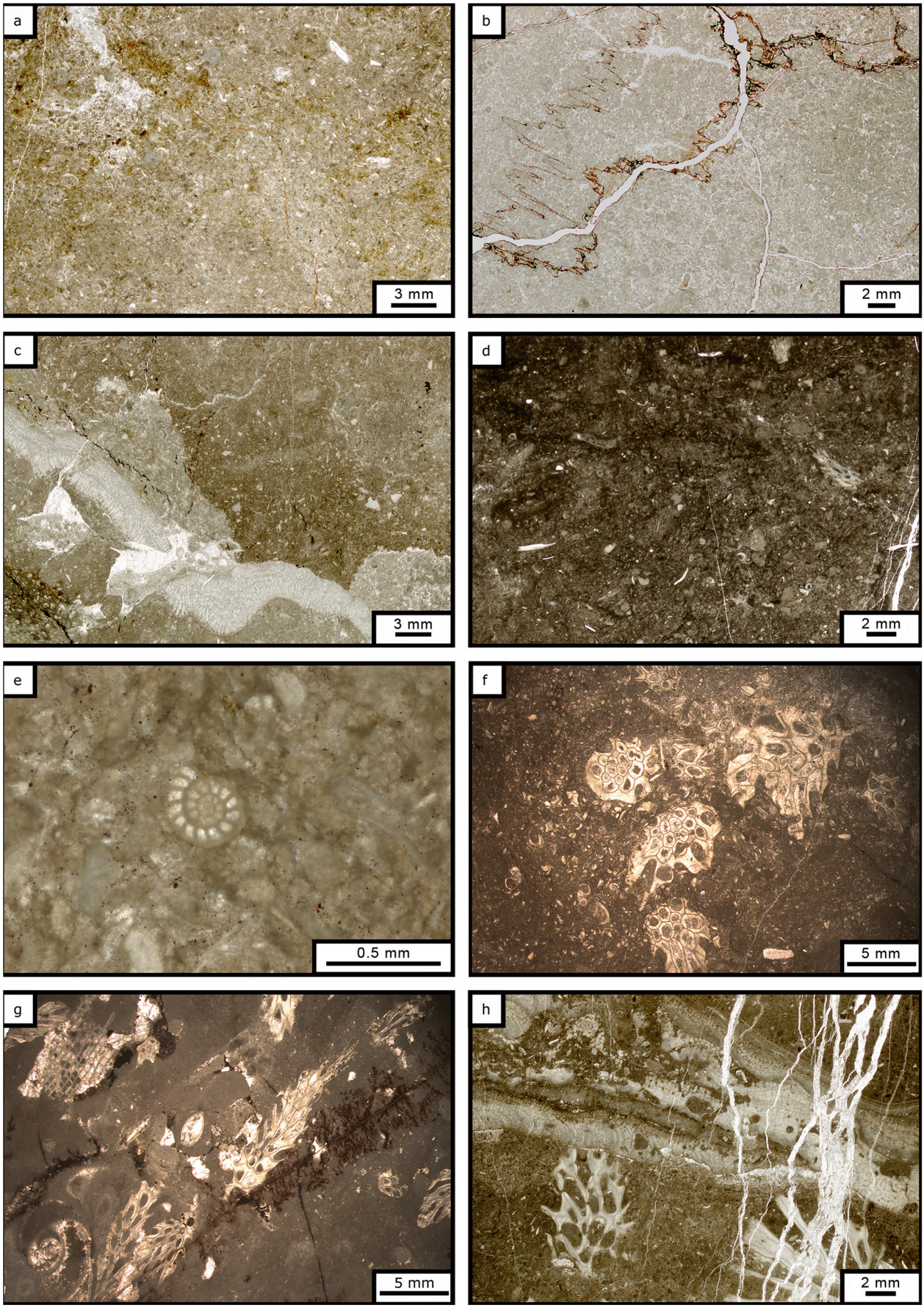
a
3 mm
b
2 mm
c
3 mm
d
2 mm
e
0.5 mm
f
5 mm
g
5 mm
h
2 mm

◀ **Fig. 8** Microfacies types of the Eisborn Member of the Beul outcrop. **a** MF-B1, peloidal and bioclastic mud-wackestone with crinoid debris, shell hash and some ostracods in a peloidal matrix, locally with washed out micrite (Bed B2) **b** MF-B2, peloidal grainstone without macrofauna and with high-amplitude stylolites (base of Bed B1) **c** MF-B3, bioclastic wackestone with fine crinoid debris, shell hash and rare calcispheres above a laminar stromatoporoid (*Stachyodes (Keega) australe*) (Bed B4, thin-section II) **d** MF-B4, organic-rich, bioclastic wacke-packstone, with debris of thamnoporids, echinoderms, shell pieces, some calcispheres and ostracods in a dark, bioturbated matrix (Bed B6) **e** MF-B4, detail of bioclastic wackestone with the planispiral foraminifer *Nanicella,* crinoid, coral, and shell debris (Bed B10b) **f** MF-B5a, thamnoporid floatstone with small gastropods and many undetermined bioclasts in a dark, bioturbated micrite matrix (Bed E1, thin-section I) **g** MF-B5a, thamnoporid floatstone with bioturbated, fine, dense micrite matrix, iron-manganese mineralizations and oblique cross-section of the euomphalid *Coloniacirrus* (lower left corner) showing its typical, convex growth lirae, biostrome on backside (Sample top 1B, thin-section I) **h** MF-B5b, organic-rich thamnoporid-stromatoporoid floatstone with *Th.* ex. gr. *polyforata*, laminar *Stachyodes (Keega) australe*, peloidal, fine bioclastic micritic matrix, and branching calcite veins (Bed B9)

brachiopods), fragmentary thamnoporids, ostracods, gastropods (beds B5, B8a, abundant in Sample B11-1), and rare calcispheres. Typical is a small amount of coiled, multichambered foraminifers (*Nanicella*, Fig. 8e). Rare cross-sections of uniserial foraminifers (beds B7, B10b, Sample B11-1) may represent *Tikhinella* or *Paratikhinella*. In conodont residues, rare sponge spicules, including heteractinids (compare Löw et al. 2022, this issue, for the initial reef phase) were found. Diagenetic overprint caused flaser-bedding (pressure solution) and calcite-healed fractures. MF-B4 grades into the less bituminous MF-B3 and into the bituminous MF-B5b (Bed B8b), MF-B5c (Bed B8a, Sample B11-2), MF-5d (Sample B10c-2), and MF-5f (Bed B7).

Interpretation: MF-B4 differs from MF-B3 by the increased amount of C_{org}, reflecting higher primary productivity. The more typical, unusually advanced (for the time) *Nanicella* had a pantropical distribution (Dubicka 2017). In Rhenish Massif reef complexes, it has previously been recorded from platy limestones of the reef drowning stage of the Bergisch Gladbach region (= *Rhenothyra* Beckmann, 1950), from organic-rich mudstones of the Eifel Mountains (Faber 1980), from peloidal micritic limestones of the Wülfrath Reef (Städter 1989), organic-rich back-reef limestones of Lindlar (Hering 1995), and from reef detrital, turbiditic grainstones (Beisinghausen Limestone, May 1994a). In the Frasnian reefs of the Holy Cross Mountains, it occurs also in reef slope facies with microbial stromatoporoid-alveolitid mounds (Racki and Soboń-Podgórska 1993), in Belgium in the bioclastic facies of biostromes (Dumoulin et al. 1996), and in the Moroccan Meseta both in biostromal brachiopod-coral floatstones (Eichholt and Becker 2016) or crinoidal brachiopod-coral-stromatoporid limestones (Termier et al. 1975). Özkan et al. (2019) found *Nanicella* in several MF types around basal Frasnian biostromes of Anatolia, but with maximum abundance in bioclastic packstones on the off-reef side. In summary, *Nanicella* is typical for eutrophic (organic-rich) reefal facies with moderate water agitation and open water influx.

Distribution: MF-B4 resembles the bioturbated, bituminous mud facies of Eifel biostromes (Faber 1980). It is more fossiliferous and not as rich in foraminifers/calcispheres as the common dark mud-wackestones of back-reef settings (e.g. Franke 1973; Krebs 1974; calcisphere mud facies of Faber 1980; MF-Typ 5 of Koch-Früchtl and Früchtl 1993).

MF-B5: Coral float-rudstone

Description: Macroscopically, these are light- to dark-grey, thin-bedded limestones with moderately common to very abundant reef builders, mostly tabulate and rugose corals, sometimes with stromatoporoids. In many variants, reef builders float in a fine-grained matrix, representing destructed "coral-stromatoporoid gardens". *Alveolites* is mostly preserved in situ and shows only few signs of damage, whereas dendroid Tabulata are heavily broken. Floatstones can change laterally and vertically to rud-boundstones, which are autoparabiostromes and parabiostromes sensu Kershaw (1994). The following variants grade into each other:

MF-B5a: Thamnoporid floatstone (Fig. 8f–g)

Examples: Beul, top of Bed B4, Bed E1, Sample top reef 1B.

Thamnoporid fragments/branches float in a middle-grey, bioturbated matrix of mudstone (Sample top reef 1B) or bioclastic wacke-packstone with variably abundant bioclasts, such as gastropods (Bed E1, Sample top reef 1B: porcelliid *Coloniacirrus*, Fig. 7g), small brachiopods (Sample top reef 1B), thamnoporid debris, shell filaments, rare foraminifers, a minor amount of peloids (top of Bed B4), and dense micrite. Grading into MF-B5g (Sample top reef 1B).

MF-B5b: Organic-rich thamnoporid-stromatoporoid floatstone (Fig. 8h)

Examples: Beul, top of Bed B8, Bed B9.

Fragmentary thamnoporids and subordinate stromatoporoids (*Stachyodes*) float in a dark-grey, organic-rich matrix of slightly peloidal, bioclastic wackestone with abundant bioclasts, such as fragmentary echinoderms (crinoids and echinid spines), thamnoporids, shell debris, gastropods (upper part of Bed B8), and ostracods.

MF-B5c: Organic-rich alveolitid-gastropod floatstone (Fig. 9a)

Examples: Beul, e.p. Bed B8a, Sample B11-2.

Large alveolitids and subordinate stromatoporoids (Sample B11-2: *Stromatoporella* sp.) or encrusting syringoporids (Sample B11-2) in a (moderately) dark, bioturbated, bioclastic wacke-packstone matrix with abundant fine echinoderm

(crinoids, echinid spines), shell and thamnoporid debris, abundant gastropods, ostracods, calcispheres, peloids (Sample B11-2), and micrite.

MF-B5d: Alveolitid-stromatoporoid floatstone (Fig. 9b)
Examples: Beds B12a, B12b, B13a, B13b; B102, within lower part of Bed -26.
Alveolitids, *Platyaxum (Roseoporella),* and stromatoporoids (*Stachyodes*) floating in a bioturbated, middle- to dark-grey, partly organic-rich, bioclastic wacke-packstone matrix with abundant debris of echinoderms (crinoids, echinid spines), thamnoporids, brachiopods, some ostracods, rare calcispheres, rare peloids (Bed B12b), coated grains, and micrite. As a variant in B102, laminar stromatoporoids and alveolitids are under- and overlain or float in middle-grey bioclastic wackestone matrix.

MF-B5e: Alveolitid-thamnoporid floatstone (Fig. 9c)
Examples: Beul, samples B11-3, B13 undifferentiated, B13e-3 (= top Bed 13), top reef 2C, top biostrome; B102, beds -27, -26 (18.35–19.25 m)
Variably abundant alveolitids and fragmented thamnoporids, subordinate stromatoporoids (top biostrome) and dendroid Rugosa (*Disphyllum*) floating in a light- to middle-grey mudstone (top biostrome) or, more frequently, bioclastic and micritic wackestone matrix with diverse bioclasts, such as shell filaments, thamnoporid and echinoderm (crinoids, echinid spines) debris, and rare ostracods. There is intergradation to MF-B5a, MF-B5d, MF-B5h, and MF-B5i (e.g. within Bed B11).

MF-B5f: Organic-rich rugose floatstone (Fig. 9d)
Example: Beul, Bed B7.
Solitary Rugosa (*Thamnophyllum*, Bed B7) floating in a dark-grey wacke-packstone matrix with shell filaments, echinoderm (crinoids, echinid spines) and brachiopod debris, ostracods, calcispheres, rare algal thalli (probably *Flabellia*), and micrite. Grading into MF-B5g (Sample top reef 1D).

MF-B5g: Rugose-thamnoporid floatstone (Fig. 9e)
Examples: Beul, beds B13d, B13e-1, B13e-2, e.p. C, samples D-1, D-2, e.p. top reef A, top reef 1-D, top reef 1E.
Colonial Rugosa (*Hexagonaria* and two species of *Disphyllum*, beds B13d–e), thamnoporids, associated with subordinate alveolitids, calcareous algae (Bed B13e-1), crinoid ossicles, pleurotomariid gastropods (samples D-1, top reef 1D; Fig. 9f), and stromatoporoids (*Stachyodes*, Sample B13e-2, Bed C), floating in a bioturbated, middle-grey mudstone (samples D-1, e.p. top reef 1D) to bioclastic wackestone matrix, partly with small sparitic fenestrae, various small bioclasts, such as shell filaments, thamnoporid and echinoderm debris, rare ostracods, calcispheres (Sample D-2), foraminifers (*Radiosphaera*), and sponge spicules. Grading into coral rudstone (MF-B5i). Rarely with pockets of peloidal grainstone (Sample top reef 1D).

Fig. 9 Microfacies types of the Eisborn Member of the Beul outcrop. **a** MF-B5c, organic-rich alveolitid-gastropod floatstone with *Stromatoporella* and commensalic *Syringopora,* laminar *Alveolites (Alveolites)* (top right), small gastropods, coral and shell debris in a bioturbated matrix with some micrite (Bed B11, thin-section I) **b** MF-B5d, alveolitid-stromatoporoid floatstone, contact of fragmented *Thamnopora polyforata* branches, *Stachyodes (Keega) australe*, and *Alveolites* sp. (lower part), surrounded by variably dense, organic-rich, mud-wackestone matrix with crinoid and shell debris (Bed B13) **c** MF-B5e, alveolitid-thamnoporid floatstone with *Alveolites (Alveolites)* sp. (upper part), *Th.* ex gr. *polyforata* (larger branches), and *Th.* ex gr. *micropora* (smaller branches) in a bioturbated, organic-rich mud-wackestone matrix with partly washed out micrite (Bed B13e = Top 13) **d** MF-B5f, organic-rich rugose floatstone with *Thamnophyllum*, crinoid and shell debris, and ostracods in a bioturbated, fine bioclastic wacke-packstone matrix (Bed B7) **e** MF-B5g, rugose-thamnoporid floatstone with branches of *Th.* ex gr. *polyforata* and *Disphyllum breviseptatum* in micrite-rich, dense wackestone matrix with poorly preserved crinoid debris and several generations of calcite veins, including short sigmoidal cracks (lower left half) (Bed D) **f** MF-B5g, detail of a rugose-thamnoporid floatstone with a *Th.* ex gr. *polyforata* branch next to a spirally ribbed, pleurotomariid gastropod with geopetal sparite filling, surrounded by dense, organic-rich, micritic mudstone (Bed D, Sample B–D) **g** MF-B5h, alveolitid-rugose boundstone with *Alveolites (Crassialveolites)* sp., overlain by wave-laminated mudstone, embedding *Disphyllum rugosum*, and overlain by peloidal mud-grainstone (top biostrome, Sample top 1C) **h** MF-B5i, tabulate-rugose rudstone with alveolitids (lower right and upper left), fragmented *Thamnopora* sp., and *Disphyllum rugosum* in a bioturbated to brecciated, wacke-packstone matrix with fine debris (top biostrome, Sample top 1A)

MF-B5h: Alveolitid-rugose floatstone (Fig. 9g)
Examples: Beul, e.p. samples top reef 1A, top reef 1C; HON_1101, Bed -20 (79.03–79.10 m).
Alveolitids and dendroid Rugosa (*Disphyllum*) floating in a variable matrix, ranging from cross-bedded peloidal grainstone and laminated microbial bindstone (Sample top reef 1C) to micritic, bioclastic wackestone with thamnoporid and echinoderm debris (Sample top reef 1A). Grading into MF-B5e and MF-B5i.

MF-B5i: Tabulate-rugose rud-boundstone (Figs. 7h, 9h)
Examples: Beul, e.p. Bed C, e.p. samples top reef 1A and top reef A; HON_1101, Bed -20 (79.12–79.32 m); B102, main Bed -25 (17.90–18.96 m).
Framework of alveolitids, thamnoporids, and colonial (*Disphyllum, Haplothecia*) rugose corals with occasional stromatoporoids and interspersed mudstone (Sample top reef A) or bioclastic wacke-packstone matrix with echinoderm debris, thick-shelled brachiopod fragments, and rare ostracods. Grading into MF-B5h (Sample top reef 1A) and MF-B5g (Sample top reef A).
Interpretation: In relation to MF-B1 to MF-B4, MF-B5 is characterised by a higher content of reef builders leading up to biostromal rud-boundstones, which were strongly influenced by episodic storms. Deposition took place on the drowned platform below the fair-weather wave base and within the mesophotic zone. The micrite was mostly not washed out by permanent

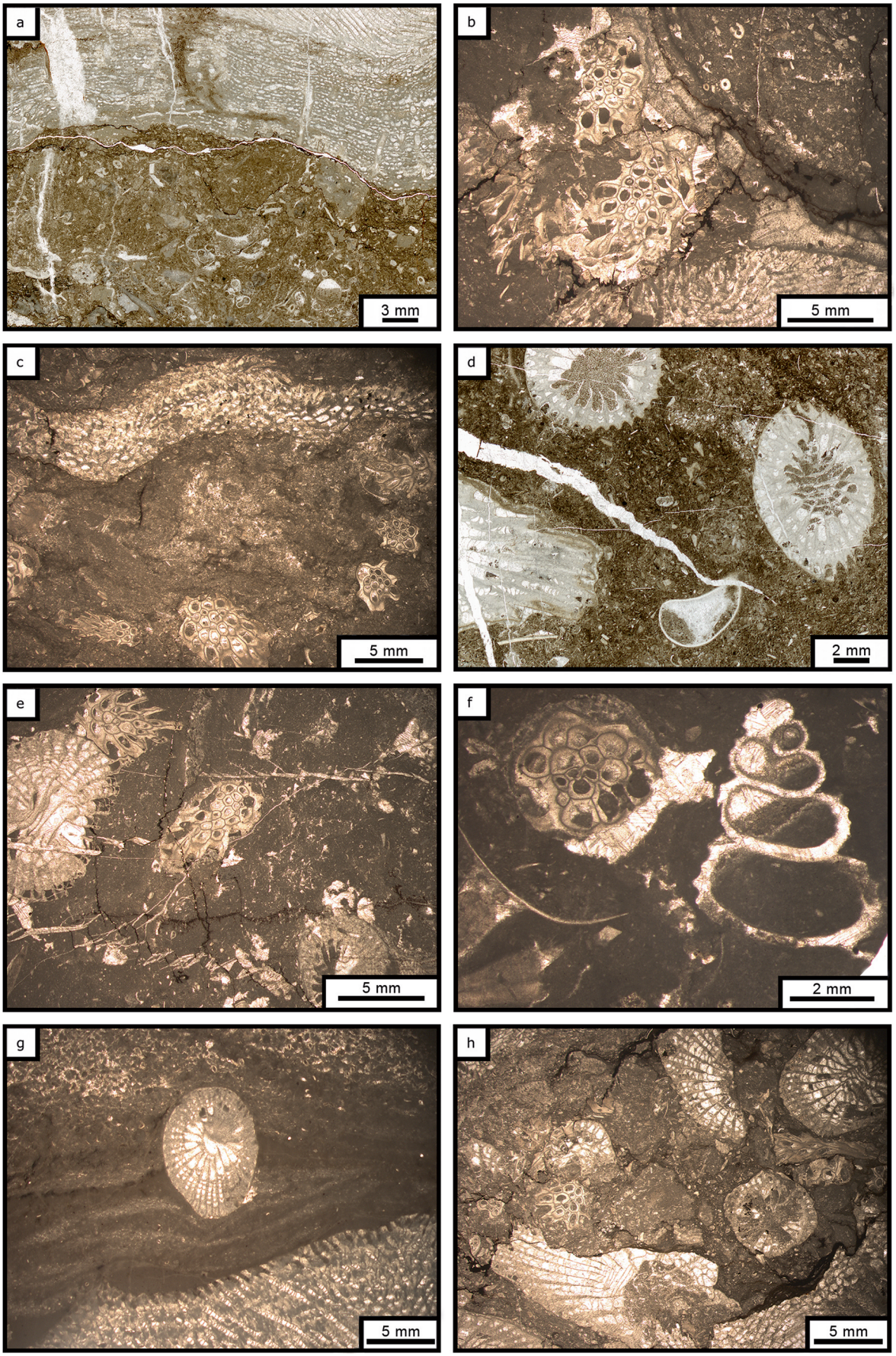
a
3 mm
b
5 mm
c
5 mm
d
2 mm
e
5 mm
f
2 mm
g
5 mm
h
5 mm

currents. Alveolitids and rugose corals are common, unlike as in typical back-reef facies of the biohermal Dorp Facies. The different subtypes suggest a small-scale lateral ecological differentiation, with patches dominated variably by thamnoporids, alveolitids, or dendroid rugose corals. The three organic-rich subtypes (MF-B5b, B5c, and B5f) reflect phases of increased primary productivity, obviously a favourable condition for gastropods, as it is known from gastropod-rich back-reef facies (e.g. Malmsheimer et al. 1991; Weller 1991: Type Ha5-2; Schudack 1993). The rud-boundstones indicate slightly shallower conditions with improved light supply for improved growth of frame builders. This is supported by the parallel decline of conodont faunas. Persisting storm influence prevented a preservation as in-situ autobiostromes (Kershaw 1994). The growth of tabulate corals outpaced that of stromatoporoids, perhaps due to the recurrent influx of detritus as a limiting factor. It is not uncommon, that *Alveolites* overgrew other taxa or rather their fragments, such as laminar stromatoporoids or thamnoporid branches (Fig. 7h).
Distribution: Givetian equivalents can be found within the initial, biostromal Schwelm Facies of Krebs (1974). Faber (1980) briefly described the "pioneer reef community" from the top of the Rohr Horizon in the Eifel Mountains, characterised by masses of thamnoporids and with alveolitids and stromatoporoids. Koch-Früchtl and Früchtl (1993, fig. 8) illustrate from the initial phase of the Hagen-Balve Reef an equivalent of MF-B5i as bindstone with incrusting alveolitids, stromatoporoids, thamnoporids, and rugose corals. Weller (1991) described as Type Hc2 alveolitid floatstones from the top of the Elbingerode Reef. This is the only known previous example from a reef drowning setting. Eichholt and Becker (2016: MF C3) described equivalents of MF-B5i from a biostrome of the Moroccan Meseta. The coral rudstones of Beul show no evidence for gravitational transport on a steep outer slope, as the many crinoidal coral-stromatoporoid rudstones of the literature (e.g. Weller 1991: Hb1-1 to 1-5; Machel and Hunter 1994: Zone IVf; Rieck and Stritzke 1999: Facies II 3).

MF-B6: Auloporid pack-rudstone (Fig. 7f)

Example: HON_1101, top of Bed -20.
Description: Pieces of fragmented encrusting tabulate corals (*Roemerolites*) are so abundant, that they form pack-rudstones.
Interpretation: This facies type is restricted to the top of the Asbeck Member of HON_1101 and was formed obviously in a time of increasing condensation, when the sea floor was colonised by encrusting corals that became subject to storm/current reworking and re-deposition.
Distribution: Previously, equivalents of MF-B6 have not been described from Rhenish reefs. Zatoń et al. (2015) described an auloporid-dominated facies from an upper Frasnian biostrome of the Russian Platform characterised by fluctuating hydrodynamic regimes.

MF-C: Post-reefal facies set (Beul Formation)

The reefal fauna has completely disappeared and was replaced by a pelagic assemblage with tentaculitoids (in the Frasnian), cephalopods, deeper-water brachiopods (including lingulids, see Batruvkova 1967 and Becker et al. 2016d), bivalves and ostracods, pelagic conodonts (*Palmatolepis* biofacies), and abundant agglutinating foraminifers, as typical for low sedimentation rates at slopes of starved basins (Gutschick and Sandberg 1983) and on pelagic carbonate platforms (Becker 1993, pp. 109–110).

MF-C1: Dacryoconarid wacke-packstone (Fig. 10e–g)

Examples: HON_1101, Bed -17 (76.90–77.08 m); B102, Bed -24 (15.40–15.60 m).
Description: Macroscopically, this facies type is developed as light-grey, fine-grained flaser- to nodular limestone with occasional pelagic macrofauna (goniatites, orthoconic cephalopods, rare trilobites). Thin-sections show a strongly bioturbated, micritic matrix with flaser-bedding (Fig. 10f) due to pressure solution during diagenesis. There are moderate to large

Fig. 10 Microfacies types of the Beul Formation. **a** MF-C4, bioturbated bioclastic wackestone with abundant mollusk shells, including early cheiloceratids with typical wide and low whorls (HON_1101, 55.85–56.03 m, Bed -6, level of samples -6a/b) **b** MF-C2/3 transitional to MF-C5, recrystallized, organic-rich ostracod wackestone with dacryoconarids (*white arrows*), overlain by a thin layer of light-grey mud-wackestone (MF-C4) with geopetals (*black arrow*) and distinctive burrows (*Bt*) exploring the underlying C_{org}-rich bed, sharply overlain by bioturbated mollusk wacke-packstone (MF-C2) with a larger bivalve shell (HON_1101, lower part of Upper Kellwasser level, ca. 58.89–58.92 m, lower part of Sample -9b) **c** MF-C2, partly well-stratified, with bedding plains marked by pyrite seams, but internally bioturbated, middle-grey mollusk wacke-packstone with a large goniatite filled by dense micrite, with embryonic to juvenile goniatites (right side), overlain by a *Frutexites*-like enrichment of iron minerals (*black arrow*), and followed by a packstone layer with geopetal filling of an ostracod (*white arrow*) (HON_1101, middle part of Upper Kellwasser layer, ca. 58.85–58.89 m, middle part of Sample -9b) **d** MF-C4 grading into C5, flaser-bedded ostracod wacke-packstone, mass occurrence of ostracods and fragmented pelecypods, with associated small-sized orthocones (*white arrows*), possible dacryoconarids (*black arrow*), and bioturbated micrite matrix (B102, 5.38–5.43 m, Bed -15) **e** MF-C1, mass occurrence of styliolinids together with fragmented crinoids (*white arrows*) (HON_1101, 76.90–77.08 m, Bed -17) **f–g** MF-C1, numerous styliolinids and few ostracods (*white arrows*), embracing as a result of bioturbation, without sharp boundary, a clump of styliolind packstone (*black arrow*, enlarged in g) (B102, 15.40–15.60 m, Bed -24) **h** MF-C3, recrystallized, organic-rich, peloidal, and bioclastic packstone with an assemblage of orthoconic cephalopods (*C*), ostracods (*white arrows*), broken pelecypods (*P*), and a questionable dacryoconarid cross-section (*D*) (HON_1101, Lower Kellwasser Limestone, 59.80–59.91 m, Bed -12)

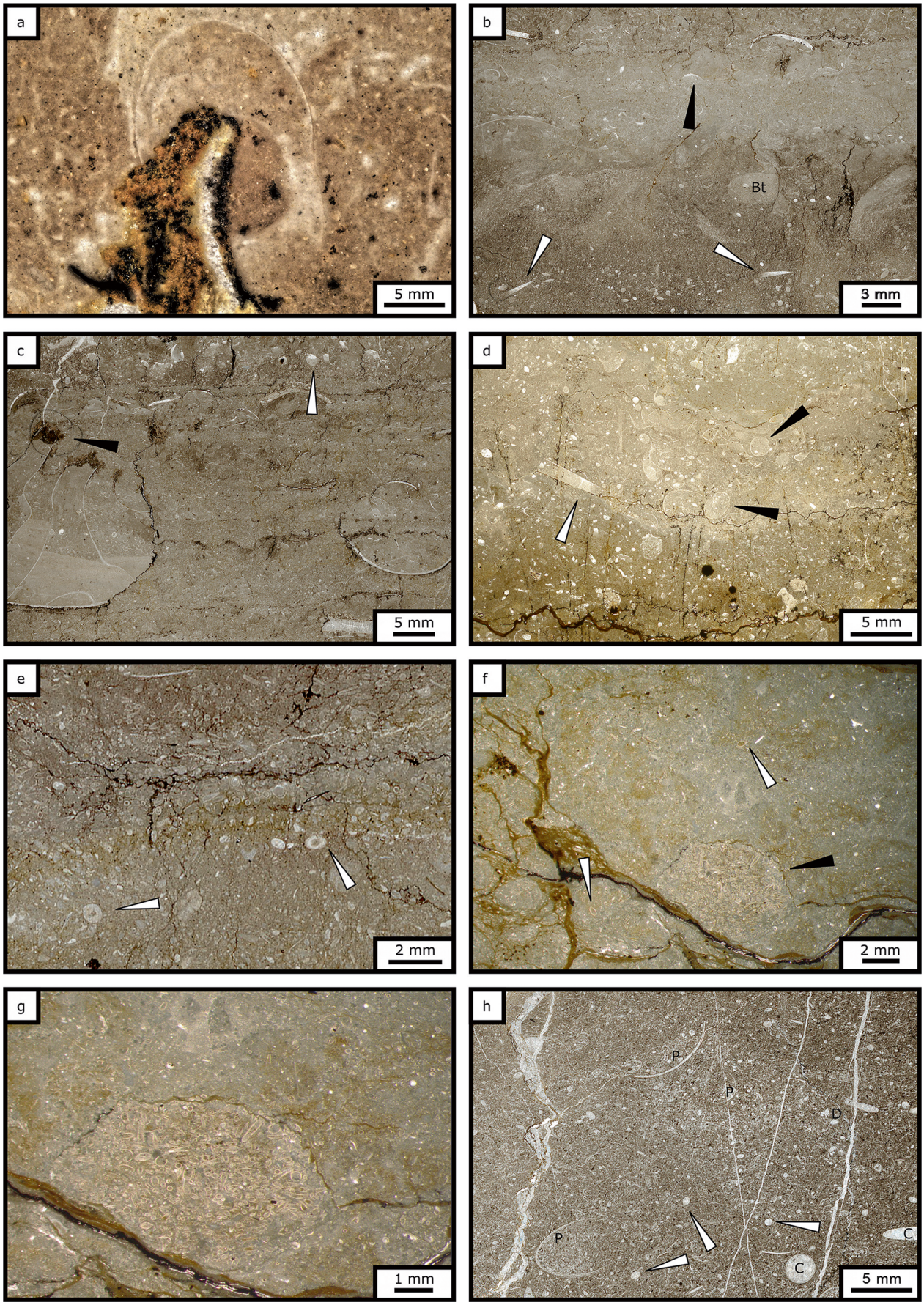
a
5 mm
b
Bt
3 mm
c
5 mm
d
5 mm
e
2 mm
f
2 mm
g
1 mm
h
P
P
D
P
C
C
5 mm

amounts of small styliolinids (Fig. 10e), sometimes found in distinctive packstone aggregates that show no current alignments (Fig. 10g). These grade without defined margins into wackestone areas and may represent coprolite remains. Associated are ostracods, thin-shelled bivalves, and poorly preserved crinoid debris.

Only in HON_1101, Bed -11 (at ca. 59.24–59.25 m), there is a subtype (**MF-C1***) with abundant small (ca. 0.1 mm in diameter), poorly preserved, circular cross-sections, interpreted as calcispheres (probably single-chamber foraminifers).

Interpretation: As typical for (hemi-)pelagic environments, photic zone organisms, such as hermatypic corals, stromatoporoids, algae, and other calcimicrobes, are absent. Instead, there is a dominance of pelagic plankton (dacryoconarids, entomozoans, unilocular foraminifers) and nekton (cephalopods). The pure micrite accumulation suggests that the current energy was low, but high enough to prevent the settling of large amounts of clay, which deposited at the same time in the adjacent Flinz basins (Fig. 3). Bioturbation and abundant agglutinating foraminifers reveal fully oxic, good living conditions on and within the upper substrate, sufficient for burying endobenthonic organisms of unknown affinities. Episodic mass occurrences of dacryoconarids suggest eutrophic facies, with relative shell enrichments during reduced micrite supply and deep-water bottom turbulence.

The classical microfacies model sensu Wilson (1975), which is based on the concept of Flügel (1972), was developed for Upper Triassic carbonate platforms. Therefore, we use the differentiated classification of Devonian (hemi-)pelagic to neritic carbonates of Hartenfels (2011). MF-C1 was deposited after the reef platform was transformed into a low-relief submarine rise. The calcisphere-rich variant MF-C1* indicates relative enrichments because of low sedimentation rates.

Distribution: Similar dacryoconarid packstones are known from pelagic ramp settings of Morocco (e.g. Aboussalam 2003; Rytina et al. 2013; Ward et al. 2013; Becker and Aboussalam 2013a), the Montagne Noire, southern France (e.g. Aboussalam 2003), and from pelagic submarine rises of the eastern Rhenish Massif (e.g. Stritzke 1989, 1990, his crinoid-tentaculite micrite facies; Aboussalam 2003).

MF-C2: Moderately organic-rich, mollusk wacke-packstone (Fig. 10b–c)

Examples: HON_1101, Sample -9b (58.80–58.94 m, **Upper Kellwasser level**), Bed -8 (58.40–58.50 m, lower Famennian); B102, Bed -16.

Description: MF-C2 is macroscopically a well-bedded, middle-grey limestone with macrofauna, such as cephalopods (orthocones and goniatites, Fig. 10c). There are no photic zone organisms. In thin-sections, a lamination is partly preserved by pyrite seams (Fig. 10c), partly destroyed by intervals of bioturbation, with distinctive burrows reaching from light-grey mud-wackestone intervals (MF-C4) into underlying darker layers that are richer in C_{org} (Fig. 10b). The micritic matrix is partially replaced by microsparite; peloids occur. There is a variable amount of small- to large-sized mollusk debris, including juvenile goniatites, without any sorting or gradation, and without current-controlled, "convex-up" embedding of curved shells. Ribbed bivalve fragments probably belong to buchiolids. Large cephalopods are partly filled by dense, layered micrite containing embryonic goniatite shells (Fig. 10c). Associated are common ostracods (smooth-shelled specimens and ribbed entomozoans), rare dacryoconarids and homoctenids, a few crinoid ossicles, and a single trilobite fragment. Repeatedly, large shell fragments exhibit traces of borings and beginning micritization. Fine iron mineralizations, originally probably pyrite, are dispersed. Iron oxide enrichments follow pressure solution contacts, former bedding planes, macrofossil margins, or occur in small nests. Sometimes blackish cauliflower microstromatolites encrusted skeletal remains (Fig. 10c), resembling *Frutexites*-type structures sensu Böhm and Brachert (1993). They were previously described by Préat et al. (2008), Hartenfels (2011), Jakubowicz et al. (2014), and Hartenfels and Becker (2016b), amongst others.

A variant without goniatites and with only very rare, probably reworked homoctenids occurs in the basal Famennian of HON_1101 (Bed -8). It is characterised by abundant gastropods, ostracods, fragmented mollusk shells and a few, sparite-filled, small orthocones.

Interpretation: MF-C2 represents an open marine, subphotic environment with abundant (hemi-)pelagic fauna (cephalopods, dacryoconarids, thin-shelled bivalves, conodonts, and entomozoans) deposited well below the storm wave base and under eutrophic conditions. Pyrite, which coats some bedding planes, and the alternating bioturbation suggest fluctuations between episodes of dysoxic and fully anoxic conditions. Some endofauna exploited the buried organic matter of underlying strata. The dominant shell fragmentation, lack of sorting by bottom currents, and original micrite matrix, normally evidence for calm deposition, are in contrast. Shell crushing occurred outside the area of deposition, with subsequent transport by occasional bottom currents. *Frutexites*-type structures have been regarded as typical for dysaerobic conditions (Préat et al. 2008) but Koptíková et al. (2010) and Hartenfels (2011) showed that they can also co-occur with a normal benthic fauna.

Distribution: MF-C2 differs from typical Rhenish Upper Kellwasser facies (Schindler 1990; Gereke 2007) but shows some similarity with the more peloidal, shallower Kellwasser facies developed on top of the microbial Wülfrath Reef (Becker et al. 2016b).

MF-C3: Recrystallized, organic-rich, peloidal, and bioclastic pack-grainstone (Figs. 10h, 11e, 11g (upper part))

Examples: HON_1101, Sample -15e (61.56–61.57 m, ***semichatovae* Event Interval**), Bed -12 (59.80–59.91 m,

Lower Kellwasser Limestone), base of Bed -9b (**basal Upper Kellwasser level**); B102, Bed -18 (7.14–7.24 m, ***semichatovae* Event Interval**).

Description: MF-C3 consists of dark-grey, organic-rich, fossiliferous limestone with goniatites (*Manticoceras* and *Sphaeromanticoceras*) and bivalves, such as *Buchiola*. In thin-sections, abundant, bivalved ostracods (smooth forms and ribbed entomozoans), orthoconic cephalopods with subspherical protoconchs (Orthoceratida or Bactritida), goniatites, rare (Fig. 10h) to moderately common (base of Fig. 10b) dacryoconarids and homoctenids, and thin-shelled bivalves lie in a recrystallized pack-grainstone matrix with peloids and masses of small mollusks (cephalopod-bivalve fragments). There is no size sorting or current orientation. Ostracods and mollusks are either filled by orthosparite or peloidal grainstone. Recrystallization transformed micrite into microspar or even pseudospar and affected also small bioclasts, such as crinoid debris and shell hash.

The microfacies of the basal Upper Kellwasser level of HON_1101 (base of Bed -9b) is transitional towards MF-C2 and MF-C5. The marly level with goniatites and large ostracods, sandwiched between black shales in B102 within Bed -18 (Fig. 11e), is intermediate between MF-C3 and MF-C6.

Interpretation: Recrystallization and the (hemi-)pelagic faunal assemblage, especially the entomozoans, cephalopods, and buchiolids, are typical for Kellwasser limestones of other sections (Schindler 1990). The local rarity of dacryoconarids in the Hönne Valley is distinctive. The high C_{org} content, abundance of fossils, and some pyrite indicate eutrophic conditions but the absence of lamination/weak bioturbation suggests that the facies was dysoxic, not anoxic. This agrees with the reworking of micrite as peloids, a sign of weak bottom turbulence.

Distribution: Gereke (2007) illustrated a Lower Kellwasser example with even higher fossil content from section Volkersbach in the southern Rhenish Massif ("Frankenbacher Schuppenzone"). There are also similarities with the very fossiliferous Kellwasser facies developed on the Tafilalt Platform of southern Morocco (Wendt and Belka 1991).

MF-C4: Mud-wackestone (Figs. 10a–b, 10d, 11a, 11b (lower and upper part), 11c–d, 11g (lower part))

Examples: HON_1101, Bed -2 (45.69–45.83 m), Bed -3 (48.15–48.21 m), Bed -4 (50.42–50.56 m), Bed -5 (52.95–53.05 m), Bed -7 (56.25–56.37 and 57.28–57.40 m), Bed -9a (58.97–59.08 m), Bed -11 (59.18–59.26 m), Bed -13 (60.40–60.53 m), Bed -14 (61.40–61.48 m), lower part of Bed -15 (61.75–71.90 m), top Bed -16; B102, base of Bed -18 (7.33–7.40 m), Bed -19 (7.40–7.42 m), Bed -24 (15.40–15.60 m); Beul, samples top 2 and top 3.

Description: Macroscopically, this facies type occurs as light- to middle-grey, beige, reddish, or yellowish-brown nodular and flaserlimestone, partly with cephalopods (orthocones) and fragmented shells. There is no debris of reefal fauna (in contrast to bioclastic wackestones of MF-B3). The colour reflects fluctuating contents and oxygenation levels of very fine iron-manganese pigments that occasional led to the formation of dendrites (Beul: Sample top 3). The dense, bioturbated micrite may contain thin, fragmented shells, orthoconic cephalopods, goniatites (gephuroceratids), gastropods, smooth ostracods, rare entomozoans, calcispheres/unilocular foraminifers (very abundant in Beul, Sample top 3, including *Parathurammina* and *Archaesphaera*), trilobites, gastropods (HON_1101, top Bed -16; Beul, Sample top 2), rare, small-sized deep-water Rugosa (HON_1101, Bed -19), and crinoid debris. Subordinate styliolinids and rare ribbed homoctenids occur only in Frasnian beds (e.g. HON_1101, Bed -14; B102, lower part Bed -18); these are transitional towards MF-C1. Especially larger shells show borings and a beginning micritization. Some thin-sections display *Frutexites*-type encrustations, thin silt layers (as a transition towards MF-C7), and mudclasts. The matrix is either micritic or microsparitic, with recrystallization spreading from bed boundaries or dissolution seams. Wide calcite veins were filled by blocky cement and were locally dolomitized. They are crossed by dark brownish stylolites, which may be associated with accumulations of pyrite grains, and younger, smaller calcite veins.

As an exception, the lower part of Bed -14 of HON_1101 is characterised by several irregular, dense accumulations of sponge spicule networks and calcispheres; the former are interpreted as remnants of deeper-water hexactinellid sponges.

Interpretation: This facies type represents a quiet and deep (hemi-)pelagic, subphotic palaeoenvironment well below the storm wave base. This is supported by bedding-parallel geopetals. *Frutexites*-type encrustions indicate very low sedimentation rates (Hartenfels and Becker 2016b). The presence of authigenic pyrite suggests local hypoxic conditions within the substrate, which, however, did not prevent the bioturbation. As normal in the Devonian, the burrowing organisms are not preserved; the very fine mud reflects an originally very soft substrate ("soupground", Etter 1995; Wetzel and Uchmann 1998). Mudclasts (e.g. Fig. 11b, lower right) can be formed by burrowing or by gravitational transport of weakly lithified lime mud on slopes.

Distribution: Hartenfels (2011) described equivalents of MF-C4 from the Famennian of adjacent Rhenish localities (Effenberg Quarry and Oese) as well as from Thuringia and the Wildenfelser Zwischengebirge (Saxothuringia), the Holy Cross Mountains (Poland), and the Maider and Tafilalt of SE Morocco. It corresponds to the "low component micrite facies" of Stritzke (1989, 1990: facies type II5), which was deposited on the submarine rise formed by the drowned Brilon Reef.

MF-C5: Ostracod Packstone (Fig. 11f)

Example: B102, middle Bed -14 (5.37–5.38 m).

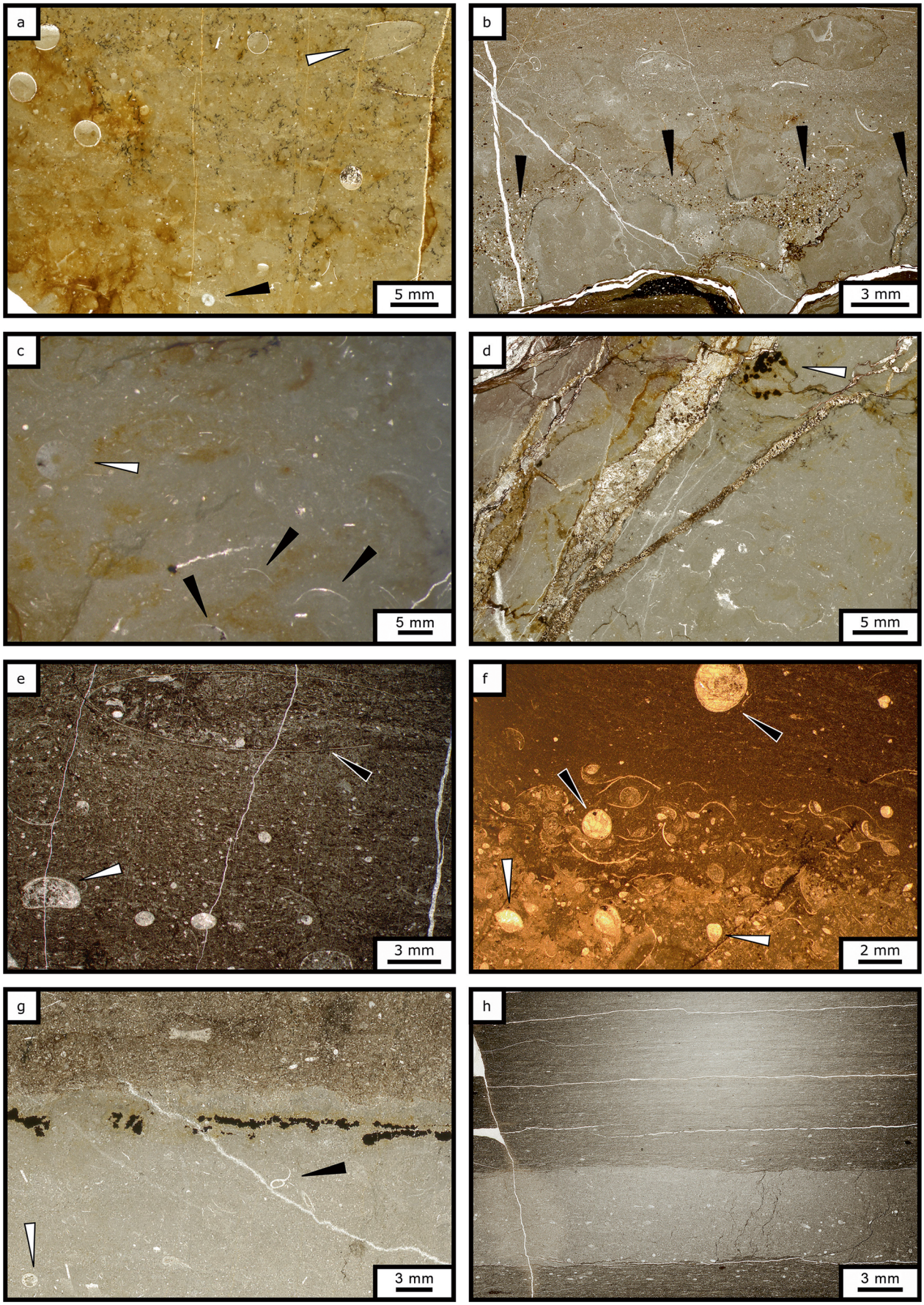
a
5 mm
b
3 mm
c
5 mm
d
5 mm
e
3 mm
f
2 mm
g
3 mm
h
3 mm

◀ **Fig. 11** Microfacies types of the Beul Formation. **a** MF-C4, bioturbated mud-wackestone with orthocones, goniatite (*white arrow*), crinoid ossicles (*black arrow*), fine iron-manganese mineralizations, and fine vertical sparite seams (B102, 2.10–2.17 m, Bed -3) **b** MF-C4 in the lower and upper parts, strongly bioturbated mud-wackestone with well-defined mudclasts, truncated in irregular burrows and pockets by MF-C7, silty mudstone to calcareous siltstone (*black arrows*), and at the top with MF-C8, fine-grained peloid packstone, which includes densely packed shell debris and rare larger shell fragments (HON_1101, 60.40–60.53 m, Bed -13) **c** MF-C4, bioturbated mudstone with fragmented pelecypods (*black arrows*), poorly preserved crinoids (*white arrow*), and dense micrite matrix (B102, 14.40–14.50 m, Bed -24) **d** Detail of the same MF and bed showing dolomitized branching veins and associated iron oxide mineralizations (*white arrow*) **e** MF-C3 transitional to MF-C6, argillaceous, strongly recrystallized, slightly peloidal mud-wackestone with unusually large-sized, partly ribbed ostracods (*white arrow*) and goniatites (crushed *Manticoceras*, *black arrow*) (B102, 7.14–7.24 m, Bed -18, *semichatovae* Event interval) **f** MF-C5, organic-rich ostracod packstone layer with geopetal fillings (*white arrows*) and bivalve debris, grading upwards into organic-rich, argillaceous mud-wackestone with rare ostracods and orthocones (*black arrows*) (B102, 5.32–5.38 m, Upper Kellwasser level, basal part of Bed -14) **g** MF-C4, light-grey, bioturbated mud-wackestone (Bed -15d) with broken shells, a minute gastropod (*black arrow*), and juvenile orthocone (*white arrow*), overlain above an undulating disconformity by a recrystallized detrital layer of partly organic-rich, flaser-bedded, microsparitized wacke-packstone (MF-C3, Sample -15e) with crinoid debris and dacryoconarids (HON_1101, 61.56–61.62 m, middle *semichatovae* Event Interval) **h** MF-C6, fine laminated, organic-rich shales with very thin sparite partings (beds -15f and -15h), interrupted with sharp boundaries by a light-grey, strongly micro- to pseudosparitic layer (Bed -15g) with small ostracods, shell hash and broken dacryoconarids (HON_1101, 61.52–61.56 m, upper *semichatovae* Event Interval)

Description: MF-C5 is restricted to a thin, dark-grey layer of marly limestone at the base of the Upper Kellwasser level in core B102. Below, in the upper part of Bed -15 (Fig. 10d), there is a transition from MF-C4 by bioturbated ostracod wackestones. Ostracods include ribbed entomozoans as well as smooth forms and are preserved as single or complete shells, the latter partly with geopetal fillings. Additional fauna ist represented by subordinate bivalves and orthocones.

Interpretation: An increased occurrence of ostracods instead of dacryoconarids or homoctenids and a higher amount of C_{org} differentiates MF-C5 from the dacryoconarid wacke-packstone of MF-C1. Ostracod blooms indicate eutrophication processes that favoured selective organism groups, which has previously been recognised within the Kellwasser Crisis Interval (Schindler 1990). But episodic primary condensation cannot be ruled out (Brett and Allison 1998). A slight increase in bottom currents may have reduced the clay and micrite accumulation (Aigner 1985; Schülke and Popp 2005; Hartenfels 2011), which is supported by partial shell disarticulation. Piper and Stow (1991) interpreted this kind of preservation as a result of distal turbidites or tempestites, respectively, but the pelagic setting was well below the storm wave base and, therefore, minor contourites intersecting the sea floor should be considered (see Hüneke et al., in prep.).

Distribution: A similar facies type was described from the Famennian by Hartenfels (2003: Franconia, 2011: Rhenish Massif, Thuringia, Wildenfelser Zwischengebirge of Saxony, southern Morocco). Schülke and Popp (2005) documented from the Beringhauser Tunnel, a volcanic submarine rise section south of the Brilon Reef, a similar MF named wrongly as "ostracod mud- to wackestone" (their MF 3b).

MF-C6: Laminated, organic-rich, black shale/argillaceous limestone (Fig. 11h)

Examples: HON_1101, samples -15a, -15c, -15f, -15h (between 61.51–61.75 m, ***semichatovae* Event Interval**); B102, within Bed -18 (7.14–7.24 m, probably ***semichatovae* Event Interval**), Bed -14 (5.32–5.37 m, **Upper Kellwasser level**).

Description: The macroscopic lamination of the C_{org}-rich, dark-grey to black marly shale or argillaceous limestone is evident in thin-sections. There is variation of the C_{org} content. Shales/marls with a higher amount of carbonate show diagenetic, small-scale flaser-lamination or microsparitization (B102, top of Bed -14). There are rare ostracods, bivalve shells, and some silt grains. Interbedded, but separated by sharp boundaries, are recrystallized (micro- to pseudospartic) and bioturbated mud-wackestones, variants of MF-C4, rarely of MF-C3 (Fig. 11g), including intermediate, marly variants (Fig. 11e).

Interpretation: Laminated, C_{org}-enriched marly shales represent phases of eutrophication (e.g. Murphy et al. 2000; Sageman et al. 2003) during transgressive pulses, which enabled by reduced bottom turbulence the settling of the clay fraction. The fine lamination and lack of bioturbation indicate anoxic conditions at the sea floor and within the sediment. Lighter, less organic-rich layers suggest fluctuations of nutrient influx and primary production. All organic matter is amorphous, which suggests blooms of cyanobacteria (e.g. Pacton et al. 2011). In Carboniferous deposits, the colonization of oxygen-depleted, organic-rich sediments has been described, amongst others, by Nyhuis and Amler (2013) and Nyhuis et al. (2014). Sharp upper boundaries of black shales, without exploration (bioturbation) from above, suggest that the mud was euxinic and could not be used as a resource after deposition.

Distribution: Gereke (2007) illustrated numerous equivalent black shales/marls from the Lower and Upper Kellwasser intervals of the eastern Rhenish Massif.

MF-C7: Silty mudstone/calcareous siltstone (Fig. 11b (parts))

Example: HON_1101, Bed -13 (60.40–60.53 m).

Description: Irregular fillings of burrows by variably abundant, moderately sorted silt grains consisting of quartz and iron minerals and intervening calcareous mud.

Interpretation: The silt accumulations probably formed originally a horizontal layer that was disarticulated by strong bioturbation. The unit records a locally rare and short influx

of non-clayey siliciclastics, probably from a rather distant source. The slightly increased depositional energy is in contrast with the fine calcareous matrix, which was not washed out. The weak sorting and rounding of the grains speak against transport as airborn particles.

Distribution: Siltstones are very rare in the upper Frasnian of the northern Rhenish Massif (e.g. Piecha 1993; Gereke 2007). They do not become more common before the eustatic regression at the end of the lower Famennian.

MF-C8: Peloidal and bioclastic packstone (Fig. 11b (top part))

Examples: HON_1101, within Bed -13 (at 60.40 and ca. 60.48–60.49 m).

Description: Thin intervals of abundant mud peloids with very fine skeletal detritus and some larger shells, such as smooth and ribbed bivalves. In the shown example (top Fig. 11b), the base is relatively sharp but upwards there is a gradation into bioclastic wackestone with trilobites and a juvenile, evolute goniatite with depressed cross-section (*?Ponticeras*), which conch is filled by fine micrite. Laterally, there is a 10 mm large mudclast that differs in its lithology from the rest of the unit. A second layer of MF-C8, again with a well-defined base, occurs at the top of Bed -13.

Interpretation: The sharp base, peloid formation by mud reworking, and detrital content suggest short intervals of slightly increased bottom currents. The mudclast may have been moved at the peak of turbulence. Since the biofacies below and above, supported by the pelagic goniatite, indicates overall conditions well below the storm wave base, we suggest deposition by minor bottom currents.

Distribution: Peloidal packstones deposited only rarely and episodically on the top of other pelagic submarine rises of the Rhenish Massif, both in the upper Frasnian and Famennian (e.g. Hartenfels 2011; Hartenfels et al. 2016).

Conodont stratigraphy (Fig. 12)

Drill core HON_1101 (Figs. 13, 14, 15, 16 and 17)

The lagoonal lower ca. 50 m of the borehole (Fig. 13, Bed -39 to top of Bed -31) were barren (11 samples taken). Above a deep weathered marly interval (Bed -30), which probably represents a fault zone, a productive sample was taken from near the top of a ca. 2 m thick interval of flaserlimestone (top Bed -29, at 107.20–107.42 m, Fig. 13). It yielded a deeper-water assemblage with *Pa. jamieae savagei* M2 (Fig. 14b), *Pa. ljaschenkoae* M2 (Fig. 14a), *Pa. hassi*, *Ag.* cf. *triangularis* (Fig. 14c), *Ad. nodosa* (Fig. 14d), *Po. paradecorosus*, *I. symmetricus* (Fig. 14e), and *"Oz."* aff. *nonaginta* (Fig. 14f). *Palmatolepis jamieae savagei* M2 enters in the *Pa. feisti* Zone/Subzone (MN Subzone 11a) of Martenberg (Saupe and Becker 2022, this issue.), where *Ag. triangularis* becomes common. Typical *"Oz." nonaginta* are not known from above the *Pa. housei* Zone (MN Zone 8, see Klapper et al. 1996).

The fault interval may also encompass Bed -28, which was not sampled. Above follow more than 20 m of typical reef limestones (Fig. 13, beds -27 to -20), the top part of the Asbeck Member. Nine samples from Bed -27 to the top of Bed -22 were barren. Conodonts, as open-water indicators of the Eisborn Member, commence at the base of Bed -21. Two samples (-21a at 83.30–83.51 and -21b at 82.49–82.75 m) yielded *Po. alatus* (Fig. 14g) and *Ad. rotundiloba* fragments; the latter are a clear indicator for the basal Frasnian (MN zones 1 or 2). Three samples from Bed -20 (-20a, 79.12–79.32 m, -20b, 79.03–79.10 m, -20c, 78.00–78.15 m) contained each different species (Fig. 13) that are all typical for lower Frasnian shallow-water facies. *Icriodus subterminus*, found in Sample -20c, does not range above the top of the lower Frasnian (Narkiewicz and Bultynck 2010).

From Bed -18 on, conodont faunas become diverse, belong to the pelagic *Palmatolepis* biofacies, and are partly so rich that we concentrate our report on the successive entry of biostratigraphic markers and unusual forms. At the base of Bed -18 (77.56–77.71 m), poorly preserved *Ad. nodosa* (Fig. 14h) and narrow relatives of *Pa. transitans*, possibly *Pa. keyserlingi*, appear. The first indicates the *Ad. nodosa* Zone of Becker and Aboussalam (in Pisarzowska et al. 2020), which base correlates with the top of the *Pa. transitans* Zone (top MN Zone 4). *Palmatolepis keyserlingi* was described by Kuz´min (1998) from the Lower Member of the Domanik Formation in the Timan, which falls in the *Pa. punctata punctata* Zone (MN Zone 5, House et al. 2000; regional *Po. efimovae-Pa. punctata* Zone of Ovnatanova and Kononova 2008). The next sample from the upper part of Bed -18 yielded *Pa. transitans,* juvenile *Ad. nodosa* that could be mistaken as representatives of older ancyrodellids (Fig. 14i), and both *Pa. punctata punctata* (Fig. 14j) and *Pa. punctata bohemica* (Fig. 14k). The latter is an alternative marker for the *Ag. primus* Zone (MN Zone 6; e.g. Klapper et al. 1996; Klapper 1997). Associated are a possibly new species of *Palmatolepis* (Fig. 14l) and a distinctive variant of *Z. ovalis* (Fig. 14m).

An *Ag. primus* with short, leaf-shaped side lobe occurs in Bed -17 (at 76.90–77.08 m), where it is associated with *Ad. lobata*, index species of the *Ad. lobata* Zone of Becker and Aboussalam (in Pisarzowska et al. 2020), which composite range begins near the top of the *Ag. primus* Zone (in the upper MN Zone 6, Klapper 1997). Sample -16a (at 76.80–

Fig. 12 Top-Givetian to lower middle Famennian chronostratigraphy, conodont zones, and their defining species (aligned to the left), selected index species that enable a further refinement (aligned to the right), and the position of global events. *Ad. Ancyrodella, Ag. Ancyrognathus, "Oz." "Ozarkodina", Po. Polygnathus, Pa. Palmatolepis, Sk. Skeletognathus*

chronostratigraphy	conodont zones/subzones		global events
middle Famennian	*Pa. marginifera utahensis*	Upp. *marginifera*	
	Pa. marginifera marginifera	Low. *marginifera*	
lower Famennian	*Pa. gracilis gracilis*	Upp. *rhomboidea*	Upp. Condroz
	Pa. rhomboidea	Low. *rhomboidea*	Low. Condroz
	Pa. glabra pectinata	Uppm. *crepida*	
	Pa. glabra prima	Upp. *crepida*	
	Pa. termini	M. *crepida*	
	Pa. crepida	Low. *crepida*	
	Pa. minuta minuta	Upp. *triangularis*	
	Pa. delicatula platys	M. *triangularis*	
	Pa. triangularis	Low.	
	Pa. subperlobata	*triangularis*	
upper Frasnian	*Pa. ultima*	MN 13c	
	Ag. ubiquitus		Upp. Kellwasser
	Pa. linguiformis	MN 13b	
	Pa. bogartensis	MN 13a	
	Ag. asymmetricus	top MN 12	Low. Kellwasser
	Pa. winchelli	MN 12	
	Pa. nasuta	MN 11b	*semichatovae*
middle Frasnian	*Pa. feisti*	MN 11a	
	Pa. plana	MN 10	
	Pa. proversa	MN 9	
	Pa. housei	MN 8	
	„Oz." trepta	MN 7	Upp. Rhinestreet
	Ag. primus	MN 6	Low. Rhinestreet
	Pa. punctata punctata	MN 5	
	Ad. nodosa	top MN 4	Middlesex
	Pa. transitans	MN 4	
lower Frasnian	*Ad. pramosica*	MN 3b	Timan
	Ad. alata		
	Ad. rugosa	MN 3a	
	Ad. rotundiloba rotundiloba	MN 2b	Genundewa
	Ad. rotundiloba soluta	MN 2a	
	Ad. rotundiloba pristina	MN 1	Lower Frasnes
upper Givetian	*Sk. norrisi*		Ense
	Po. dengleri dengleri		

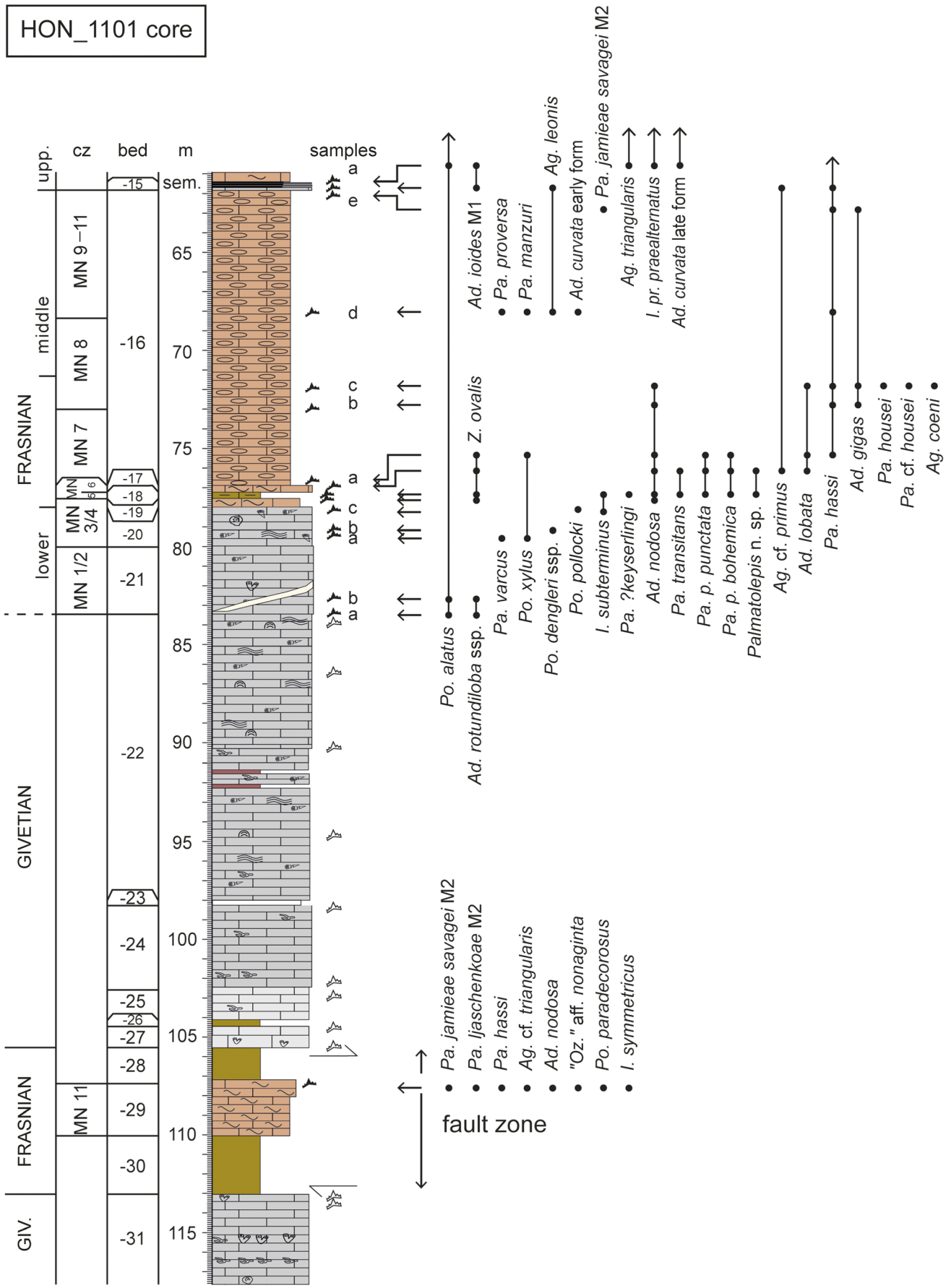
HON_1101 core
GIV.
FRASNIAN
GIVETIAN
FRASNIAN
upp.
middle
lower
cz
bed
m
samples
MN 11
MN 1/2
MN 3/4
MN 5/6
MN 7
MN 8
MN 9–11
-15
-16
-17
-18
-19
-20
-21
-22
-23
-24
-25
-26
-27
-28
-29
-30
-31
sem.
65
70
75
80
85
90
95
100
105
110
115
a
e
d
c
b
a
c
b
a
b
a
Po. alatus
Ad. rotundiloba ssp.
Z. ovalis
Ad. ioides M1
Pa. proversa
Pa. manzuri
Ag. leonis
Ad. curvata early form
Pa. jamieae savagei M2
Ag. triangularis
I. pr. praealternatus
Ad. curvata late form
Pa. jamieae savagei M2
Pa. ljaschenkoae M2
Pa. hassi
Ag. cf. triangularis
Ad. nodosa
"Oz." aff. nonaginta
Po. paradecorosus
I. symmetricus
fault zone
Po. xylus
Po. dengleri ssp.
Po. pollocki
I. subterminus
Pa. ?keyserlingi
Ad. nodosa
Pa. transitans
Pa. p. punctata
Pa. p. bohemica
Palmatolepis n. sp.
Ag. cf. primus
Ad. lobata
Pa. hassi
Ad. gigas
Pa. housei
Pa. cf. housei
Ag. coeni

◀ **Fig 13** Ranges of selected conodonts in the lower part of core HON_1101. For legend see Fig. 5; sample = bed numbers with lettered subdivisions

76.90 m) produced early, weakly ornamented *Pa. hassi*, the same *Z. ovalis* variant as below, and *Pa. punctata punctata* with a rather posterior position of the side lobe (Fig. 14n). In the absence of the index species, the base of the *"Oz." nonaginta* Zone (MN Zone 7) is not recognisable. Slightly higher, the entry of *Ad. gigas* s. str. (= *gigas* M3) in Sample -16b (at 72.90–72.98 m) suggests that the *Pa. housei* Zone (MN Zone 8) has been reached (see composite range of Klapper 1997). Accordingly, Sample -16c (at 71.75–72.28 m) yielded several variants of *Pa. housei* (Fig. 14o–p), a unusual specimen identified as *Pa.* cf. *housei* (Fig. 15a), and *Ag. coeni*, as an alternative zonal marker (Klapper 1997). Based on its index taxon (Fig. 15b), the *Pa. proversa* Zone (MN Zone 9) is identified in Sample -16d (at 67.90–68.28 m). Associated are, amongst others, *Pa. ljaschenkoae* (M2/3 sensu Saupe and Becker 2022, this issue; Fig. 15c), *Pa. manzuri* (Fig. 15d), which has been regarded as a variant of *Pa. amplificata* (Klapper and Kirchgasser 2016), the early form of *Ad. curvata* (Fig. 15f), and *Ag. leonis* (Fig. 15e). At the top of Bed -16 (Sample -16e, at 61.90–62.05 m), we found a *Pa. jamieae savagei* M2 (Fig. 15g) as indicator of the *Pa. feisti* Zone/Subzone (MN Subzone 11a, Saupe and Becker 2022, this issue), in association with *Ad. hamata*.

A next younger level at the middle/upper Frasnian transition (Fig. 16) is marked in the lower part of Bed -15 (at 61.75–61.90 m) by the onset of *Ad. ioides* M1 sensu Klapper (2021). Our sample provides evidence that *Ad. ioides* M1 enters within the *Pa. feisti* Subzone (MN Subzone 11a). The associated *Pa. punctata martenbergensis* does not extend above the *Pa. feisti* Zone (MN Zone 11; Saupe and Becker 2022, this issue). In Sample -14a (at 61.40–61.48 m), we found further *Ad. ioides* M1 (Fig. 15j), *I. praealternatus praealternatus* (Fig. 15h), and typical *Ag. triangularis* (Fig. 15i). The latter two species occur commonly in the *Pa. feisti* Zone (MN Zone 11) but their FADs are slightly older. Unfortunately, we obtained neither *Pa. feisti* nor any *Pa. nasuta*, which define the two subzones of the *Pa. feisti* Zone (Saupe and Becker 2022, this issue). At the top of Bed -14 (Sample -14b, 60.53–60.61 m), typical *Ad. ioides* and *I. alternatus alternatus* enter, indicative of the *Pa. winchelli* Zone (MN Zone 12; compare Klapper 1997; Hartenfels et al. 2016). The zonal index, *Pa. winchelli,* begins with Sample -13a (ca. 60.40–60.53 m), followed in Sample -13b (59.91–60.00 m) by *Pa. muelleri* and *Pa. orlovi*, which are typical for the same level in the Canning Basin of Western Australia (Klapper 2007).

Sample -12a is poor in *Palmatolepis* but rich in icriodids (sudden surge of *I. symmetricus*, *I. praealternatus praealternatus*, *I. vitabilis*, and *I. alternatus alternatus*), and polygnathids (sudden late appearances of juvenile *Po. capollocki* and *Po. zinaidae*), an ecostratigraphic pattern first noted in Lower Kellwasser beds of the Frasnian/Famennian boundary GSSP section at Coumiac (Klapper et al. 1993). We did not find the Lower Kellwasser level index species *Ag. asymmetricus*, but a late variant of *Ad. hamata* in which the secondary carinas of the side lobes rise and develop short free blades (Fig. 15k). The same feature is long-known from late forms of *Ad. curvata* (see Fig. 15l). In the upper part of Bed -12 (Sample -12b, at 59.33–59.42 m), there are abundant *Pa. bogartensis* (Morphotype B, Fig. 15m–n), the index species of the *Pa. bogartensis* Zone (MN Zone 13a). The thin interval of Bed -11 (with Sample -11a from the base and Sample -11b from 59.13–59.22 m) to Bed -10 represents the middle and upper parts of the *Pa. bogartensis* Zone (MN Zone 13a). Sample -9a (at 58.97–59.08 m) has a sparse fauna. Apart from several forms that are difficult to assign to one of the common terminal Frasnian species, we recognised *Pa. boogardi* and *Pa. beckeri* in a very rich assemblage of Sample -9b (at 58.80–58.94 m). *Palmatolepis beckeri* enters very late in the *Pa. bogartensis* Zone (top of MN Zone 13a) in its type section of Australia (Klapper 2007), just below the regional Upper Kellwasser equivalent (*Manticoceras guppyi* Bed, Becker et al. 1991). Sample -9c (at 58.68–58.80 m) yielded *Pa. beckeri* variants that are somewhat homeomorphic to the older *Pa. semichatovae*. *Palmatolepis linguiformis*, the index species of the top-Frasnian *Pa. linguiformis* Zone (= MN Zone 13b/c), was not found. It is long-known that it was rather facies sensitive and absent or very rare in several regions (Girard et al. 2005).

Between the top of Bed -9 and the base of Bed -8 (at 57.70–57.80 m), all Frasnian palmatolepids, ancyrodellids, and ancyrognathids disappear; only the *I. alternatus* Group continues locally. The association of *Pa. ultima* (Fig. 17a), *Pa. subperlobata* (Fig. 17o), intermediates between the two species (Fig. 15p), and *Pa. delicatula delicatula* characterises the basalmost Famennian *Pa. subperlobata* Zone/Subzone. However, the lower Famennian is strongly discontinuous since in Sample -7a (at 57.45–57.60 m), *Pa. subperlobata* (Fig. 17b) is outnumbered by *Pa. lobicornis* (Fig. 17c), associated with *Pa. delicatula platys* (Fig. 17d) and *Pa. regularis* (Fig. 17e). *Palmatolepis minuta minuta* dates the unit as *Pa. minuta minuta* Zone (former Upper *triangularis* Zone). This leaves just 10 un-sampled cm (57.60–57.70 m) for the *Pa. triangularis* Subzone and *Pa. delicatula platys* Zone (former Middle *triangularis* Zone).

The *Pa. crepida* (= Lower *crepida*) Zone is reached in Sample -7c (at 56.60–56.70 m), based on the FODs of *Pa. crepida* (Fig. 17f) and *Pa. minuta loba*, associated with *"Ag." sinelaminus* (Fig. 17g). Just slightly higher, in Sample -7d (at 56.45–56.56 m), the index species of the *Pa. termini* Zone (former Middle *crepida* Zone) enters. The same zone lasts through samples -7e to -6d (from 56.37–55.12 m). In Sample -6e (at 54.95–55.09 m), *Pa. glabra prima* M3 enters, the index of the *Pa. glabra prima* Zone (former Upper *crepida* Zone). The *Pa. glabra pectinata* Zone (former Uppermost *crepida* Zone) begins with Sample -3a

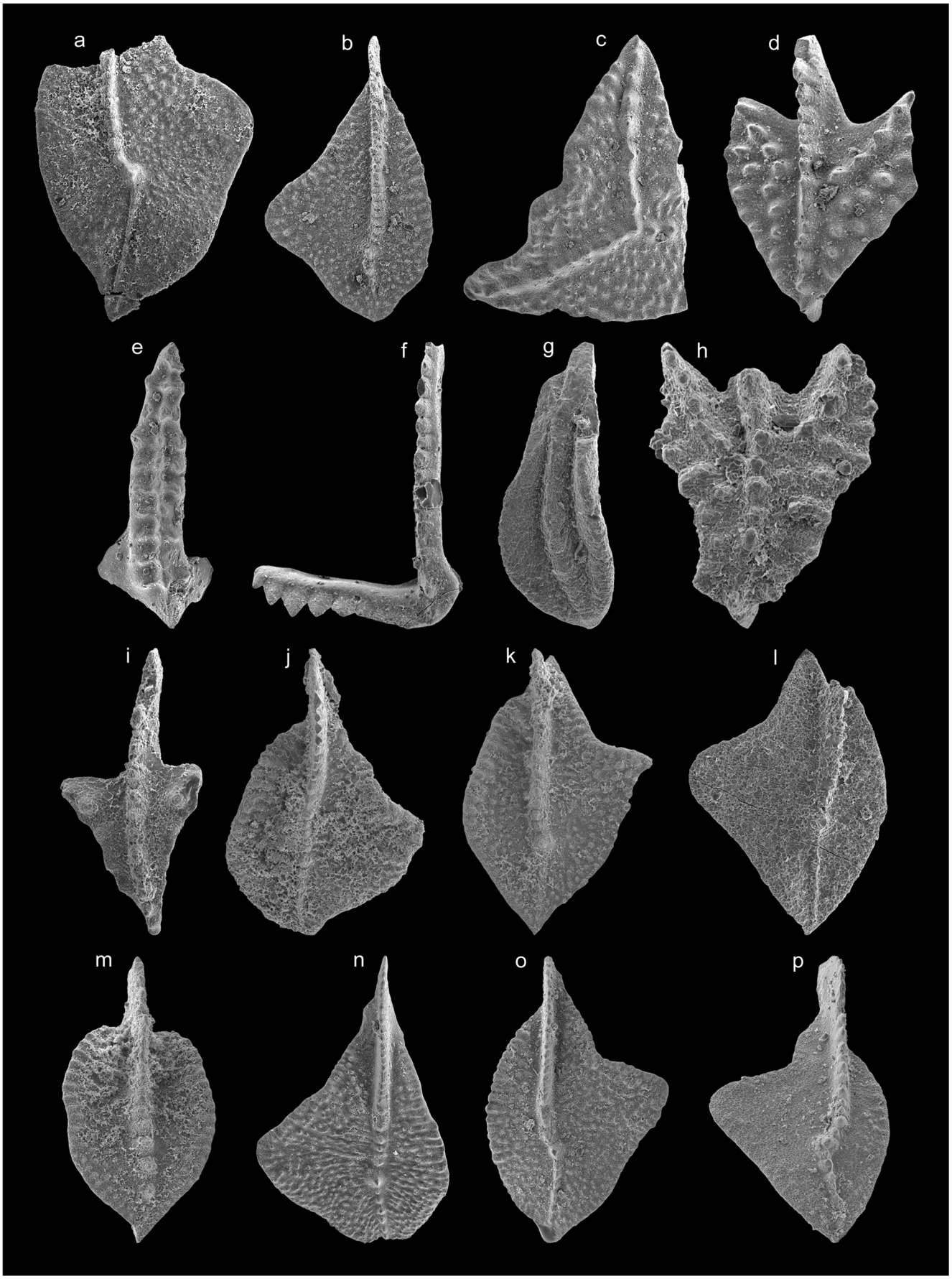
a
b
c
d
e
f
g
h
i
j
k
l
m
n
o
p

◀ **Fig 14** Conodonts from the upper Frasnian intercalation within the Asbeck Member (Bed -29) and the lower/middle Frasnian of the Beul Formation, core HON_1101; specimens B9A.14.1–16. **a** *Palmatolepis ljaschenkoae* M2, Bed -29, x 55 **b** *Pa. jamieae savagei* M2, Bed -29, x 45 **c** *Ancyrognathus triangularis* s.l., morphotype with wide platforms and without free blade, Bed -29, x 35 **d** *Ancyrodella nodosa*, Bed -29, x 60 **e** *Icriodus symmetricus* M1, Bed -29, x 50 **f** *"Ozarkodina"* aff. *nonaginta*, Bed -29, x 65 **g** *Polygnathus alatus*, Bed -21b, x 65 **h** *Ad. ?nodosa*, with ornament trend towards *Ad. gigas*, Sample -18a, x 90 **i** *Ad. nodosa* juv., resembling the older *Ad. rotundiloba pristina*, Sample -18b, x 80 **j** *Pa. punctata punctata*, Sample -18b, x 30 **k** *Pa. punctata bohemica*, Sample -18b, x 45 **l** *Palmatolepis* n. sp., small-sized, with straight carina, narrow platform, and shagreen ornament, Sample -18b, x 80 **m** *Zieglerina ovalis*, morphotype with pointed posterior platform, Sample -18b, x 40 **n** *Pa. punctata punctata*, variant with posteriorly shifted side lobe, Sample -16a, x 35 **o-p** *Pa. housei*, Sample -16c, x 40 and x 45, two variants

(at 49.15–49.30 m). Apart from *Pa. glabra pectina* M1, *Pa. arta* and *Pa. linguiloba* occur among several other species (Fig. 16). The zonal marker of the *Pa. rhomboidea* (= Lower *rhomboidea*) Zone enters in Sample -2a (at 47.98–48.13 m), together with the only local occurrence of *Pa. minuta subgracilis*. They are followed slightly higher, in Sample -2b (at 47.28–47.46 m), by *Pa. gracilis gracilis* that was used by Spalletta et al. (2017) to define their *Pa. gracilis gracilis* Zone at the top of the lower Famennian. The entry of *Br. ampla* in Sample -2c (at 47.05–47.28 m) confirms a previous oldest record from the Upper *rhomboidea* Zone of the Ardennes by Dreesen and Dusar (1975; see range discussion in Lüddecke et al. 2017, p. 597).

The first record for the basal middle Famennian was obtained from Sample -2e (at 45.69–45.83 m) and includes, amongst others, *Pa. marginifera marginifera* in association with *Pa. quadrantinodosa inflexa*, *Pa. quadrantinodosa inflexoidea*, *Pa. perlobata maxima*, and *Pa. glabra lepta* late morphotype. Due to a return to very low sedimentation rates, the *Pa. marginifera utahensis* Zone follows just above, in Sample -2f (at 43.50–43.65 m). There are both *Pa. marginifera marginifera* (Fig. 17h) and *Pa. marginifera utahensis* (Fig. 17i), which are rarely found together in Rhenish sections (Lüddecke et al. 2017). Associated late representatives of *Pa. quadrantinodosa inflexoidea*, Fig. 17j) confirm the previously controversial range overlap with *Pa. marginifera utahensis*.

Subsequently, two samples from the lower, ca. 5.5 m thick red marls (Bed -1, Hemberg Formation) were not productive. The upper ca. 43 m of the borehole consist of basinal marls and shales that are not calcareous enough for conodont sampling.

Drill core B102 (Figs. 18, 19, and 20)

The lagoonal lower ca. 87 m of core B102 have not been sampled for conodonts (Fig. 18). A sample from the debris interval at the top of the Hagen-Balve Formation, the local Eisborn Member interval (upper part of Bed -27), was barren and beds -26 and -25 could not be sampled.

Accordingly, the small amounts of dissolved core material of most B102 samples from the Beul Formation yielded only few conodonts. At the base, Sample -24f produced an assemblage with a fragmentary *Ag. amplicavus* (Fig. 19a), a specimen identified preliminarily as *Pa.* cf. *housei* (Fig. 19b), *Po. paradecorosus* (Fig. 19c), and *Ad. lobata*. The first enters at the base of the *"Oz." nonaginta* Zone (MN Zone 7, Klapper et al. 1996) while typical *Pa. housei* define MN Zone 8. Faunas representing the lower half of the middle Frasnian are missing. In Sample -24e, *Ad. lobata* (Fig. 19d) is associated with a *Pa.* cf. *plana* that appears to be transitional from *Pa. housei* (Fig. 19f). This gives some uncertainty whether the *Pa. plana* Zone (MN Zone 10) level has been reached. In Sample -24d, *Pa. hassi* with a short side-lobe (Fig. 19e) enters, associated with *Ad. gigas*. The middle/upper part of Bed -24 is conodont-poor. Sample -24c yielded another *Ad. gigas* (Fig. 19g), Sample -24b an incomplete specimen with short side lobe identified as *Ag.* aff. *barbus*; typical *Ag. barbus* are not known from above the *Pa. housei* Zone (MN Zone 8; Klapper 1997).

Bed -22 yielded a sparse fauna with *Pa. kireevae* (Fig. 19h) and *Ad. nodosa*, showing a trend towards *Ad. ioides*, but not yet as strong as in *Ad. ioides* M1 sensu Klapper (2021; Fig. 19i). The first taxon ranges from the upper part of the *Pa. housei* Zone (MN Zone 8) into the lower part of the *Pa. winchelli* Zone (MN Zone 12, Klapper et al. 1996). Above a black shale unit, higher parts of Bed -18 yielded many juveniles of *Po. webbi*, *Po. alatus*, *Po. politus*, *I. alternatus alternatus*, *Bel. resima*, *Ad. nodosa*, *Palmatolepis* sp., and *Ad. ioides* s. str. (Fig. 19j). The latter indicates the *Pa. winchelli* Zone (MN Zone 12, e.g. Klapper 2007) but its index species does not occur; the precise relationships of the FODs of *Pa. winchelli* and *Ad. ioides* s. str. require refinements. Among larger specimens, there are well-preserved *Ag. triangularis* (Fig. 19k), several *Pa. nasuta*, rare *Pa.* cf. *mucronata*, and *Pa. uyenoi* (Fig. 19l). The latter species occurs both in MN Zone 11 and 12 (Klapper 2007, p. 529). After a short interruption by core loss, the fauna from higher parts of Bed -16 includes a questionable *Ag. tsiensi* (Fig. 19m), the late morphotype of *Ad. curvata* (Fig. 19n), *Pa. muelleri*, and questionable *Pa. rhenana*. *Palmatolepis nasuta* continues from below (Fig. 190). *Ancyrognathus tsiensi* (sensu the holotype) and the closely related *Ag. asymmetricus* have similar lower ranges in the "upper *rhenana* Zone" (Sandberg et al. 1992, p. 58; high in MN Zone 12). *Palmatolepis muelleri*, which was also found in Bed -15 (Fig. 19p), ranges from the *Pa. nasuta* Subzone (middle MN Zone 11) to the upper *Pa. winchelli* Zone (MN Zone 12; Klapper et al. 1996). The upper part of Bed -15 yielded a variant of *Ag. iowaensis* with narrow platform (Fig. 20a). Typical *Ag. iowaensis* do no reach the top of MN Zone 12 in the Iowa Basin (Day and Witzke 2017). The incompletely preserved top of the Frasnian provided no conodont faunas of the *Pa. bogartensis* (MN Zone 13a) and *Pa. linguiformis* (MN zones 13b/c) zones.

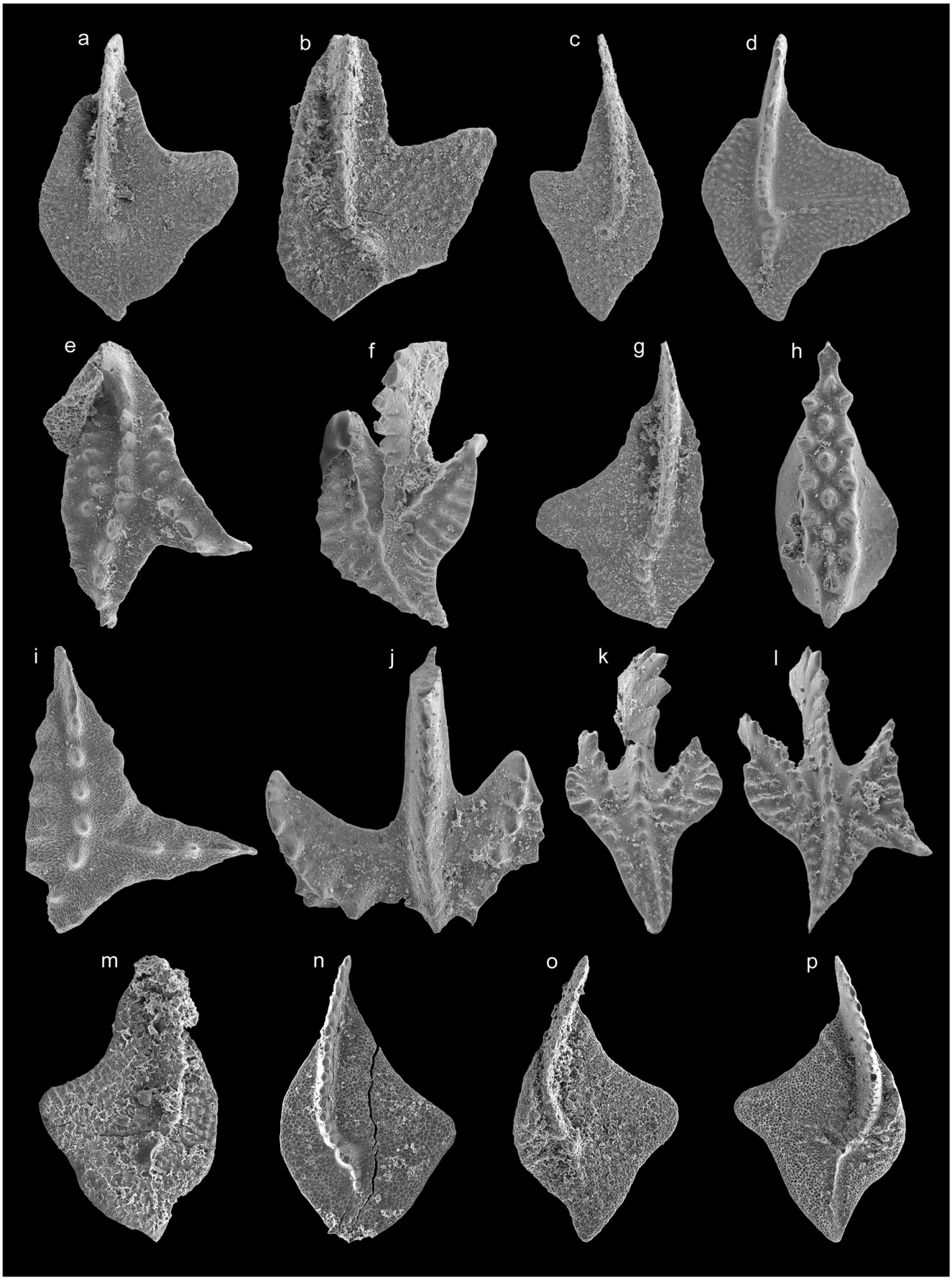
a
b
c
d
e
f
g
h
i
j
k
l
m
n
o
p

◀ **Fig 15** Conodonts from the higher middle Frasnian to basal Famennian of core HON_1101, specimens B9A.14.17–32. **a** *Palmatolepis* cf. *housei*, form grading towards *Pa. proversa* and *Pa. semichatovae*, Bed -16c, x 40 **b** *Pa. proversa*, Sample -16d, x 65 **c** *Pa. ljaschenkoae*, intermediate between M2 and M3, Sample -16d, x 55 **d** *Pa. manzuri*, Sample -16d, adult, x 30 **e** *Ancyrognathus leonis*, Sample -16d, x 65 **f** *Ancyrodella curvat*a, early form, Sample -16d, x 45 **g** *Pa. jamieae savagei* M2, Sample -16e, x 40 **h** *Icriodus praealternatus praealternatus*, juvenile, Sample -14a, x 95 **i** *Ag. triangularis*, typical form, Sample -14a, x 80 **j** *Ad.* cf. *ioides* M1 sensu Klapper 2021, fragmentary, Sample -14a, x 65 **k** *Ad. hamata*, late form with short, secondary free side blades, Sample -12a, x 50 **l** *Ad. curvata*, late form, sample -12a, x 50 **m** *Pa. bogartensis* Morphotype B, Sample -12b, x 55 **n** *Pa. bogartensis* Morphotype B, juvenile with different posterior platform outline, Sample -12b, x 90 **o** *Pa. subperlobata*, top Bed -8, x 65 **p** *Pa. subperlobata* with some nodes on the inner anterior platform, transitional from *Pa. ultima* (see Klapper et al. 2004, p. 382), top Bed -8, x 65

It is intriguing that lower Famennian samples of core B102 are in general richer than samples from Frasnian strata. The assemblage of Bed -13, with *Pa. ultima*, *Pa. triangularis* (M2, including *Pa. praeterita*, Fig. 20b), narrow *Pa. subperlobata* (Fig. 20c), *Pa. canadensis*, *Pa. delicatula delicatula*, *"Ag." sinelaminus, I. alternatus alternatus*, *I. alternatus helmsi*, *Ct. brevilaminus*, and *Po. procerus*, is typical for the basal, but not basalmost Famennian (*Pa. triangularis* Subzone, upper part of former Lower *triangularis* Zone; compare Schülke 1995; Spalletta et al. 2017). In Bed -12, transitional forms towards *Pa. lobicornis* appear and there is *Pa. triangularis* s. str. (= M1). The FOD of *Pa. clarki* in Bed -11 proves that the former Middle *triangularis* Zone (= *Pa. clarki* Zone sensu Hartenfels et al. 2016 and *Pa. delicatula platys* Zone sensu Spalletta et al. 2017) has been reached. Some specimens show first morphological trends towards *Pa. minuta minuta*. The assemblage of Bed -10 is similar apart from the FOD of *I. cornutus*, which is known from higher parts of the *Pa. delicatula platys* Zone (e.g. Sandberg and Dreesen 1984; Schülke 1995). Bed -8 still has basal Famennian taxa, such as *Pa. ultima* (Fig. 20d), *Pa. triangularis* (M2), *Pa. delicatula delicatula* (Fig. 20e), and a fragmentary *I. alternatus mawsonae* (Fig. 20f). In Bed -5, *Pa. lobicornis* (Fig. 20g) and *Pa. regularis* (Fig. 20h) are present, which enter both in the upper part of the *Pa. minuta minuta* Zone (= Intervall 2 of the Upper *triangularis* Zone sensu Schülke 1995). Associated is a juvenile identified as *I.* cf. *alternatus* (Fig. 20i).

All of the subsequent Famennian to upper Tournaisian is missing in a long gap below cherts of the Hardt Formation (beds -1 and 0).

Beul outcrop (Figs. 21, 22, and 23)

The preliminary outcrop conodont biostratigraphy was outlined in Becker et al. (2016c) but further sampling requires updates, especially a shift of the position of the Givetian/Frasnian boundary. Samples from the Eisborn Member mostly have a very low conodont yield, often less than 5 Pa elements (mostly polygnathids) per kg of limestone. A few richer samples (ca. 15–20 Pa elements/kg) indicate deepening intervals. The nodular limestones of the Beul Formation are much richer, partly with several hundred of Pa elements in a normal-sized (2–3 kg) sample, but many specimens are juveniles. The complete local species ranges are given along the section log in Fig. 21. Since published conodont data are very scarce for Frasnian Rhenish reef facies and directly overlying strata, abundances are compiled in Tables 2 and 3.

Four samples from the thick lowest bed (Bed B1) yielded almost exclusively small numbers of *Po. alatus,* which normally does not occur before the topmost Givetian *Sk. norrisi* Zone (Aboussalam and Becker 2007). The associated single *Po. paradecorosus* represents a species that enters at the same level. Loose slabs with brachiopods, laminar stromatoporoids, and rare trilobites yielded the same almost monotypic fauna. A slight increase of polygnathid diversity in beds B3 to B5 is caused by local late entries of long-ranging middle/upper Givetian to lower Frasnian species, such as *Po. varcus* and *Po. dubius*, in association with *Po. alatus* (Fig. 22c). Two *Ad. rotundiloba pristina* date Bed B3 as basal Frasnian *Ad. rotundiloba pristina* Zone (MN Zone 1). Previously, the first record was from Bed B11 (Becker et al. 2016c), resulting in a significant downwards shift of the local Upper Devonian base. Since the larger specimen (Fig. 22d–e) displays an advanced morphology (high number of platform nodes combined with a very large basal cavity), the Frasnian base may lie even slightly lower. Beds B6 to B10b have mostly the same poor assemblages as at the section base, apart from curved variants of *Po. dengleri sagitta*. The subspecies enters in southern Morocco in the upper Givetian but ranges into the basal Frasnian (Aboussalam and Becker 2007). A more advanced ancyrodellid with 28 platform nodes, identified as *Ad. rotundiloba soluta*, enters in Bed B10c (Fig. 22f–g) and indicates the base of the *Pa. rotundiloba rotundiloba* Zone (*Pa. rotundiloba soluta* Subzone, MN Zone 2a). It is associated with *Po. pollocki*, which is a typical lower Frasnian species. Entries of *Po. pennatus* and *Po. webbi* in Bed B11 represent further facies-controlled delayed FODs. A single *Zieglerina* from Bed B11 (Fig. 22h-i) represents a new species (*Zieglerina* n. sp. B).

Icriodids, which normally characterise shallow-water limestones, appear suddenly in Bed B13a. The locally oldest *I. subterminus* and *I. symmetricus* represent delayed entries (see icriodid zonation of Narkiewicz and Bultynck 2010). Subsequent beds were difficult to sample in the steep cliff; the small-sized samples retreived proved to be conodont-poor. In thin-bedded limestones at the top (beds E1 and E3), faunas become richer. Specimens of *Po. dengleri dengleri* from Bed E1 (Fig. 22j) with an incipient anterior platform collar are transitional towards *Po.* cf. *dengleri* sensu Aboussalam et al. (2020, fig. 20.10) that occurs in the top-lower Frasnian of Morocco. There is the late record of an ancestral looking anyrodellid (Fig. 22k) that is morphologically intermediate between *Ad. rotundiloba pristina* and *Ad. binodosa*. Some *Po. dubius* (Fig. 22o), *Po. paradecorosus* (Fig. 22p), *Po. xylus*, *I. symmetricus* M2 sensu Saupe and Becker (2022,

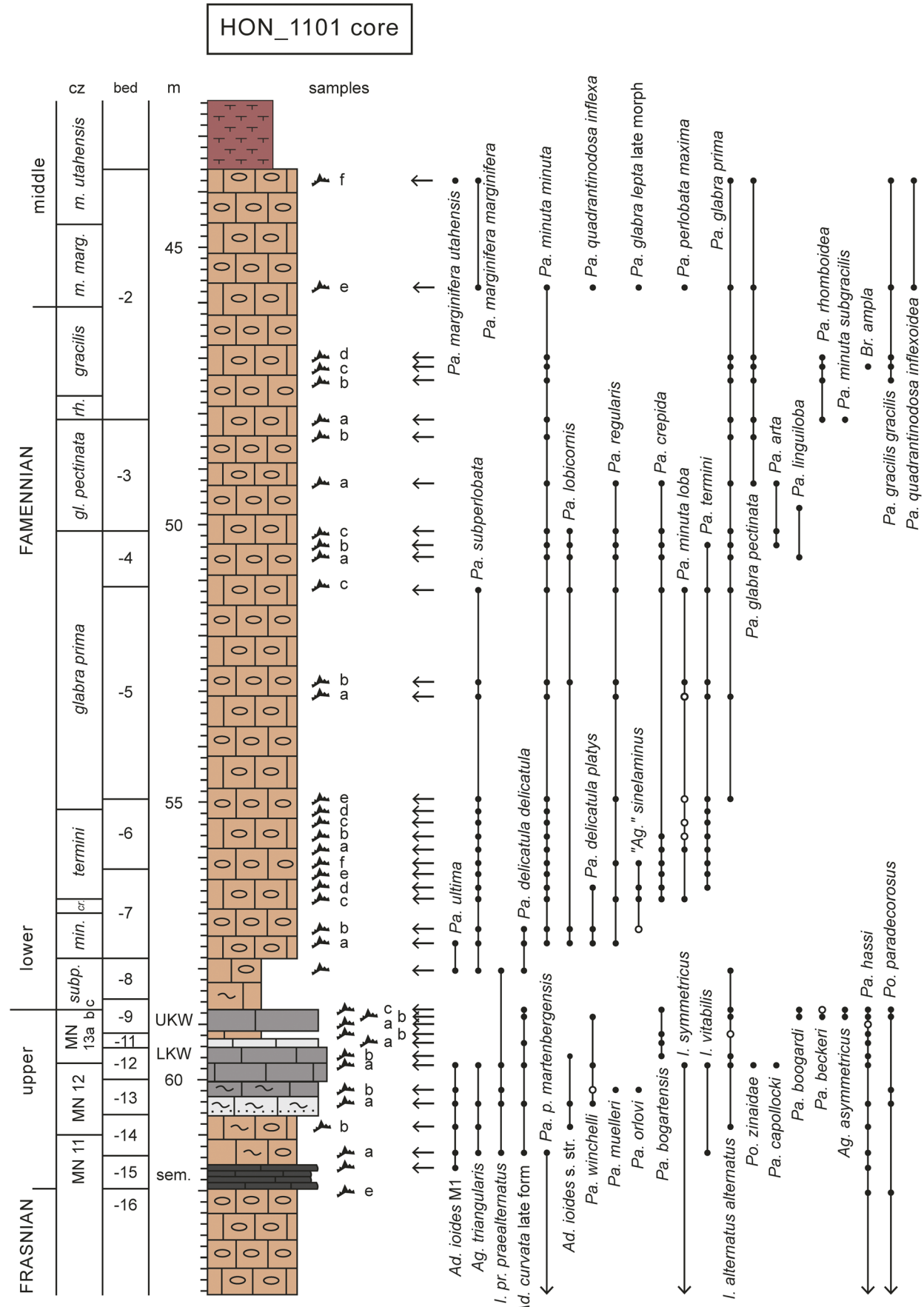
HON_1101 core
FRASNIAN
FAMENNIAN
upper
lower
middle
cz
bed
m
samples
MN 11
MN 12
MN 13a
subp.
min.
cr.
termini
glabra prima
gl. pectinata
rh.
gracilis
m. marg.
m. utahensis
sem.
LKW
UKW
Ad. ioides M1
Ag. triangularis
I. pr. praealternatus
Ad. curvata late form
Ad. ioides s. str.
Pa. winchelli
Pa. muelleri
Pa. orlovi
Pa. bogartensis
I. symmetricus
I. vitabilis
I. alternatus alternatus
Po. zinaidae
Pa. capollocki
Pa. boogardi
Pa. beckeri
Ag. asymmetricus
Pa. hassi
Po. paradecorosus
Pa. p. martenbergensis
Pa. ultima
Pa. subperlobata
Pa. delicatula delicatula
Pa. delicatula platys
"Ag." sinelaminus
Pa. minuta loba
Pa. termini
Pa. glabra pectinata
Pa. arta
Pa. linguiloba
Pa. minuta minuta
Pa. lobicornis
Pa. regularis
Pa. crepida
Pa. marginifera utahensis
Pa. marginifera marginifera
Pa. quadrantinodosa inflexa
Pa. glabra lepta late morph
Pa. perlobata maxima
Pa. glabra prima
Pa. rhomboidea
Pa. minuta subgracilis
Br. ampla
Pa. gracilis gracilis
Pa. quadrantinodosa inflexoidea

◀ **Fig 16** Ranges of selected conodonts in the upper Frasnian to middle Famennian of core HON_1101. For legend see Fig. 5; *cz* conodont zones (see Fig. 12), sample = bed numbers with lettered subdivisions, open dots indicate uncertain identifications

this issue), and *I. subterminus* (Fig. 22m) are associated with a single, last *I. difficilis* (Fig. 22n). This species is normally restricted to the Givetian (e.g. Narkiewicz and Bultynck, 2010, fig. 10) but Bultynck (2003, fig. 2) noted a questionable lower Frasnian range in North America.

Several *Ad. recta* (Fig. 22r) date Bed E3 as upper part of the *Ad. rotundiloba rotundiloba* Zone (MN Subzone 2b, Table 3; see lower range of *Ad. recta* in Kralick 1994). Associated are six species of *Polygnathus*, including a re-appearance of *Po. webbi* (Fig. 22q). The final, poorly exposed coral biostrome yielded hardly any conodonts during several initial sampling trials, a typical feature of reefal facies. A single *Mes. guanwushanensis* (Fig. 22s) represents a new morphotype, M3 (see taxonomic notes). In southern Morocco, the same form reaches the basal middle Frasnian *Pa. punctata punctata* Zone (MN Zone 5, Becker and Aboussalam 2013b) but it is more common in the lower Frasnian. A later sample from coral floatstone (Sample "top reef") turned out to be relatively rich in *Pa. paradecorosus*, including specimens with rather long free blade (compare *Po.* aff. *paradecorosus* of Aboussalam et al. 2020). Associated are a single *I. cedarensis*, a long-ranging species (Narkiewicz and Bultynck 2010), and *Po. dengleri dengleri*. The latter taxon is not known from above the top of the lower Frasnian (top of *Pa. transitans* Zone, see composite range in Klapper 1997; Gouwy et al. 2007). This constrains the youngest age.

The first conodont sample from the lower Beul Formation ("top 2", lower sample from Bed top 2-3 in Fig. 21) yielded a flood of juvenile palmatolepids and *Pa. housei* (Fig. 22t), the index species of the *Pa. housei* Zone (MN Zone 8) in the upper part of the middle Frasnian. Associated are *Pa. punctata martenbergensis*, which is long-ranging in the middle Frasnian, *Po. pennatus* (Fig. 22u), questionable *Ad. lobata* (Fig. 22v), and *Ag. amplicavus* (Fig. 22w), which ranges from MN Zone 7 (*"Oz." nonaginta* Zone) to the base of MN Zone 10 (*Pa. plana* Zone, Klapper et al. 1996). The index species of MN Zone 7, *"Oz." nonaginta,* occurs abundantly (Fig. 23a);

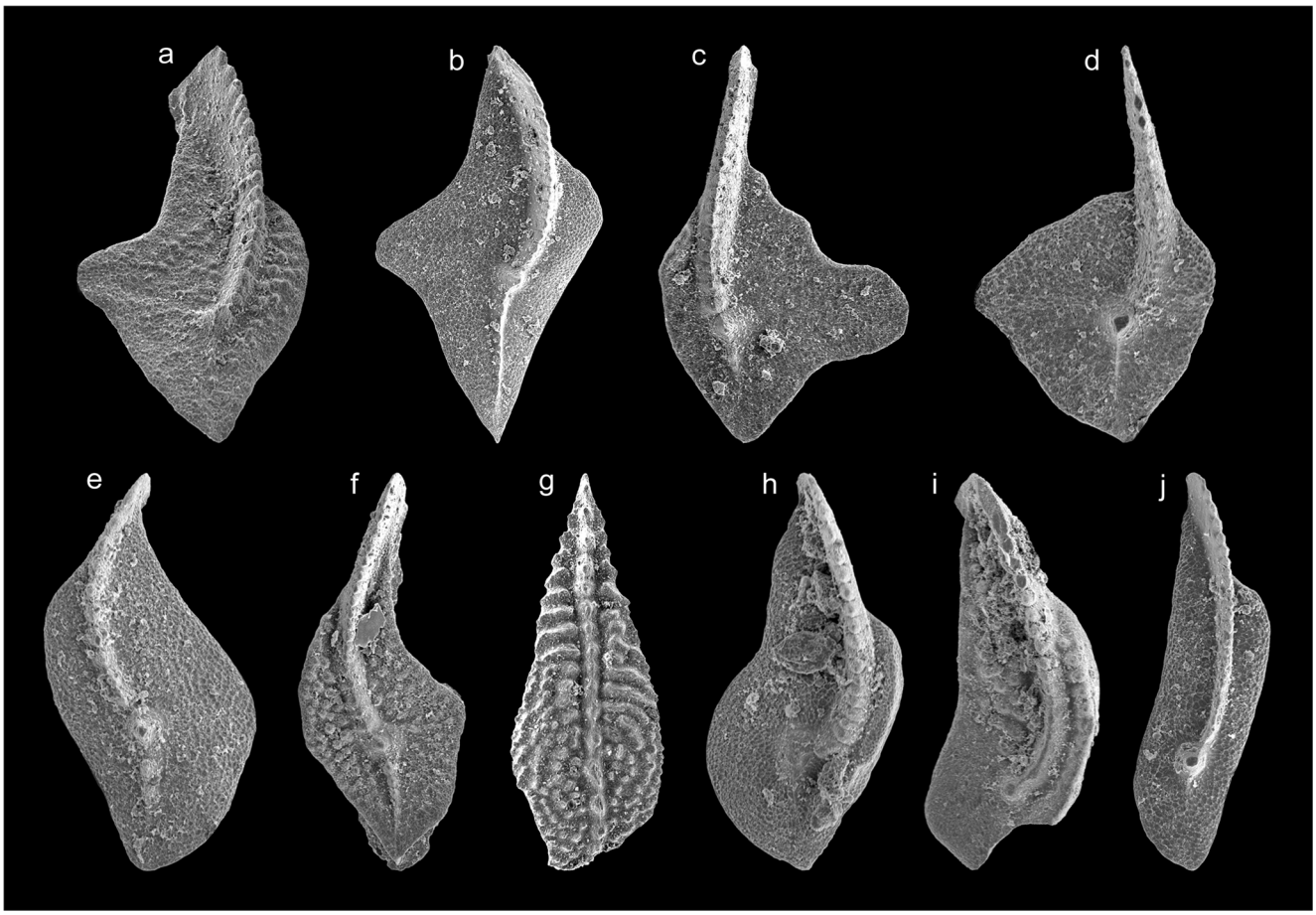

Fig 17 Conodonts from the lower and middle Famennian of core HON_1101, specimens B9A.14.33–43. **a** *Palmatolepis ultima*, top Bed -8, x 70 **b** *Pa. subperlobata*, elongate variant, Sample -7a, x 65 **c** *Pa. lobicornis*, Sample -7a, x 65 **d** *Pa. delicatula platys*, Sample -7a, x 105 **e** *Pa. regularis*, Sample -7a, x 105 **f** *Pa. crepida*, Sample -7c, x 50 **g** *"Ancyrognathus" sinelaminus*, Sample -7c, x 30 **h** *Pa. marginifera marginifera*, Sample -2f, x 90 **i** *Pa. marginifera utahensis*, Sample -2f, x 70 **j** *Pa. quadrantinodosa inflexoidea*, Sample -2f, x 85

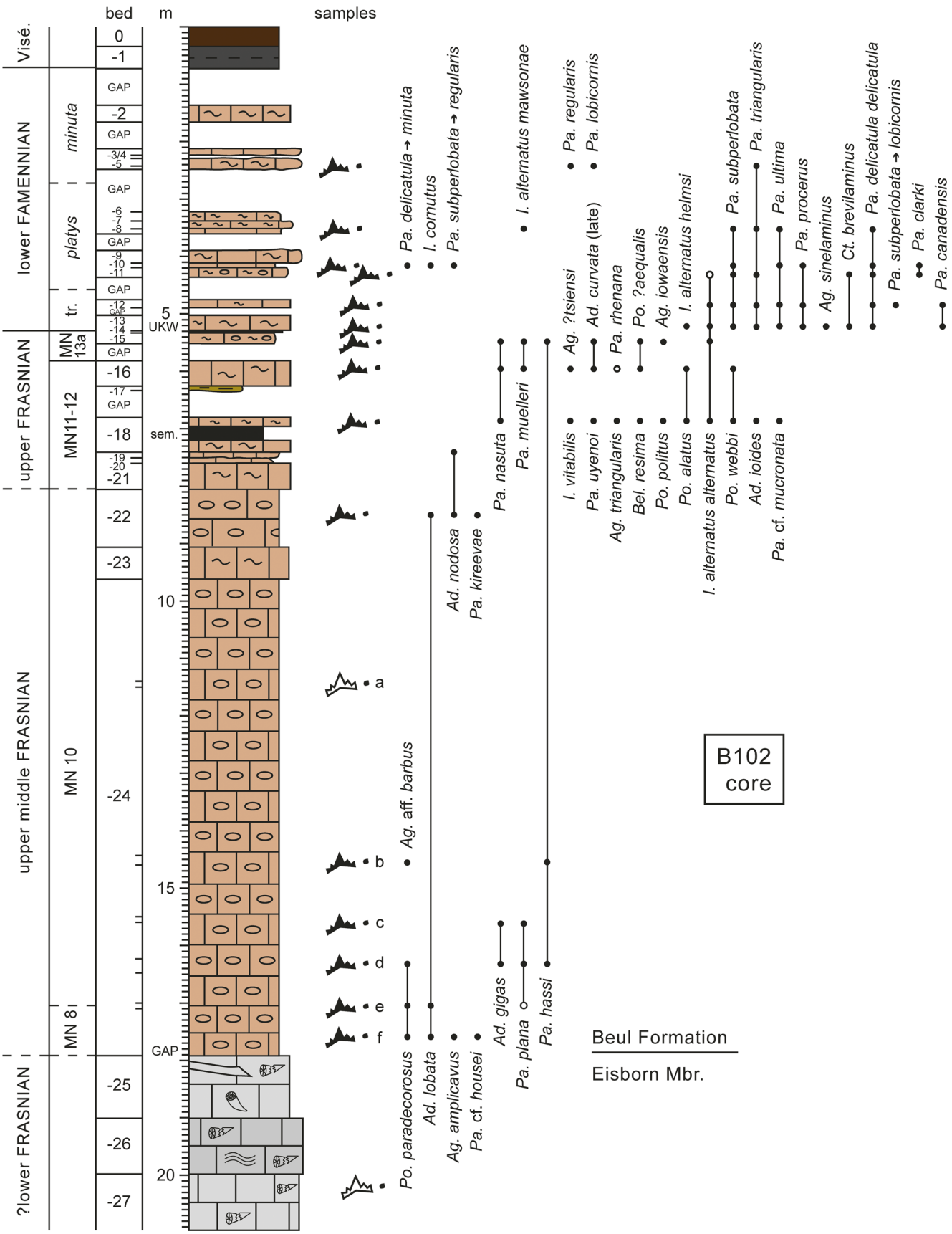

Fig. 18 Ranges of conodonts, conodont zonation, and lithology of core B102. For legend see Fig. 5; sample = bed numbers with lettered subdivisions, open dots indicate uncertain identifications

in the Timan it is also known from the *Pa. housei* Zone (MN Zone 8, Klapper et al. 1996).

Apart from typical *I. symmetricus*, there is a curved related form, named as *I.* cf. *tafilaltensis* (Fig. 23b), and a polygnathid with flat, weakly nodose platform, a rare morphology in middle Frasnian strata (*Polygnathus* sp., Fig. 23c). Although only two species of *Palmatolepis* are identified, there are three types of *Nothognathella* ("sp. 1–3", Fig. 23d–f), the supposed Pb element of the genus. A distinctive feature of the fauna is the relative abundance of a form resembling the mostly Givetian *Po. varcus*, preliminary identified as *Po.* aff. *varcus* (Fig. 23g).

Sample "top 3-1" (middle sample from Bed top 2-3 in Fig. 21) yielded a typical assemblage of the *Pa. plana* Zone (MN Zone 10), including its index species and *Pa. ljaschenkoae* M3. There are two unusual "ozarkodinids", a possible homeomorph of the Givetian *"Oz." plana* (Fig. 23h) and a specimen identified as *"Oz."* aff. *sannemanni* (Fig. 23i). Typical *"Oz." sannemanni* have not yet been described from the middle Frasnian (see upper range in Narkiewicz and Bultynck 2010). Sample "top 3-2" (upper sample from Bed top 2-3 in Fig. 21) produced a more divers palmatolepid assemblage, including *Pa. hassi*, *Pa. plana*, *Pa. ljaschenkoae*, *Pa. proversa*, *Pa. adorfensis* (Fig. 23j), and *Pa. jamieae savagei* M2 (Fig. 23k). The latter two taxa enter at Martenberg in the eastern Rhenish Massif also in the *Pa. plana* Zone (Saupe and Becker 2022, this issue). The composite range of *Avignathus decorosus*, locally represented by a single typical Pb element, begins accordingly in the *Pa. plana* Zone (MN Zone 10; Klapper 1997).

Other stratigraphic markers of the Beul Formation

Shark teeth of the basal Beul Formation of the outcrop belong to *Phoebodus latus*, which is known from the higher middle Frasnian of the Urals, and *Ph. fastigatus* (Fig. 22a–b), which ranges from the Givetian to the upper Frasnian (Ginter and Ivanov 2000). Both species have previously not been reported from the Rhenish Massif (see recent review by Ivanov 2021).

The presence of mesobeloceratids in the oldest Beul Formation of the outcrop, typical for UD I-G_2, agrees with the middle Frasnian conodont age (Becker and House 2009). The slightly younger *Beloceras* is long-known from slightly higher cliffs (e.g. Becker et al. 2016c). Beloceratidae are usefor for water depth calculations (Hewitt 1996).

Comments on the reefal macrofauna

The cores of the Asbeck Member yielded typical stromatoporoids of Givetian and Frasnian lagoonal facies, such as *Stachyodes (St.) costulata* Lecompte, 1952, *St. (Sphaerostroma) crassa* (Lecompte, 1952), *Amphipora* ex gr. *laxeperforata* Lecompte, 1952, and *Actinostroma clathratum* Nicholson, 1886. Representatives of *Stromatopora* and *Parallelopora* could not be identified to species level. In the reef core/margin setting of HON_1101, Bed -22, *Schistodictyon* sp., with overgrown *Syringopora hanshanensis* Zhou, 1980, *Salairella buecheliensis* (Bargatzky, 1881), and *Act.* ex gr. *filitextum* have to be added (compare May 2005). In the slightly younger, probably basal Frasnian Bed -26 of core B102 (Eisborn Member), there is also *Schistodictyon* sp., associated with *Clathrocoilona (Cl.) obliterata* (Lecompte, 1951), *Parallelopora* sp., *Stromatopora* sp., other stromatoporoids, and the tabulate corals *Alveolites (Alveolites)* sp. and *Aulopora (Mastopora)* sp.

Based on additional thin-sections, some previous identifications of supposed solitary Rugosa (*Temnophyllum, Chostophyllum*) from the Eisborn Member of the Beul outcrop (Becker et al. 2016c) have to be revised. These represent branches of the dendroid genus *Disphyllum*. *Disphyllum breviseptatum* (Frech, 1886) is known from the lower Frasnian of Refrath in the western Rhenish Massif, while *Dis. rugosum* (Wedekind, 1922) occurs in the lower/middle Frasnian of the Rhenish Massif (Refrath), France, and Canada (e.g. Schröder 2005; McLean 2010). The assumed *Spinophyllum* is based on the transsect of a fragmentary *Haplothecia schlotheimi* Pickett, 1967 (see Fig. 24b), which is a Frasnian genus. Due to the strictly straight polypar walls and strong carinae, the sectioned hexagonariid colony is not *Hexagonaria hexagona*, but a relative of *Hex. davidsoni* (Milne-Edwards and Haime, 1851), identified here as *Hex.* aff. *davidsoni* (Fig. 24a). The typical form is cosmopolitan in the Frasnian (compare description by Falahatgar et al. 2018).

Among the tabulate corals of the Beul outcrop, many alveolitids are closer to *Alveolites (Alv.) edwardsi edwardsi* Lecompte, 1939 than to *Alv. (Alv.) edwardsi frasnianus* Nowinski, 1993. The latter seems to be typical for higher parts of the Frasnian. Only in the biostrome at the top of Beul, *Alv. (Alv.) suborbicularis* de Lamarck, 1801, probably the typical subspecies, and an *Alv. (Crassialveolites)* were recognised. Most thamnoporids belong to the group of *Thamnopora* ex gr. *polyforata* (Schlotheim, 1820) but in addition there are some smaller-sized *Th.* ex gr. *micropora* Lecompte, 1939; for Rhenish thamnoporid systematics see May (1993a).

Based on the new material, the *Stachyodes (Keega)* specimens from Beul are now assigned to *St. (K.) australe* Wray, 1967, not to *St. (K.) jonelrayi*. The first is known globally, including the eastern Sauerland (May 1993b). Other stromatoporoids are rare and not well preserved; they are assigned to *?Euryamphipora*, *?Clathrocoilona*, and *Stromatoporella*.

Brachiopods form a subordinate element of the Beul Facies. A distinctive spiriferid valve (Fig. 24c–d) agrees in its spinous micro-ornamentation with *Adolfia pseudomultifida* (Vandercammen, 1955; see Vandercammen 1957, pl. 1, figs. 9, 10, 11, and 12). It was originally described as a *Guerichella* species from the middle Frasnian of the Ardennes and

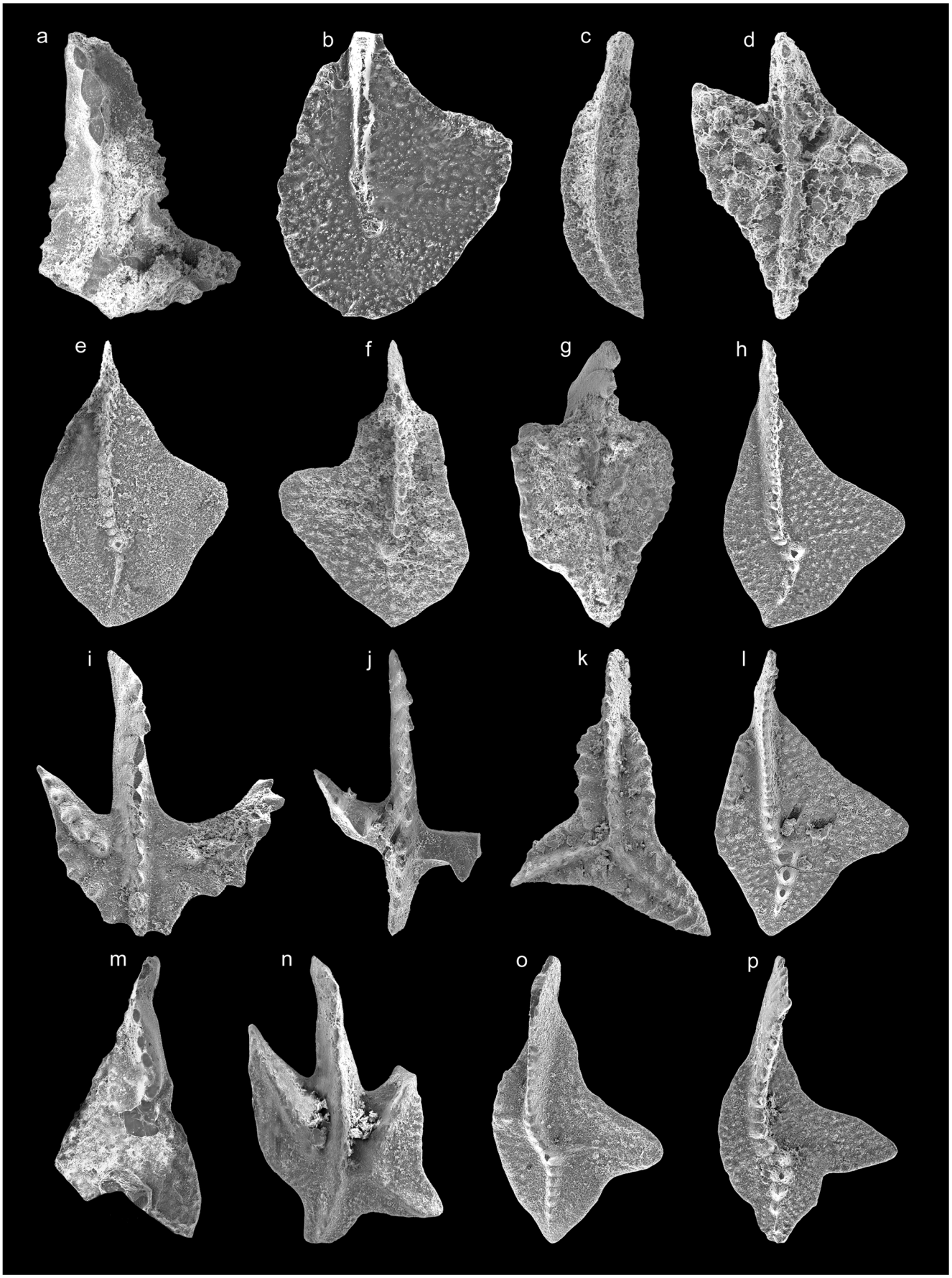
a
b
c
d
e
f
g
h
i
j
k
l
m
n
o
p

◀ **Fig. 19** Conodonts from the middle/upper Frasnian of core B102; specimens B9A.14.44–59. **a** *Ancyrognathus amplicavus*, poorly preserved, Sample -24f, x 45 **b** *Palmatolepis* cf. *housei*, unusual form lacking a posterior carina, Sample -24f, x 50 **c** *Polygnathus paradecorosus*, Sample -24f, x 55 **d** *Ancyrodella lobata*, Sample -24e, x 60 **e** *Pa. hassi*, atypical early form with short side-lobe, Sample -24d, x 55 **f** *Pa.* cf. *plana*, variant with reduced posterior carina, Sample -24c, x 65 **g** *Ad. gigas*, Sample -24c, x 30 **h** *Pa. kireevae*, Bed -22, x 60 **i** *Ad. nodosa*, showing a trend towards *Ad. ioides* M1 sensu Klapper 2021, Bed -22, x 60 **j** *Ad. ioides* s.str., small specimen, base Bed -18, x 80 **k** *Ag. triangularis*, typical form, base Bed -18, x 40 **l** *Pa. uyenoi*, base Bed -18, x 40 **m** *Ag. ?tsiensi* (or possibly *Ag. asymmetricus*), fragmentary but showing the typical, asymmetrically positioned fin, Bed -16, x 35 **n** *Ad. curvata* late form, Bed -16, x 45 **o** *Pa. nasuta*, Bed -16, x 45 **p** *Pa. muelleri*, Bed -15, x 35

transferred to the genus *Judinica* Oleneva, 2019. Outline and macro-ornamentation resemble those of other species of *"Adolfia"*, such as *"Adolfia" angustisellata* (Paeckelmann, 1913) from the "Iberger Kalk" of Metzenberg near Wülfrath; in that species the micro-ornamentation has also been described as "densely standing, rounded verrucae" (written comm. U. Jansen, Frankfurt a.M.). Our specimen suggests a range extension into the lower Frasnian.

A rare new odontopleurid trilobite is described in a separate note (Helling and Becker 2022, this issue). It was found on a slab with *Po. alatus*, *St. (Keega) australe*, and *Th.* ex gr. *polyforata*.

Facies developments

Drill core HON_1101 (Figs. 4, 13, 16)

Asbeck Member: In drill core HON_1101, the upper ca. 80 m of the Asbeck Member (excluding a ca. 8 m interval of intercalated post-reefal strata) were penetrated between ca. 78 and 165 m. In its lower ca. 7 m (beds -39 to -36, 158.15–165.00 m), the palaeoenvironment is characterised by shallow lagoonal conditions (MF-A1, micritic, dendroid stromatoporoid float-rudstone, Fig. 6b). *Amphipora* and *Stachyodes* (represented by *St. (St.) costulata*) are variably dominant and associated with bulbous stromatoporoids. This suggests the lateral growth of delicate *Amphipora* and more robust *Stachyodes* thickets depending on the level of water agitation. The setting was relative stable for some time, presumably caused by a carbonate production that

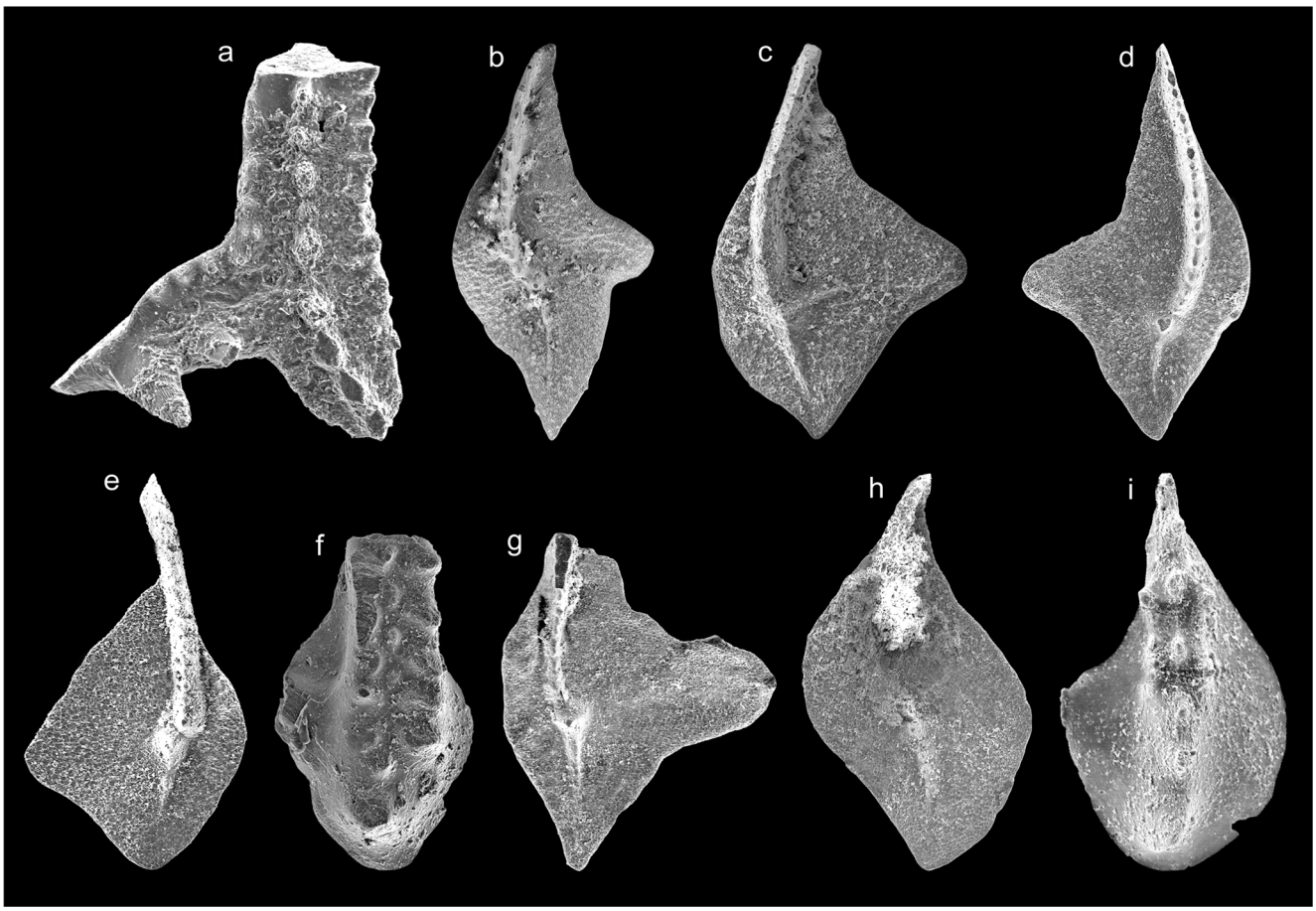

Fig. 20 Conodonts from the upper Frasnian and lower Famennian of core B102, specimens B9A.14.60–68 **a** *Ancyrognathus iowaensis*, small, narrow form, Bed -15, x 85 **b** *Palmatolepis triangularis, praeterita* morphotype, Bed -13, x 30 **c** *Pa. subperlobata*, Bed -13, x 65 **d** *Pa. ultima*, Bed -8, x 35 **e** *Pa. delicatula delicatula*, Bed -8, x 95 **f** *Icriodus alternatus mawsonae*, fragmentary, Bed -8, x 80 **g** *Pa. lobicornis,* Bed -5, x 60 **h** *Pa. regularis*, Bed -5, x 50 **i** *I.* cf. *alternatus*, juvenile, Bed -5, x 135

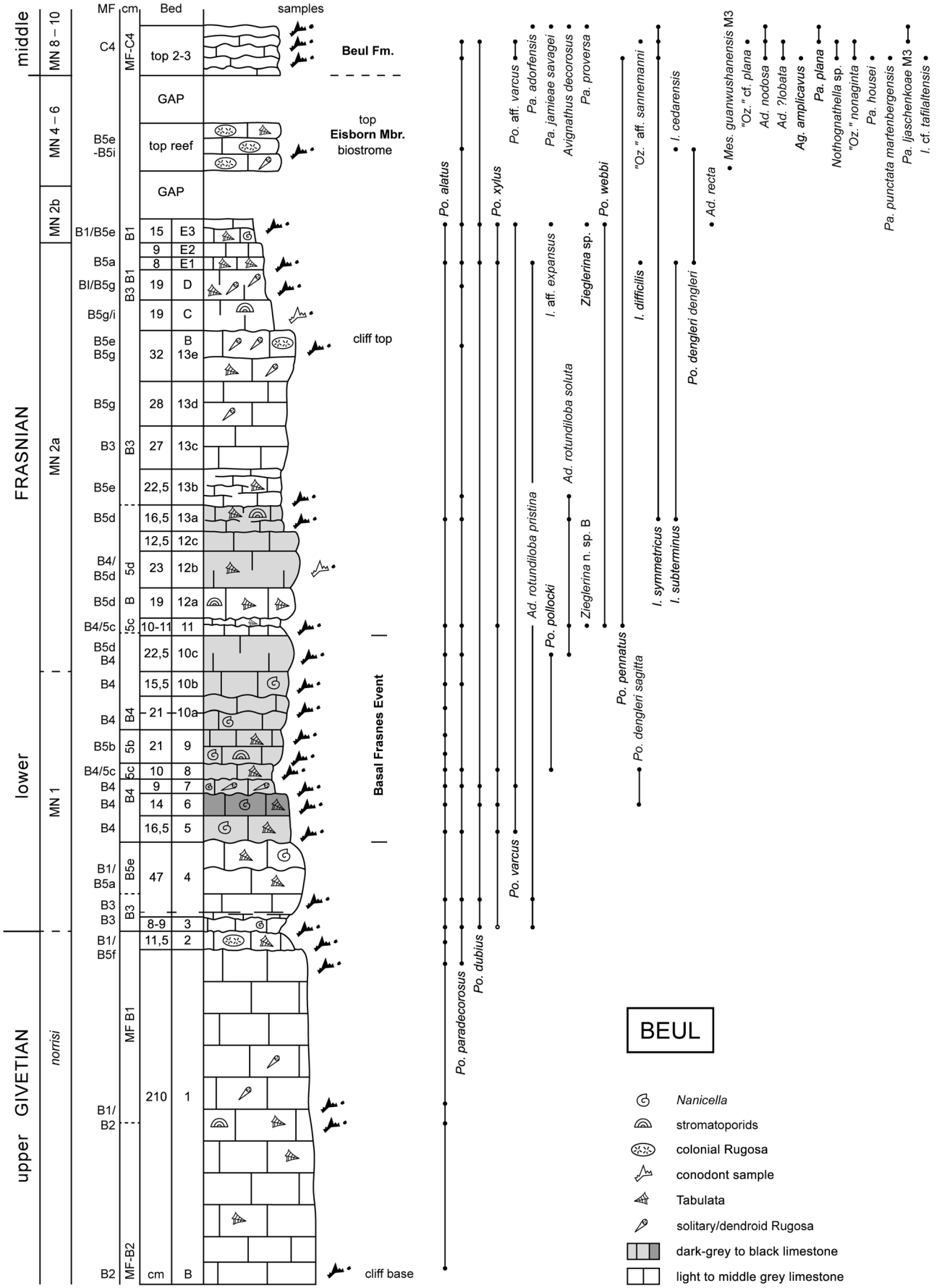
middle
lower
upper
FRASNIAN
GIVETIAN
norrisi
MN 1
MN 2a
MN 2b
MN 4 – 6
MN 8 – 10
MF
cm
Bed
samples
C4
MF-C4
top 2-3
Beul Fm.
GAP
top reef
top Eisborn Mbr. biostrome
GAP
B1/B5e
B5a
Bl/B5g
B5g/i
B5e B5g
B5g
B3
B5e
B5d
B5d
B4/ B5d
B5d
B4/5c
B5d B4
B4
B4
B5b
B4/5c
B4
B4
B4
B1/ B5a
B3
B3
B1/ B5f
B1/ B2
MF-B2
B2
B1
B3 B1
B3
5d
B
5c
5c
B4
B4
5b
5c
B4
B5e
B3
MF B1
15
E3
9
E2
8
E1
19
D
19
C
32
B 13e
28
13d
27
13c
22,5
13b
16,5
13a
12,5
12c
23
12b
19
12a
10-11
11
22,5
10c
15,5
10b
21
10a
21
9
10
8
9
7
14
6
16,5
5
47
4
8-9
3
11,5
2
210
1
cm
B
cliff top
Basal Frasnes Event
cliff base
Po. alatus
Po. paradecorosus
Po. dubius
Po. xylus
Po. varcus
Po. aff. varcus
Pa. adorfensis
Ad. rotundiloba pristina
Pa. jamieae savagei
Po. pollocki
I. aff. expansus
Avignathus decorosus
Ad. rotundiloba soluta
Pa. proversa
Zieglerina n. sp. B
Zieglerina sp.
Po. webbi
Po. pennatus
I. difficilis
Po. dengleri sagitta
"Oz." aff. sannemanni
I. symmetricus
I. subterminus
I. cedarensis
Po. dengleri dengleri
Ad. recta
Mes. guanwushanensis M3
"Oz." cf. plana
Ad. nodosa
Ad. ?lobata
Ag. amplicavus
Pa. plana
Nothognathella sp.
"Oz." nonaginta
Pa. housei
Pa. punctata martenbergensis
Pa. ljaschenkoae M3
I. cf. tafilaltensis
BEUL
Nanicella
stromatoporids
colonial Rugosa
conodont sample
Tabulata
solitary/dendroid Rugosa
dark-grey to black limestone
light to middle grey limestone

◀ **Fig. 21** Section log, conodont ranges, and microfacies succession in the Beul outcrop. Due to the outcrop conditions, no thicknesses can be given for the biostrome at the top of the Eisborn Member and for the basal Beul Formation, open dots indicate uncertain identifications

kept up with subsidence. *Amphipora* (MF-A3, represented by *Am.* ex gr. *laxeperforata*) became dominant in Bed -35, indicating calm episodes. In the more than 4 m thick Bed -34 (Fig. 6f), the change to the high-energy conditions of MF-A2 (detrital stromatoporoid grain-rudstone, including *Parallelopora* sp.) reflects storm events or the lateral shift of a channel adjacent to a patch reef. *Amphipora* float-rudstones (MF-A3) from Bed -33 to the base of Bed -31 (ca. 146.50–151.55 m, Fig. 6) indicate a return to calmer conditions overprinted by episodic storms. In the almost 35 m thick main part of Bed -31, the predominant MF-A1 (e.g. at 124.61–124.85 m, Fig. 6c, with *Am.* ex gr. *laxeperforata*, *St. (Sphaerostroma) crassa*, and *St. (St.) costellata*) is interrupted by a few *Amphipora* floatstone phases (MF-A3a, Fig. 4) and coarse reefal debris, probably storm deposits, at 127.79–127.89 m. An interval of MF-A5 (crinoidal stromatoporoid-coral rudstone) in the upper part (116.30–116.57 m) is interpreted as an interval, when storms delivered material from the reef core, possibly through channels. This is supported by the subsequent rapid return to the lagoonal MF-A1 and MF-A3b. At the top of Bed -31 (113.50–113.60 m, Fig. 7c), the sporadic appearance of MF-A4 (fenestral pack-grain-bindstones) indicates a shift from subtidal to intertidal conditions and, therefore, a minor sea level fall. As conodonts avoided back reefs and lagoons, it was not possible to date this phase.

Between 113.00 and 105.50 m (Fig. 13), the carbonate succession is interrupted by strongly weathered clayey sediment, which probably belongs to a fault zone. An intercalated, ca. three-metres thick limestone unit (Bed -29) is in bioturbated and bioclastic wackestone facies (MF-C2) revealing open shelf conditions, which is supported by pelagic palmatolepid biofacies. The dating as upper Frasnian proves that it is an intercalation of Beul Formation that does not belong to the reefal succession.

The "normal" reef development continues at 105.50 m (Bed -27) with lagoonal stromatoporoid float-rudstones (MF-A1, Fig. 6d, with *Actinostroma clathratum*) of the Asbeck Member. As typical for back-reef settings, there is no conodont record. At the top of Bed -25 (102.80–103.00 m), MF-A1 yielded, as below, the dendroid *St. (St.) costulata* (Fig. 6a). A short sea level fall is noticeable at 102.00 m by MF-A4b, indicating an intertidal to supratidal environment. At 94.98 m, peloidal stromatoporoid rudstones (MF-A5, Fig. 7d) occur, which yielded dendroid *St. (St.) costulata* and *Thamnopora* sp., but also *Alveolites (Crassialveolites)* sp. This was only a brief episode, directly followed by a return to the lagoonal MF-A4a (fenestral pack-grain-bindstones, Fig. 7a). The close association records either an influx of outside detritus by a major storm or a short transgressive pulse shifting reef facies onto the lagoon. The last MF-A4a is found at 90.00 m.

The final phase of the reef complex (Asbeck Member) is marked in core HON_1101 by a package (ca. 83.40–90.00 m, Bed -22) of MF-A5. Large stromatoporoids, including *Schistodictyon* sp., *Salairella buecheliensis*, *Actinostroma* ex gr. *filitextum*, and others dominate rudstones with some *Stachyodes*, *Th.* ex gr. *micropora* (as in the Eisborn Member, see below), subordinate solitary rugose corals, and a peloidal grainstone matrix that includes fragmented crinoids. This is clearly a reef core to outer margin facies.

Eisborn Member: Deepening is supported by the incoming of open shelf organisms (basal Frasnian conodonts) in Bed -21 of the basal Eisborn Member. The sudden facies shift above the thick lagoonal sequence reflects a significant reef margin backstepping, which correlates in time with the eustatic floodings of the global **Frasnes Events** (e.g. House 1985; Ebert 1993; Aboussalam and Becker 2007, 2017; = *Mesotaxis* Event of Racki 1993). Its severe effect on reefal platforms and its varied biota is long known from the Ardennes, where the thick Fromelennes Reef Complex was flooded at the base of the Frasnian (e.g. Bigey et al. 1982; Devleeschouwer et al. 2010). Far away, in the eastern Taurides of southern Turkey, biostromes were submerged in a similar way by two top-Givetian and lower Frasnian sea level rises that correlate with the Frasnes Events (Özkan et al. 2019). This example underlines the eustatic nature of sea level changes.

In Bed -20, alveolitid-dominated rudstones (Fig. 7h, 79.12–79.32 m) with *Alv. (Alv.)* ex gr. *edwardsi*, some *Th.* ex gr. *polyforata*, subordinate rugose corals, a small amount of crinoid debris, and rare polygnathids follow. The dominant laminar growth of tabulates and the presence of crinoid debris reveal the transformation into a drowned biostromal platform. The deepening also caused the replacement of most stromatoporoids by corals. The microfacies is assigned to MF-B5h/i of the Eisborn Member, correlating laterally with the top lower Frasnian biostrome of the Beul outcrop (see below).

The drowning of the reef platform involved an incredible decrease (up to 120 times) of carbonate production. The up to 1.000 m thick top-lower to middle Givetian strata of the main Asbeck Member, a time span in the order of 3 Ma (Becker et al. 2020), gives an accumulation of ca. 333 m/Ma. This contrast with 6–7 m for all of the lower Frasnian, lasting ca. 2.5 Ma, giving ca. 2.8 m/Ma. This trend is accompanied by the unique pack-rudstones with the auloporid *Roemerolites* sp. (MF-B6, Fig. 7f, 78.00–78.15m, Bed -20). The *I. subterminus* fauna from the top shows that the reef remained in the open shallow-water realm (see Narkiewicz and Bultynck 2010).

Frasnian Beul Formation: Starting with the thin Bed -19, no reefal fauna is noticeable anymore. The rapid change to

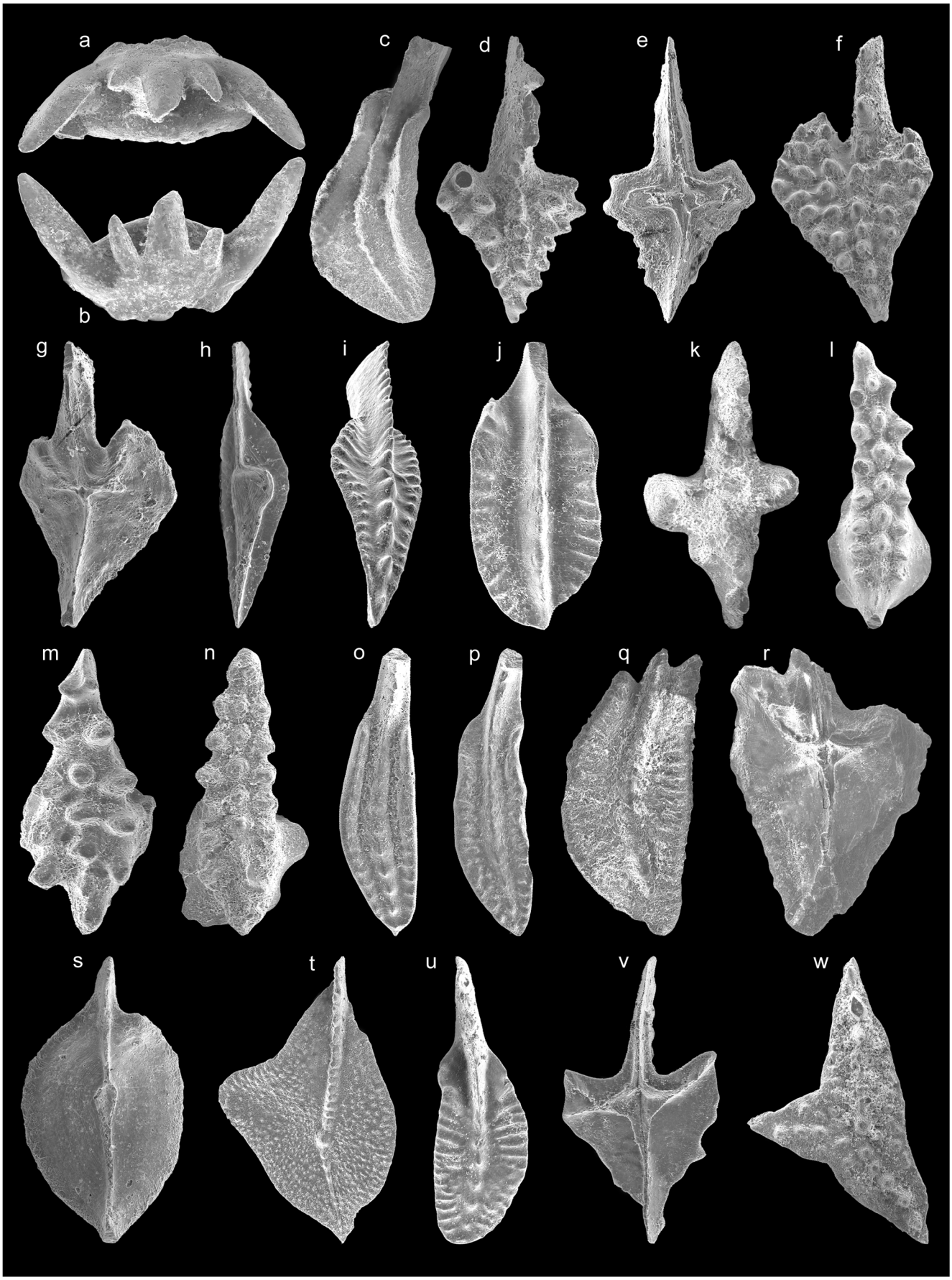
a
b
c
d
e
f
g
h
i
j
k
l
m
n
o
p
q
r
s
t
u
v
w

◀ **Fig. 22** Shark teeth (a–b, specimens A1C.7.1–2) and conodonts (c–w, specimens B9A.14-69–81) from the top-Givetian and Frasnian of the Beul outcrop. **a–b** *Phoebodus fastigatus*, Sample top 2, x 45 **c** *Polygnathus alatus*, Bed B3, x 40 **d–e** *Ancyrodella rotundiloba pristina*, upper and lower views, Bed B3, x 45 **f–g** *Ad. rotundiloba soluta,* upper and lower views, Bed B10C, x 35 **h–i** *Zieglerina* n. sp. B, lower and upper views, Bed B11, x 60 and 65 **j** *Po. dengleri dengleri*, with incipient anterior platform collar, Bed E1, x 70 **k** *Ad. rotundiloba pristina*, small specimen transitional towards *Ad. binodosa*, Bed E1, x 80 **l** *Icriodus* aff. *expansus*, Bed E1, x 80 **m** *I. subterminus*, Bed E1, x 90 **n** *I. difficilis*, unusually late representative, Bed E1, x 65 **o** *Po. dubius*, Bed E1, x 65 **p** *Po. paradecorosus*, Bed E1, x 50 **q** *Po. webbi*, Bed E1 **r** *Ad. recta*, lower view with typical orientation of side carinas Bed E3, x 45 **s** *Mesotaxis guanwushanensis* M3, lower view, top biostrome, x 40 **t** *Palmatolepis housei*, Sample top 2, x 45 **u** *Po. pennatus*, Sample top 2, x 45 **v** *Ad. ?lobata* juv., lower view, Sample top 2, x 80 2 **w** *Ancyrognathus amplicavus*, Sample top 2, x 45

micritic limestones with pelagic and subphotic fauna correlates with the eustatic rise of the global **Middlesex Event** near the base of the middle Frasnian. Its development in the eastern Rhenish Massif, global distribution, and isotopic signatures have been summarised by Pisarzowska et al. (2020). In many regions, but not everywhere, the Middlesex Event is characterised by the sudden spread of hypoxia (black shales). In the distal slope setting south of the Brilon Reef, there is geochemical evidence both for enhanced primary production and oxygen deficiency. At the Beul, the event caused extreme condensation, probably with unconformities due to non-deposition, but no increased deposition of C_{org}, and the facies remained oxic. The *Pa. punctata punctata* and *Ag. primus* zones (MN zones 5/6, lasting up to 1 Ma; Becker et al. 2020) are represented by just ca. 70 cm of beds -18 and -17. The latter, a solid limestone layer at 77.00 m, is a bioclastic, stylioline-dominated, pelagic wacke-packstone (MF-C1, Fig. 10e).

Pelagic conditions continue in an overlying, ca. 15 m thick package of flaser- or nodular limestone (Bed -16), which spans the *"Oz." nonaginta* (MN Zone 7) to basal *Pa. feisti* Zone (MN Zone 11). At 65.26–65.34 m, middle Frasnian nodular limestones belong to MF-C2 (bioturbated wackestone), with a decreasing amount of bioclasts to the top of Bed -16 (MF-C4, 61.90–62.05 m) and at the base of Bed -15 (MF-C4, 61.75–61.90 m). Just above, there is a ca. 27 cm alternation of black to

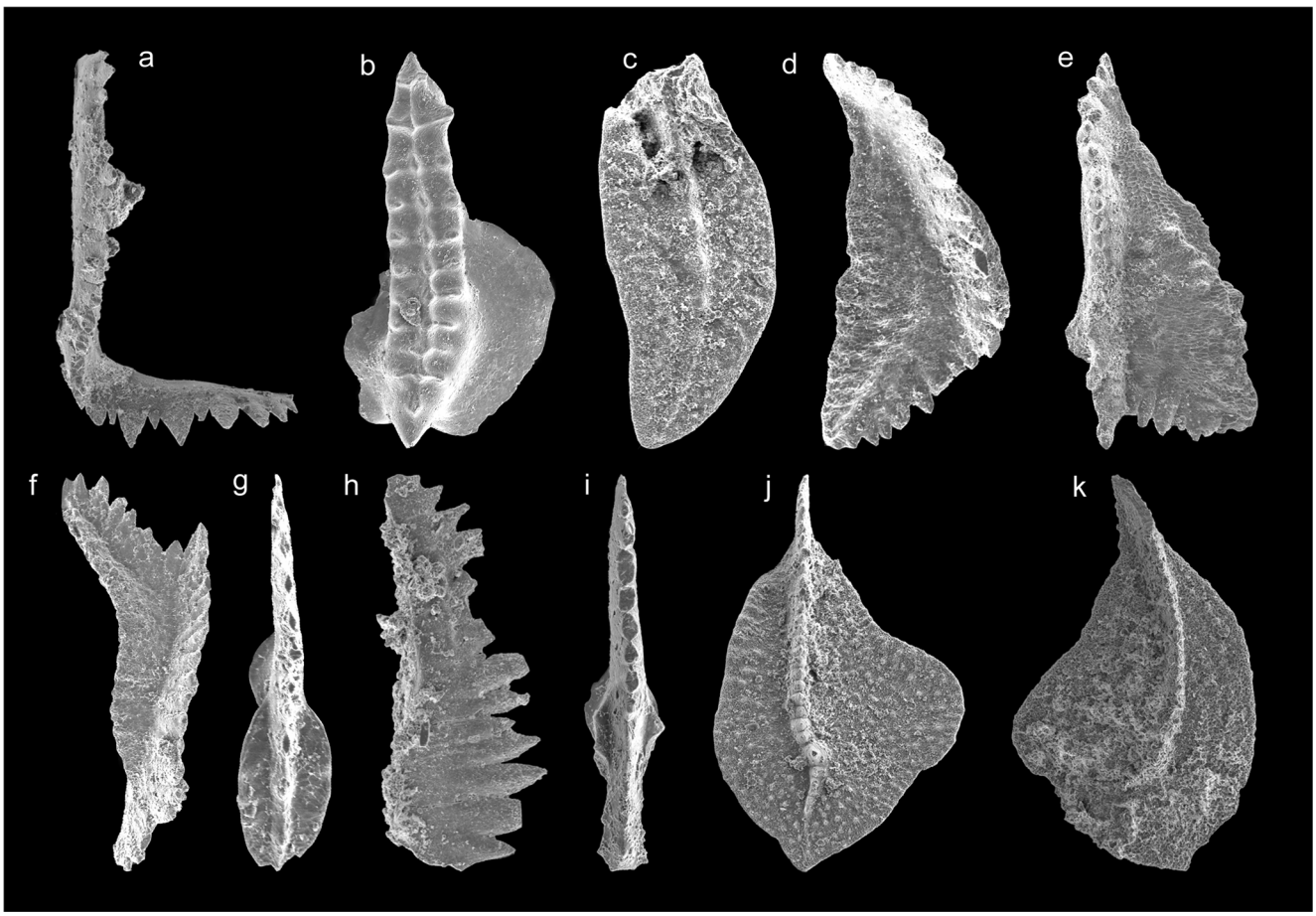

Fig. 23 Conodonts from the Frasnian of the Beul outcrop, specimens B9A.82–98. **a** *"Ozarkodina" nonaginta*, Sample top 2, x 65 **b** *Icriodus* cf. *tafilaltensis*, Sample top 2, x 55 **c** *Polygnathus* sp., rare Frasnian form with flat, finely nodose platform, Sample top 2, x 70 **d** *Nothognathella* sp. 1, Sample top 2, x 90 **e** *Nothognathella* sp. 2, Sample top 2, x 85 **f** *Nothognathella* sp. 3, Sample top 2, x 80 **g** *Po.* aff. *varcus*, upper view, Sample top 2, x 125 **h** *"Oz."* cf. *plana*, probable homoeomorph, Sample top 3-1, x 60 **i** *"Oz."* aff. *sannemanni*, form with very narrow platforms with small nodes, Sample top 3-1, x 90 **j** *Palmatolepis adorfensis*, Sample top 3-1, x 40 **k** *Pa. jamieae savagei* M2, Sample top 3-1, x 65

Table 2 Conodont ranges and abundances in the Beul outcrop (main cliff = beds B1–13)

species/bed no.	1b	1m1	1m2	1o	2	3	4	5	6	7	8	9a	9b	10a	10b	10c	11	13a	13b	13e
zones/subzones	*Sk. norrisi*					*Ad. rotundiloba pristina*										*Ad. rot. soluta*				
Po. alatus	1	1	3	9	1	11	3	9	30	48	10	2	12	8	8	3	9	1	-	-
Po. paradecorosus				1	-	1	1	3	1	6	1	-	-	-	2	3	2	18	2	1
Po. dubius						1	1	-	4	6	-	-	-	-	-	-	-	-	-	-
Po. xylus						1?	-	1	1	-	1	-	-	-	-	-	1	-	-	-
Ad. rot. pristina						2	-	-	2	-	-	-	-	-	-	-	1	-	-	-
Po. varcus								1	-	2	-	-	-	-	-	-	-	-	-	-
Po. dengl. sagitta									1	-	2									
Po. pollocki										1	-	-	-	-	-	1				
Ad. rotund. soluta																1	-	2	1	
Po. pennatus																	2	-	-	-
Zieglerina n. sp. B																	1			
Po. webbi																	3	-	-	-
I. symmetricus																		1	-	-
I. subterminus																		6	-	-

dark brownish-grey, laminated shales (MF-C6) and pelagic mud-wackestones. These represent locally the eustatic ***semichatovae* Event Interval,** which transgressive base defines the global Depophase IId sensu Johnson et al. (1985). In the Ardennes, it caused the drowning of the Lion Mudmounds and corresponding reefs (Sandberg et al. 1992). Its global distribution and event stratigraphy are reviewed and refined by Saupe and Becker (2022, this issue). The local succession is polyphased, with four black shales, which may record four Milankovitch cycles, as it has been proposed for other Devonian black shale events (De Vleeschouwer et al. 2013). The latter are fractured in the core; therefore, we provide a thin-section based detailed log, with representative illustrations of microfacies:

Bed -15a (61.71–61.75 m) laminated, very organic-rich black shale with rare ostracods; **anoxic pulse 1**

Bed -15b (61.68–61.71 m) light-grey, bioturbated mud-wackestone with dacryoconarids, shell debris, some larger mollusk shells, in the lower part microsparitic and with undulating sharp base

Bed -15c (61.62–61.68 m) laminated, very organic-rich black shale with few ostracods, in the upper part (3 mm) less organic-rich and with fine silt; **anoxic pulse 2**

Bed -15d (61.57–61.62 m) light-grey, bioturbated mud-wackestone (MF-C4) with shell fragments, small gastropods, juvenile orthocones, rare dacryoconarids, some geopetals, and sharp base (Fig. 11g)

Bed -15e (61.56–61.57 m) middle- to dark-grey, flaser-bedded, partly organic-rich, microsparitic, crinoidal wacke-packstone with dacryoconarids and shell debris, a detrital layer (MF-C3) with erosional, undulating base (Fig. 11g)

Bed -15 f (61.55–61.56 m) flaser-laminated, organic-rich, dark-grey shale with some ostracods (Fig. 11h); **anoxic pulse 3**

Bed -15g (61.54–61.55 m) middle-grey, strongly recrystallized (micro- to pseudosparitic) layer of wackestone with dacryoconarids, ostracods, and shell fragments (altered MF-C4), with sharp lower and upper boundaries (Fig. 11h)

Bed -15h (61.51–61.54 m) flaser-laminated, organic-rich, dark-grey shale, subdivided by eight thin sparite seams that are partly slightly oblique and, therefore, a diagenetic feature (Fig. 11h); **anoxic pulse 4**

Bed -15i (61.48–61.51 m) light-grey, bioturbated, microsparitic layer with rare dacryoconarids (MF-C4), with a 12 mm clast sunken into the underlying, unconsolidated shale

The lack of bioturbation and lamination proves anoxic seafloor conditions, probably because of strong eutrophication, leading to cyanobacterial blooms that typically left only amorphous C_{org} (Pacton et al. 2011). The complexity of the *semichatovae* Event has previously not been documented. Therefore, its detailed sequence is provided here. The two lower shales are much darker and organic-rich than the two upper ones. In the Rhenish Massif east of the Rhine, the *semichatovae* Event was previously not recognised as an anoxic event, but it initiated hypoxic

Table 3 Conodont ranges and abundances in the Beul outcrop (cliff top and samples from the backside), xx = numerous uncounted specimens

species/bed and sample no.	D	E1	E3	biostrome	top reef	top 2	top 3-1	top 3-2
zones/subzones	*Ad. rot. soluta*		*Ad. r. rotundiloba* to *Pa. transitans*			*Pa. housei*	*Pa. plana*	
Po. alatus	-	1	1	-	3	-	1	2
I. symmetricus	-	-	-	-	-	58	60	35
Po. paradecorosus	1	3	2	-	9	234	78	28
Po. dubius	-	8	8	-	1	26	3	
Po. xylus	-	3	3					
Po. varcus	-	-	2	-	-	27 (aff.)	7 (aff.)	
Ad. rotundiloba pristina	-	1						
Po. pennatus	-	-	-	-	1	1		
Po. webbi	-	-	8					
I. aff. *expansus*	-	1	-	-	-	58	60	35
I. subterminus	-	5						
I. difficilis		1						
Po. dengleri dengleri	-	3	-	-	1			
Zieglerina sp.			1					
Ad. recta			4					
Mes. guanwushanensis M3				1				
I. cedarensis					1			
Ad. nodosa						8	3 + 2?	4
Ad. lobata						2?	1?	
Ag. amplicavus						3		
"Oz." nonaginta						19	2	
I. cf. *tafilaltensis*						2		
Polygnathus sp.						1		
Nothognathella sp. 1–3						11	21	5
Pa. housei						4		
Pa. punct. martenbergensis						4		
Palmatolepis sp. juv.						83	xx	4
"Oz." cf. *plana*							1	
Pa. plana							53	2
"*Oz.*" aff. *sannemanni*							1	
Pa. ljaschenkoae M3							1	1
Avignathus decorosus (Pb)								1
Pa. jamieae savagei M2								1
Pa. adorfensis								2
Pa. proversa								2
Pa. hassi								2

goniatite shale deposition in more western parts (Bergisch Gladbach, Eifel). On the northern Gondwana Shelf (Morocco-Algeria, e.g. Wendt and Belka 1991), it was the starting point for long-lasting high organic productivity and anoxia ("Kellwasser-type facies") associated with a major water mass change (Dopieralska et al. 2015).

The anoxic sequence ended as sharp as it began. Bed -14, which falls in the higher part of the *Pa. feisti* Zone (MN Zone 11), consists again of well-oxygenated, bioturbated flaser-limestone. The occurrence of several sponge bodies, indica- ted by spicule arrangements, is unique for the borehole. Within the following Bed -13, there are thin, strongly bioturbated layers of silt (MF-C7) and peloidal packstones (MF-C8) that indicate minor phases of increased turbulence (Fig. 11b). This is the only and rather weak local evidence for equivalents of the regressive Usseln Limestone that characterises just below the Lower Kellwasser interval basinal and submarine rise sections of the eastern and southern Rhenish Massif, Harz Mountains, and Saxothuringian Zone (Gereke 2007; Gereke and Schindler 2012; Gereke et al. 2014). The eutrophic and transgressive subsequent **Lower**

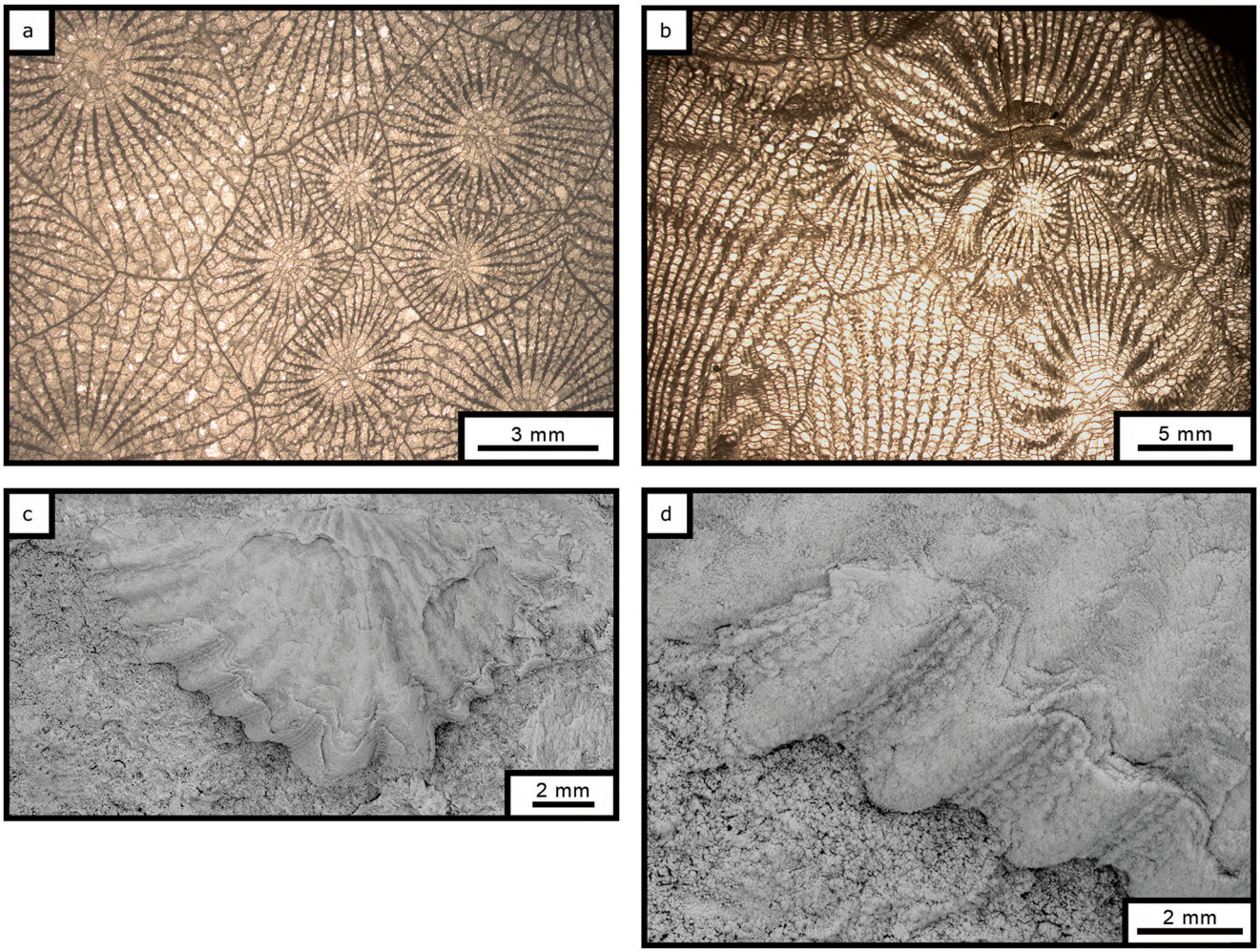

Fig. 24 Macrofauna of the Eisborn Member (Beul outcrop). **a** *Hexagonaria* aff. *davidsoni*, Bed 13e **b** *Haplothecia schlotheimi*, biostrome on the backside of the Beul outcrop **c–d** *Adolfia pseudomultifida*, single valve with micro-ornament preserved at the shell margin, loose slab with *Polygnathus alatus*

Kellwasser Event is represented by the almost 60 cm thick, dark-grey, organic-rich, recrystallized ostracod-mollusk pack-grainstones of Bed -12 (MF-C3, Fig. 10h). As elsewhere, the unit spans the boundary between the *Pa. winchelli* (MN Zone 12) and *Pa. bogartensis* (MN Zone 13a) zones. It is remarkable that there are still only a few published illustrations of Rhenish Lower Kellwasser facies types from submarine rises. In the Hönne Valley area, eutrophic conditions did not lead to sea floor anoxia. Ostracods and mollusks benefitted locally much more strongly than dacryoconarids or homoctenids. In the well-studied Schmidt Quarry (Kellerwald, LKW thickness = 50–55 cm), Benner Quarry at Bicken (Dill Syncline, LKW thickness = 41 cm), and in the Kellwasser type-section of the Harz Mountains (LKW thickness = 37 cm), the typical Lower Kellwasser limestones are rich in homoctenids and mostly laminated (Schindler 1990), representing deeper submarine rise facies.

The intra-Kellwasser succession is a thin interval (Bed -11 to lower part of Bed -9) characterised by the return to bioturbated, oxygenated, micritic mud-wackestone deposition. At the base of Bed -11, recrystallization and strong fracturing mask the facies transition. However, there is at least one reworked Lower Kellwasser clast indicating a disconformable contact. Above a thin interval with calcisphere wackestones (MF-C1*), light-grey, bioturbated mudstones (MF-C4) prove the return to a quiet and oligotrophic deep-water setting. The main part (level of Sample -9a, 58.97–59.08 m) consists of three layers that are each more bioturbated and nodular at their bases. The recrystallised (microsparitic) mudstone contains some calcispheres, shell debris, rare ostracods and dacryoconarids, as well as the single branch of a bryozoan or algal thallus.

The 14 cm thick level of Sample -9b (58.80–58.93 m) is characterised by the return to (moderately) organic-rich, middle- to dark-grey limestone, interpreted as a more shallow-water, better oxygenated **equivalent of the Upper Kellwasser Limestone** (MF-C2, Fig. 10b–c). The base is relatively sharp, with the top of the underlying subunit (Sample -9a, 58.93–59.94

m, Fig. 16) developed as a light-grey, bioturbated mud-wackestone (MF-C4) with shell debris, some ostracods, and crinoid ossicles. Right above, at 58.91–58.93 m (base of Fig. 10b), eutrophication caused an ostracod and homoctenid bloom; the microfacies is transitional between MF-C2, C3, and C5. The ostracod bloom occurs also in core B102 (see below). However, the typical Upper Kellwasser ecological succession established for Rhenish basinal and other submarine rise settings by Schindler (1990, 1993) and Gereke and Schindler (2012) is not developed.

Typical for Kellwasser Facies is the rather strong recrystallization. The subsequent middle grey, partly laminated, partly bioturbated mollusk wacke-packstones (MF-C2) are interrupted by two thin layers of light-grey, bioturbated mud-wackestone (MF-C4, Fig. 10b). From these, burrowing organisms dug downwards into the more organic-rich layers. The polyphase deposition of the local Upper Kellwasser unit is underlined by vertical fluctuations between wacke- and packstones. At least ten successive depositional intervals can be recognised, which equals the number of subunits at Steinbruch Schmidt (Schindler 1990, 1993). A small-sized, incomplete, pachyconic goniatite cross-section resembles the shell form of early *Crickites holzapfeli*. Interesting is the abundance of embryonic to early juvenile goniatite shells. These suggest recurrent worsening of environmental conditions, e.g. by changing oxygenation, which killed episodically juvenile goniatite populations before they could grow. The strong fragmentation of most shells indicates allochthonous mollusk debris, with water agitation in the source region and episodic transport by bottom currents, however, without winnowing the micrite. There are clear differences to the typical Upper Kellwasser beds of other Rhenish sections deposited in the shelf basin or on isolated submarine rises (e.g. Schindler 1990; Gereke 2007; Gereke and Schindler 2012). Becker et al. (2016b, fig. 21) illustrated a shallow-water variant, but still within the *Palmatolepis* Biofacies realm, from the Upper Kellwasser unit that drowned the microbial top part of the Wülfrath Reef. It differs in its more peloidal matrix, resembling the Lower Kellwasser Limestone of HON_1101.

Sample -9c (58.68–58.80 m, Fig. 16) appears to be lighter-grey and less organic-rich than Sample -9b but this is mostly a consequence of its much stronger recrystallization, including wide, sparite-filled cracks, iron mineralizations, and beginning dolomitization. The less affected parts of the thin-section suggest the same MF-C2 microfacies as below, with some bioturbation and micritization of larger mollusks shells. This interpretation is supported by partial goniatite cross-sections, which probably belonged to *Manticoceras*, *Crickites*, and "*Archoceras*", a typical Kellwasser assemblage, as well as by the conodont fauna.

Our data prove that both Kellwasser Events extended in the Rhenish Massif as blooms of specific organism groups and increased burial of C_{org} to shallower settings than described in most previous studies. The microfacies evidence does not answer the unsolved questions why groups adapted to Kellwasser conditions (e.g. conodonts, ammonoids, specific ostracods, and bivalves) died out at the top of the crisis interval. For reviews of the many Kellwasser hypotheses and models see Racki (2005), Carmichael et al. (2019), and Becker (in press).

Famennian Beul Formation: The basal Famennian Bed -8 is a ca. 1 m thick, poorly preserved, and deeply weathered unit consisting of heavily fractured to brecciated, middle-grey, marly limestone and flaserlimestone. It is impossible to decide whether the Frasnian-Famennian (F-F) boundary brecciation was a synsedimentary or entirely post-sedimentary, diagenetic feature. However, there is mounting evidence for seismic events right at the stage boundary (e.g. Racki 1999; Becker et al. 2016b, 2018; Hartenfels et al. 2016; Szrek and Salwa 2020). The poorly preserved interval lies at ca. 59 m depth but deep carstification is common in the Hönne Valley area and led to the formation of its famous caves. The brecciated interval may have been a path for circulating ground water. The microfacies (MF-C2) in the upper part of Bed -8 (58.40–58.50 m) still resembles the top-Frasnian interval but the goniatites, buchiolids, and homoctenids have disappeared. While basal Famennian blooms of ostracod populations are known from other sections (Casier and Devleeschouwer 1995; Becker et al., 2016e), the proliferation of gastropods is a rather unique facies pattern in the basal Famennian.

The following 14 m of the upper part of the drill core consist of nodular limestone and flaserlimestone, rather monotonous MF-C4 (mud-wackestones). The fauna contains ostracods, rare cephalopods, broken mollusk debris, associated with authigenic pyrite, and common traces of bioturbation. The setting was a stable to uniform, (hemi)pelagic, subphotic palaeoenvironment with oxic to dysoxic conditions. Beds -6 and -7 had a richer macrofauna of cephalopods and some trilobite debris. The recognition of *Cheiloceras* cross-sections at 55.85–56.03 m (Fig. 10d) is important since it confirms the onset of lower Famennian ammonoid radiation in upper parts of the *Pa. termini* Zone (see Becker 1993, p. 157). The Hönne Valley setting was too distal to clastic shelf regions and too deep to get affected by the two regressive Condroz Events at the top of the lower Famennian (Becker 1993; Becker et al. 2020) that caused the basinward progradation of a sandstone wedge in the west ("Plattensandstein", Fig. 3; Krebs 1979). Based on the conodont stratigraphy, the Condroz Events should occur within Bed -2 (within the *Pa. rhomboidea* and *Pa. gracilis gracilis* zones). The change from condensed nodular limestone to marl at the base of Bed -1 suggests a deepening trend in the middle of the middle Famennian (higher *Pa. marginifera utahensis* Zone) but there is no correlation with the refined eustatic curve (Becker et al. 2020). The typical red nodular limestones of the Hemberg Formation are locally not developed.

Drill core B102 (Figs. 13, 18)

Asbeck Member: The lower ca. 30 m (beds -97 to -69) consist of light- or middle-grey lagoonal limestones with

branching stromatoporoids, MF-A1 to A3. Macroscopically, *Stachyodes* appears in thickets, but the microfacies analysis exhibits that they are always associated with the smaller-sized *Amphipora* and/or bulbous stromatoporoids (MF-A1). The latter are more frequent than in HON_1101. *Amphipora* float- and bafflestones (MF-A3) occur in beds -95, -93, -91, -86, -81, and -71. They indicate fluctuating phases of deeper and calmer conditions in the lagoon. The almost 7 m thick interval of Bed -68 (70.50–77.30 m) is poor in reef builders (MF-A1*) and suggests a time of worsened palaeoecological conditions. This is followed by a recovery in Bed -67 (66.55–70.50 m) and new *Amphipora* float-rudstones in beds -65 and -64 (65.30–66.10 m). Some intercalations by dolomite (beds -85, -79, -71) are regarded als post-sedimentary diagenetic features.

In the interval from 53.58 to 43.79 m, there are three, variably thick units of macroscopic reefal breccia (Bed -44, 337 cm thick, Bed -42m, 105 cm thick, and Bed -39, 73 cm thick). These can be explained by two possibilities: reef backstepping during sea level rise, resulting in the shedding of reef debris from the retrograding reef core onto the previous lagoon strata, or by shallowing in the lagoon, resulting in the formation of patch reefs that were strongly affected by wave action and recurrent storms. Since the intervening beds and the overlying Bed -38 (40.42–43.79 m) are in lagoonal facies, the second interpretation seems more likely. Especially intriguing is the intercalation within Bed -43, at ca. 49 m, of fenestral fabrics (MF-A4) indicating a very shallow back-reef setting and lowstand peak. The number of stromatoporoids decreased but *Amphipora* bafflestones still occur.

From Bed -31 to Bed -30, there is a gradual increase and rise to dominance of laminar stromatoporoids, which we interprete as the beginning of the terminal reef drowning by backstepping. However, in the middle of Bed -30 (at 30.97–31.12 m), there is a last episode of fenestral and peloidal lagoonal facies (MF-A4), grading upwards (30.85–30.97 m) into fenestral stromatoporoid floatstones with peloidal grainstone matrix (intermediate towards MF-A2). The peloidal stromatoporoid rudstone with crinoid debris of Bed -28 (23.07–23.25 and 24.20–24.38 m), typical MF-A5, shows that a reef core/margin setting was reached, which lasted to the top of the bed, the top of the Asbeck Member.

Eisborn Member: Beds -27 to -25 represent the Eisborn Member, although we did not obtain conodonts from the available single sample. The microfacies of Bed -27 (19.93–20.94 m), alternating peloidal and bioclastic wacke- and grainstones with fine coral, shell, and crinoid debris, represents MF-B1/2. It indicates the drowning of the reef platform, which led to a habitat that was too deep for a rich reef builder community. Upwards, in Bed -26 (19.00–19.93 m), lenses of lamellar stromatoporoids (*Stachyodes (Keega) australe*, *Schistodictyon* sp., *Clathrocoilona (Cl.) obliterata*, *Parallelopora* sp., *Stromatopora* sp., and others), alveolitids, and chaetetids overgrow each other as well as auloporid branches. They are surrounded by a dense, micritic, bioclastic wackestone matrix with some thamnoporids and juvenile gastropods (interval of MF-B5d within dominant MF-B3). The final reef stage, Bed -25 (17.88–19.00 m), is a storm-ridden biostrome (rudstone, MF-B5i), constructed by *Alveolites (Alveolites)* sp., thamnoporids, and colonial Rugosa (probably the phaceloid *Disphyllum*), resembling closely the lower Frasnian reef top of HON_1101 and the Beul outcrop (see below).

Beul Formation: At a depth of ca. 18 m, the Beul Formation begins after a phase of extreme condensation or non-deposition, spanning at least the lower part of the middle Frasnian, possibly also parts of the lower Frasnian. The contact to the Eisborn member was obscured by diagenetic overprint (brecciation and flaser-bedding). A significant deepening is marked at the base of Bed -24 by the onset of bioturbated dacryoconarid wackestones (MF-C1, Fig. 10f–g), followed higher by mud-wackestones (MF-C4, Fig. 11c–d). In thin-sections, the fauna consists of typical pelagic organisms, such as cephalopods (orthocones and goniatites), entomozoans, smooth-shelled ostracods, dacryoconarids, rare trilobites, thin, broken bivalve shells, deformed crinoids, and gastropods. Authigenic pyrite and *Frutexites*-type microbial encrustations suggest dysoxic conditions within the sediment, similar to HON_1101. At the top of the middle Frasnian, in the lower part of Bed -18, bioturbated wackestones include as faunal newcomers various, partly juvenile goniatites and homoctenids. This facies type is sharply interrupted at 7.14–7.24 m by a package of flaser-laminated, organic-rich black shales with a few ostracods (MF-C6; Fig. 11e). The conodont record is not precise (no record of the *Pa. feisti* Zone = MN Zone 11 below), but by comparison with core HON_1101, we assume that it represents the ***semichatovae* Event Interval**. Because it predates the *Pa. winchelli* Zone (MN Zone 12), it cannot be the Lower Kellwasser level. The shales grade into a non-laminated layer of argillaceous, peloidal, and recrystallized wackestone with partly unusually large ostracods and juvenile to fully grown goniatites (probably *Manticoceras*), intermediate between MF-C6 and MF-C3 (Fig. 12e). This suggests first anoxic, then dysoxic conditions.

Above a thin, marly unit (Bed -17), no unequivocal equivalent of the **Lower Kellwasser Limestone** can be identified but the core recovery was incomplete (Fig. 18). Within Bed -16 (5.83–6.23 m), there are several layers of bioclastic wackestone with bivalves, ostracods, juvenile goniatites, and rare homoctenids, separated by pyrite-enriched, horizontal dissolution seams, which suggest episodic dysoxia. In the higher part, at 5.89 m, and as a filling of a larger orthocone near the top, there are patches of fossiliferous wackestones that are slightly darker and richer in C_{org} and, therefore, transitional towards MF-C2. But the difference to the rest of the bed, also in comparison with HON_1101, is too weak to draw conclusions. The overlying, bioturbated Bed

-15 is characterised by a gradual bloom of ostracods (Fig. 10d) culminating in a thin packstone layer (MF-C5) at the top. The conodont residue contained originally pyritic juvenile bivalves and longiorthoconic cephalopods. This indicates hypoxic conditions and a transition towards the partly laminated black, organic-rich, marly limestone (Bed -14) that forms the top of the Frasnian and represents the **Upper Kellwasser level** (Bed -14, 5.28–5.375 m; Fig. 11f). Fully anoxic facies with rather restricted fauna is typical for basinal Upper Kellwasser settings (e.g. Gereke 2007). The lack of lamination in the upper, unfossiliferous part is caused by recrystallization (micritization), not by bioturbation. The absence of ammonoids indicates hostile conditions both at the seafloor and within the water column.

The overlying flaserlimestone (Bed -13, 5.05–5.28 m) yielded a rich basal Famennian conodont assemblage, which confirms that Bed -14 is the Upper Kellwasser level. The poor core preservation prevents to document the contact at the stage boundary. The lower Famennian nodular to flaser-bedded limestones are bioclastic wackestones (MF-C4) that indicate a return to oxic pelagic facies. The local marl-limestone alternations suggest a slightly deeper setting than for HON_1101. The sedimentary and faunal record was cut off still low in the lower Famennian (near the top of the *Pa. minuta minuta* Zone), probably due to non-deposition since there is no evidence for faulting below the overlying thin Viséan strata (Fig. 5).

Beul section (Fig. 21)

Eisborn Member: At its base (beds B1–4, Fig. 21), 2.8 m of thick bedded and medium grey limestone consists of peloidal grainstones (MF-B2) grading upwards into peloidal, bioclastic wackestones (MF-B1). Tabulate corals dominate the dispersed frame builders but additionally there are rare colonial rugose corals (phaceloid *Disphyllum*), accessory stromatoporoids, crinoid and mollusk debris, as well as ostracods. This detrital variant of the Eisborn Member characterises a drowning of the platform, which caused a significantly reduced carbonate production and flooding of the protecting reef margins. This enabled the subordinate influx of open water organisms, such as conodonts, brachiopods (e.g. the spiriferid *Adolfia*, Fig. 24c–d), and trilobites (*Gondwanaspis*, Helling and Becker 2022, this issue). Moderate currents clumped fine micrite to "pseudopellets" via hydraulic forcing at the seafloor (Fåhræus et al. 1974). The sparse polygnathid fauna supports a correlation of the bioherm drowning with the first pulse of the Frasnes Events in the *Sk. norrisi* Zone (uppermost Givetian; Becker and Aboussalam 2004). Ebert (1993) coined the term **Ense Event** for this topmost Givetian eustatic rise.

At the base of Bed B3 (Frasnian base), the peloids become rarer (MF-B3), due to decreased bottom currents and micrite reworking. In the higher part of Bed B4, thamnoporids become abundant in floatstones (MF-B5a) that also include three genera of stromatoporoids, reflecting an episodic "coral-sponge garden" setting disturbed by distal storms. The next lithological change is marked at the base of Bed B5. From there to Bed B11, the percentage of organic content is increased in more thin-bedded limestones, mostly dark, bioclastic mud-wackestones (MF-B4). This suggests a higher rate of C_{org} burial but there is no corresponding rise in carbon isotope values as evidence for high primary productivity (Becker et al. 2016c). Very typical, despite their small numbers, are small-sized, planispiral, multi-chambered, calcareous foraminifers (*Nanicella*), which had a pantropical distribution in eutrophic reefal facies with moderate water agitation. Solitary, hermatypic Rugosa (*Thamnophyllum*, Becker et al. 2016c, fig. 13) occur in Bed B7. The gradation of MF-B4 into organic-rich and micritic floatstones with alveolitids and gastropods (Bed 8, MF-B5c) or thamnoporids and stromatoporoids (Bed B9, MF-B5b) confirms that the drowned lagoon stayed in the lower part of the euphotic zone. The increase of conodont abundance in beds 6–7 (Tables 2 and 3, middle part of *Ad. rotundiloba pristina* Zone = middle MN Zone 1) correlates with the main deepening pulse of the Frasnes Events in the Ardennes and North Africa (Aboussalam and Becker 2007; Narkiewicz and Bultynck 2010). It should be called **Basal Frasnes Event** in order to enable a clear distinction from the previous top-Givetian deepening.

A small peak of conodont diversity, with seven species, including a new form, is reached in Bed 11 (*Ad. rotundiloba soluta* Subzone, MN Zone 2a). The microfacies is intermediate between the bioclastic MF-B4 and floatstones of MF-B5c/d. There is a gradual return to lighter grey limestone with a higher amount of tabulate corals, such as *Alveolites* and *Platyaxum (Roseoporella)* (Becker et al. 2016c, fig. 16), and some stromatoporoids (*Stachyodes*, *Stromatoporella*). These indicate a minor shallowing but the "reefal garden" (alveolitid-stromatoporoid floatstone, MF-B5b–d) received a lot debris. In the following three beds (beds B12b–B13a), the microfacies became again more organic rich but otherwise without much change (MF-B4 grading into MF-B5d). This episode may correlate with eutrophication and deepening of the *Ad. rotundiloba soluta* Subzone known from the onset of dark, organic-rich marls at Giebringhausen in the eastern Sauerland (Aboussalam and Becker 2017), from the Blauer Bruch section in the Kellerwald (Sandberg et al. 1989, base of Unit H), and from the lower Frasnian maximum of black limestone accumulation in North Africa (Lower Styliolinite, Aboussalam and Becker 2007). The change of conodont biofacies at the top (Bed 13a, sudden income of icriodids) indicates a subsequent minor shallowing, leading to the P-I Biofacies of drowned carbonate platforms of Narkiewicz et al. (2016).

With Bed B13b, another microfacies change occurred. First, there are light-grey alveolitid-thamnoporid floatstones (MF-B5e), an oxygenated "coral garden" setting. After a brief detrital phase (Bed B13c, MF-B3), phaceloid rugose corals (*Disphyllum*) become more abundant (MF-B5g, beds B13d to D) in association with thamnoporids. This suggests

improved living conditions for more fragile reef builders, interrupted by occasional storms. Stromatoporoids and hexagonariids are rare. Interestingly, a short peak of carbon isotope values occurred within this phase (Bed C, Becker et al. 2016c) still within the *Ad. rotundiloba soluta* Subzone. At the top, the disphyllids become rare (Bed E1, MF-B5a). Above, peloidal matrix re-appears, returning at the level of oldest *Ad. recta* (oldest MN Zone 2b, Bed E3) to the setting known from the base of the section (mostly MF-B1).

Remnants of the latest reefal stage of the Hönne Valley Reef are preserved among the roots of fallen trees on the backside of the cliff. Limestone plates display abundant, nicely weathered tabulate and rugose corals in light-grey, fine-grained matrix. Dominant are large, flat alveolitid colonies and thamnoporids, while phillipsastreids (*Haplothecia*) and hexagonariids are rare. Among the Rugosa, *Disphyllum* is abundant and associated with some *Stachyodes* (Becker et al. 2016c). This "coral garden", grading into a thin coral biostrome (coral rud-boundstones, MF-B5i) represents the top of the lower Frasnian. A range of actinopterygian teeth from conodont residues show that it was a good biotope for early bony fishes. Based on the presence of last lower Frasnian conodonts in biostrome slabs and dates for the oldest Beul Formation of core HON_1101, the final biostrome extinction is correlated with the eustatic rise of the global Middlesex Event (see review in Pisarzowska et al. 2020).

Beul Formation: Exposed under more fallen trees ca. 10 metres beyond, the overlying pelagic nodular limestones (bioclastic wackestones, MF C-4) indicate a significant deepening, resulting in an oxic, subphotic setting well-below the storm wave base. We assume a water depth exceeding 80–100 m based on the lack of euphotic biota (including photosynthetic calcimicrobes, such as *Renalcis* or *Sphaerocodium*) and the upper bathymetric estimates of Franke and Walliser (1983) and Wendt and Aigner (1985). This is supported by sections in the Canning Basin (Australia), where one can walk down from reefal carbonates to micritic pelagic limestones of the lower slope (see Playford 1980, fig. 18). Calculation for the implosion depth of beloceratid ammonoids, which occur in the Beul Formation, yielded values between ca. 110 and 170 m (Hewitt 1996).

Conodont dating of the palmatolepid-dominated assemblages as ca. upper half of the middle Frasnian (*Pa. housei* to *Pa. plana* zones, MN zones 8–10) proves an outcrop gap that spans the lower part of the middle Frasnian. This is precisely the interval of extreme condensation or non-deposition in the two studied cores. Conodont residues include shark teeth and inarticulate brachiopods, which are typical in peri-reefal to pelagic facies. The poor macrofauna content suggests that the environment became oligotrophic. More ammonoid-rich upper Frasnian and Famennian nodular limestones are exposed between tree roots and in small, scattered natural cliffs higher up on the slope of the Beul hill (e.g. Wedekind 1913a, 1913b; Lange 1929; Paeckelmann 1938; Price 1982). They included an outcrop of the Upper Kellwasser Limestone with coral- and trilobite-bearing strata just below (Feist and Schindler 1994; Weyer 2016) but details are not known.

Correlation of boreholes and outcrop (Fig. 25)

In both cores, the thick, lower parts of the sections (Asbeck Member) consist of relatively monotonous, lagoonal limestones deposited in a variably calm and restricted palaeoenvironment. The microfacies fluctuates between MF-A1 to A4. It is not possible to correlate individual intervals of *Amphipora* rud-bafflestones (MF-A3) or of fenestral limestones (MF-A4); these record local palaeoecological shifts within the wide platform. This also applies to the three levels of brecciated limestone of core B102 (within the interval from Bed -44 to -39, marked as "br" in Fig. 5). Near the top, the initial drowning and backstepping in the course of the Frasnes Events, with changes from lagoonal to reef core facies (MF-A5), suggest to correlate the upper ca. 6.5 m of Bed -22 in HON_1101 with the ca. 13 m of Bed -30 to Bed -28 in B102. Based on the onset of early *Ancyrodella* in the overlying Bed -21 of HON_1101 and in Bed B3 of the Beul section, the lagoon drowning began roughly at the same time. Due to similar microfacies, the lower part of the Eisborn Member in the Beul outcrop correlates ca. with Bed -25 in core B102. The final reef phase at the top of the lower Frasnian, a biostrome with abundant tabulate and branching rugose corals, is rather similarly developed in all three sections (B102: Bed -25; HON_1101: Bed -20; Beul: top biostrome). This relative homogenization is a remarkable trend that was obviously caused by external factors, such as eustatic rise.

The base of the (hemi)pelagic Beul Formation appears to be diachronous but this is caused by the extreme condensation (HON_1101: beds -18 and -17) to local non-deposition (B102: between Bed -25 and the base of Bed -24) in the lower middle Frasnian. The discontinuous outcrop prevented sampling of the contact in the Beul section but, based on the conodonts, Sample "top 2" correlates with the sample from the basal Beul Formation in core B102. The higher part of the middle Frasnian is rather uniform but with slightly variable accumulation rates (HON_1101: 16 m, Bed -16; B102: less than 11m, Bed -24 to the lower part of Bed -18; Beul outcrop: thickness unknown). In both boreholes, the basal upper Frasnian *semichatovae* Event is apparently marked as a sudden intercalation by laminated black shales (MF-C6, HON_1101: within Bed -15; B102: within Bed -18). The overlying upper Frasnian is more condensed than the middle Frasnian (HON_1101: 2.8 m, Bed -14 to Bed -9; B102: ca. 2.15 m, upper part of Bed -18 to Bed -13). The Lower Kellwasser Limestone is thick and well-developed in HON_1101 (58 cm, Bed -12) but not identifiable in core B102. The Upper Kellwasser equivalents are also characterised by

laterally variably facies (HON_1101: 25 cm, Bed -9b/c, alternating MF-C2 to MF-C4; B102: less than 10 cm, Bed -14, MF-C5 grading upwards into MF-C4). This reflects a small-scale local palaeotopography, with deposition of laminated and marly facies in calmer depressions.

In the lower/middle Famennian, the environment was more stable and monotonous in core HON_1101 (Fig. 16). In core B102, nodular limestones alternate with marls, which caused a more punctuated conodont record that ends much earlier (high in the *Pa. minuta minuta* Zone; Fig. 18). Schäfer (1978, Sample P250) described from the northern part of the Beul a lower Famennian (*Pa. minuta minuta* Zone) reworking unit with resedimented upper Frasnian taxa. This shows that at close distance variably scouring or condensed deposition occurred. Such facies differentiation suggests a small-scale palaeorelief with fluctuating bottom currents on the drowned submarine rise.

Discussion: Causes and patterns of the Hagen-Balve Reef Complex extinction

Controls on the reef demise in the studied sections

In the classical reviews of Rhenish reefs (Jux 1960a, 1960b; Krebs, 1967, 1971, 1974), extinctions were not studied in detail, hardly discussed, or attributed to regional subsidence or block faulting. It was recognised that most reefs did not survive until the end-Frasnian Kellwasser Events but that in many cases black shales directly overlie reef carbonates. The concept that "reefs suffocated in mud due to sudden major subsidence" was also adopted for the Ardennes reef belt in the west (Lecompte 1970). Based on the study of six reefs from the Ardennes to the Wuppertal region, Wilder (1989) suggested a different model in which tectonically triggered precipitation changes caused land plant spreading and increased chemical weathering, resulting in a higher terrestrial discharge of fine detritus and nutrients that, again, led to phytoplankton blooms, increased C_{org} deposition, and euxinic conditions. The model lacked any indicators for Givetian-Frasnian humidity, vegetation cover, proxies for weathering and terrestrial runoff, or precise biostratigraphical data. Therefore, it remained highly hypothetical. For example, it did not consider other explanations, such as open marine nutrient recycling and climatically induced thermohaline upwelling (e.g. Murphy et al. 2000), to explain biogeochemical evidence for phytoplankton blooms in black shales that overlie some of the reefs.

Several processes are widely considered to cause potentially the termination of reef growth: high siliciclastic influx, drowning by rapid eustatic rise or strongly increased subsidence, emersion due to eustatic regression or tectonic uplift, the spread of anoxia, and strong fluctuations of temperature or salinity (for Devonian reefs see review of Copper 2002a). Our biostratigraphically constrained data from the Hönne Valley provide a correlation of reef drowning, backstepping and eventual extinction with three eustatic deepening pulses, the Ense Event, Basal Frasnes Event, and Middlesex Event. There are no indicators for accelerated subsidence, the reverse is true (Krebs 1974), and there was no uplift or subaerial exposure. The fully marine and stenohaline faunas indicate persisting normal salinity. Hypoxic conditions may have developed in the Eisborn Member of the Beul outcrop within the sediment due to increased influx and bacterial recycling of organic matter. But the carbon isotope trends (Becker et al. 2016c) of the dark, bituminous limestones give no support for increased primary productivity. Sea floor anoxia of the *semichatovae* and Kellwasser events arrived long after the reef was dead.

The carbonate production of reefs is normally able to keep up with slow sea level rises, unless its growth is restricted in muddy water, for which there is no regional microfacies evidence. This suggests that the three eustatic pulses in combination with continuing subsidence outpaced the reef builder capacities. This occurred in an interval of pulsed global climatic heating (Joachimski et al. 2009), which probably caused contemporaneous thermohaline upwelling in the adjacent Flinz basins. Kiessling and Simpson (2011) reviewed the potential of ocean acidification as a cause of ancient reef crises but found no evidence in the Upper Devonian.

Comparison with the western Hagen-Balve Reef Complex (Fig. 1)

The area from Hagen to Iserlohn (Fig.1) is characterised by much earlier rapid drowning, during the Taghanic Transgression near the top of the middle Givetian (May and Becker 1996), associated with a sudden onset of organic-rich, dark, pelagic facies. The overlying Flinz limestones and black shales may contain reef debris, top-middle Givetian stringocephalids, and maenioceratids (Denckmann 1902, 1905; Becker 1985), but also upper Givetian goniatites (Denckmann 1901b, 1903; Becker 1985). West of the Lenne river, in the Donnerkuhle Quarry at Hagen-Eppenhausen (Fig. 1), the sharply overlying black shales at the base of the local Eppenhausen Formation (von Kamp 1972) yielded also a pyritic, upper Givetian pharciceratid fauna (Bockwinkel et al. 2013). There was clearly a combined role of rapid sea level rise, eutrophication and suffocation by anoxia at the middle/upper Givetian boundary in that region, which predated the reef drowning in the Hönne Valley region.

Only small-sized reef caps survived, for example at the Steltenberg of Hagen-Hohenlimburg (von Kamp 1972; Fig. 1). Their reef debris is characterised by tabulates, some chaetetid sponges, and dominant solitary rugose corals that grew within the photic zone, proven by the presence of the calcimicrobes *Girvanella* and *Rothpletzella*. The lack of stromatoporoids is conspicuous (May and Becker 1996) and turbiditic limestones occur laterally. This characterises a small-scale, steep slope palaeoenvironment, which was very

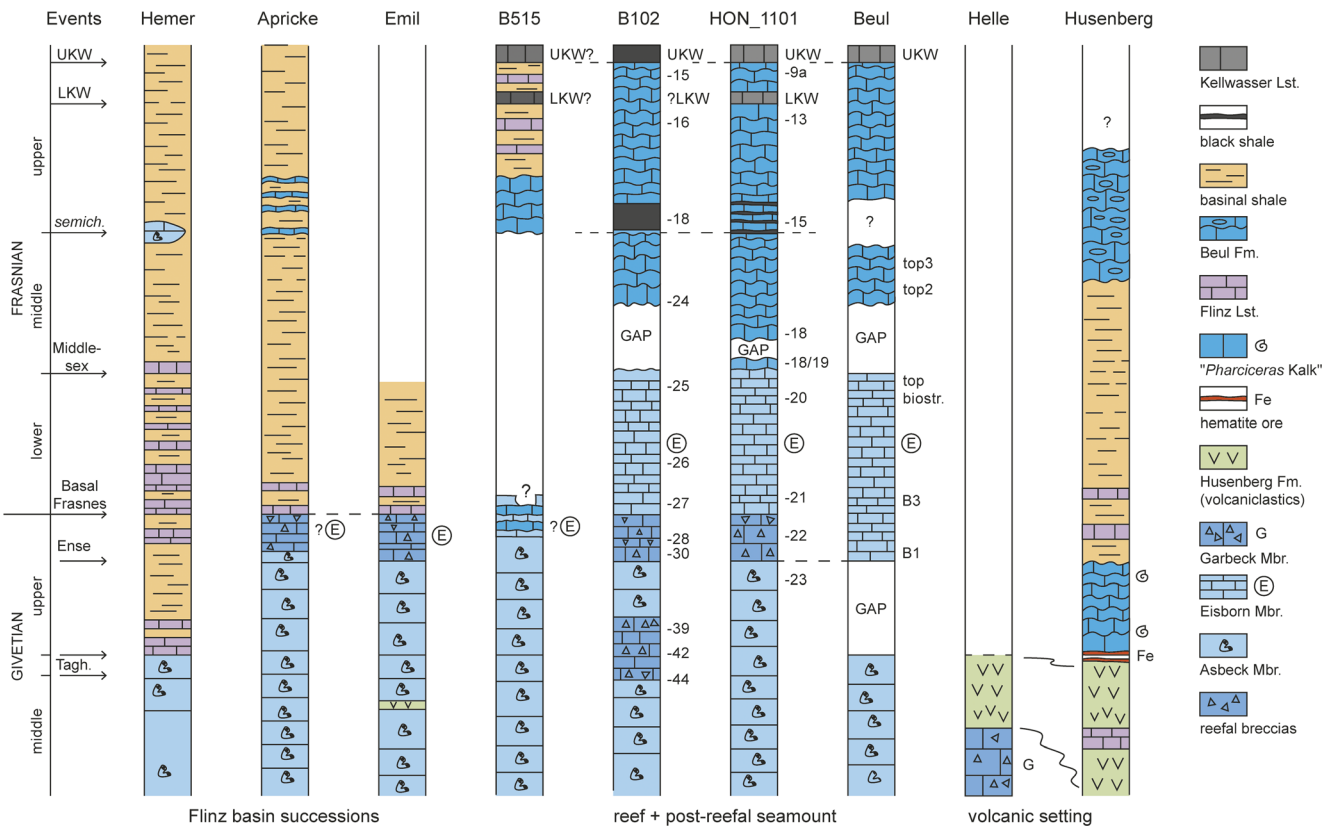

Fig. 25 Middle Givetian to upper Frasnian facies developments, showing the variable timing of reef drowning and extinction, in the eastern part of the Hagen-Balve Reef Complex, from the Hemer region in the west to Balve in the southeast (vertical scale = time, not thicknesses; for localities see Figs. 1–2). Important bed numbers are given for the three studied successions; *Emil* Emil Quarry, *B515* eastern slope of the B515 road just south of Oberrhödinghausen, *Helle* Helle Quarry at the southern end of the Balve Cave

different from the low-relief final reef phase (Eisborn Member) of the Beul area.

The small-sized caps probably did not survive into the top-Givetian but their extinction is not yet well-dated. Higher up, there is a re-surgence of limestone turbidites ("Flinzkalk-Horizont") with some reef margin debris and intercalated marls with goniatites in the lower Frasnian (Becker 1985). This suggests a top middle Givetian reef backstepping towards the southern core of the Remscheid-Altena Anticline, followed by a lower Frasnian phase of progradation, resulting in a northward shift of debris shedding. This latter pulse correlates in time with the lower part of the Eisborn Member at the Beul.

East of Iserlohn, around Bilveringsen (Figs. 1, 3), brachiopod-rich limestones form the famous Schleddenhof Member, which yielded some pre-Taghanic goniatites (Torley 1908, 1934). It represents a gentle slope setting with extremely diverse neritic assemblages. After the Taghanic deepening, the brachiopod limestones were overlain by turbiditic, dark Flinz limestones.

Eastern Hagen-Balve Reef Complex (Figs. 3, 25)

At Hemer (Figs. 1, 25), the organic-rich Flinz limestones and shales overlying the youngest reef contain upper Givetian to middle Frasnian conodonts (Clausen and Ziegler 1989). However, a 2 m thick reef limestone lense was found south of Hemer-Höcklingsen between basal upper Frasnian beds (Heinke 1978: "*Ag. triangularis* Zone"; Figs. 3, 25). Its nature, autochthonous reef growth or allochthonous glide block, is unclear. To the southeast, in the Hemer-Apricke region (Figs. 1, 25), organic-rich, basinal, turbiditic Flinz facies directly overlies the last coral limestones and yielded rich basal Frasnian conodont faunas (*Ad. rotundiloba pristina* Zone, Hoppenberg fauna of Aboussalam and Becker 2009). Therefore, the final reef extinction in that region is also linked with a very sudded change to eutrophic black shales and turbidites, in this case coinciding with the Basal Frasnes Event. It correlates in time with the initial Hönne Valley drowning but pre-dates the final biostrome of the Beul. It seems that there was a younging of the top Hagen-Balve Formation from west to east, interrupted by local cap reefs. The reef breccia noted by Jux (1960a) at the former top of Emil Quarry (Figs. 1, 25) may have been an equivalent of the final alveolitid-thamnoporid biostrome of the Beul area. It was shown to be overlain by basinal and organic-rich Flinz facies, which was confirmed during mapping by Kruse (2013). This basinal post-reefal development ends more or less with the Hönne Valley (Fig. 25).

Paeckelmann (1938) gave a section from the final reef limestones through the Frasnian to lower Famennian at the eastern slope of the B515 road that runs through the Hönne Valley (Fig. 2). It was re-studied by W. Ziegler in 1959 but only the Famennian conodont data were published in 1962. Paeckelmann (1938) noted intercalating light-grey "Adorf Limestone" and dark-grey to black Flinz limestones and shales, with black limestones with buchiolids in higher parts, probably evidence for Kellwasser beds. The important section is now overgrown but we sampled at the southern end of Oberrödinghausen, at 31 km, light-grey limestones that yielded deep-water (*Palmatolepis* biofacies) basal upper Frasnian conodonts of the *Pa. nasuta* Subzone (MN Zone 11b), as known from the Beul. There is no evidence for Frasnian Flinz facies overlying the reef limestones from there towards the east (e.g. Hacke 1999).

Dornsiepen (1973) discussed the considerable decline of reef limestone thicknesses from our study area towards the south and the implications for middle Givetian subsidence variations at short distance. There are no precise data for the reef extinction midway between Oberrhödinghausen and Balve. But Schäfer (1978) emphasised that alternating thin-bedded limestones and basinal shales of Frasnian age occur at the Radeberg NE of Beckum (Fig. 1). This suggests that the post-reefal submarine rise palaeotopography descended to the southeast. Further to the south, from the Balve Cave and adjacent Helle Quarry to Garbeck (Fig. 1), the so-called Garbeck Limestone (Eder 1971; now Garbeck Memer) consists of middle Givetian, thick marginal slope reef talus transported by debris flows and turbidites into a southern basin, where limestone deposition interfingered with the active volcanism (Dobrzinski 2001; Figs. 3, 25). The top of the volcanic succession of the Husenberg at Balve (Figs. 1, 25) was locally covered by iron ore and condensed, upper Givetian goniatite limestones ("*Pharciceras* Kalk", Paeckelmann 1938; Fig. 25). On the flanks, slightly further to the south, pelagic shales with goniatites deposited from the top-middle Givetian on (Clausen 1989). Interestingly, the nodular, micritic Beul Formation characterises not only the drowned reef submarine rise but it expanded eventually southwards, to the Husenberg area (Figs. 3, 25).

Extinctions of other Rhenish reefs

Combined effects of eustatic and hypoxic events on the Middle/Upper Devonian reef development have previously been recognised in other Rhenish reef complexes. In the Aachen region, the Middle Devonian to lower Frasnian is characterised by a biostromal limestone succession, which is sharply overlain by an argillaceous interval, long-known as "Grenzschiefer" (Holzapfel 1910) and re-named as Inde Member by Aboussalam and Becker (2016). Conodonts date the transgression as Timan Event high in the lower Frasnian (*Ad. pramosica* Zone = MN Zone 3b of Aboussalam and Becker in Pisarzowska et al. 2020). Interestingly, the Timan Event has not yet been recognised in more eastern Rhenish reef successions. A full recovery of reef growth is marked in the Aachen region by the re-onset of coral and massive stromatoporoid bearing limestone ("Frasne Reef Limestone = Hahn Member). This mostly middle Frasnian reef platform drowned in the course of the basal upper Frasnian *semichatovae* Transgression (Aboussalam and Becker 2016).

In the western part of the Velbert Anticline, the Frasnes Events are developed as black shale intercalations within the Hofermühle Reef (Hofermühle South Quarry, Ellerkamp et al. 2018). The last reef caps are overlain by a poorly known middle Frasnian siliciclastic unit ("Hülsbeck-Schluffstein-Folge", Ribbert and Lange 1993). Local reef extinction may have been caused by clastic shedding during regression. Frasnian coarse siliciclastics are restricted to the Hofermühle region. This suggests that fluctuating terrestrial discharge did play a role for reef extinctions in a restricted region and that not a single extinction model can be applied to all Rhenish reef bodies.

At the eastern end of the Velbert Anticline, the Wülfrath Reef was initiated on the siliciclastic shelf (Flandersbach Formation) by the deepening of the Basal Frasnes Event (Ribbert and Lange 1993; Becker et al. 2016b). In its upper part, dominating *Stromatactis* bindstones form the Schlupkothen Member, a microbial deep-water (dysphotic) reef platform and subtype of the "Iberg Facies" (Krebs 1974). The record of deep-water palmatolepids indicates a platform drowning, with a partly thick intercalation of black marls, before the *Pa. winchelli* Zone (MN Zone 12) but with an overprint by synsedimentary tectonic tilting (Nowak 2012; Becker et al. 2016b). The Middlesex Event that finally killed the last Hönne Valley biostrome is not yet known to have affected the Wülfrath Reef but the age of a thick black marl unit is not yet constrained. The final drowning and extinction were caused by the transgressive Upper Kellwasser Event (Becker et al. 2016b).

Further to the south, basal Frasnian black shales with goniatites directly overlie the youngest reef limestones of the poorly studied Neandertal Reef. This underlines the different significance of the Frasnes Events for major shifts of reef growth throughout the Velbert Anticline region, simultaneously with the initial Hönne Valley drowning.

In the eastern Rhenish Massif, the last marginal slope limestones with abundant reef debris of the Burgberg Atoll (no. 5 in Fig. 1) yielded conodonts from higher parts of the lower Frasnian (Hartenfels et al. 2016; Duda 2020) but dolomitization masks the final reef extinction. Just to the north, the up to 1200 m thick Brilon reef succession is mostly of Middle Devonian age (no. 4 in Fig. 1). The youngest reefal limestones are younger than in the Hönne Valley (Stritzke 1989, 1990; Brinkmann and Stoppel, in press) and were overlain by upper Frasnian (hemi-)pelagic limestones (Grottenberg Member of

Burgberg Formation, Hartenfels et al. 2016). A possible role of the *semichatovae* Transgression requires more data.

Comparisons of the Hönne Valley succession with the extinction phases of other Rhenish reefs are hampered by the still incomplete knowledge, especially for the Wuppertal (no. 1 in Fig. 1), Attendorn-Elspe (no. 6), and Warstein regions (no. 3). The combined available data for Rhenish reefs suggest a major role of eustatic and anoxic events. The overprint by local/regional factors, such as subsidence, block faulting, volcanism and siliciclastic influx, resulted in a regionally variable significance and expression of event signatures.

Conclusions

The analysis of conodont stratigraphy, reef fauna, and carbonate microfacies in two cores and the only currently available outcrop enable a high-resolution reconstruction of initial backstepping, drowning, and final extinction of the thick Hönne Valley Reef. Results suggest general patterns of Rhenish reef extinctions that occurred well before the end-Frasnian Kellwasser Crisis. The post-reefal strata give insights into the sedimentary and palaeoecological effects of Frasnian and Famennian global events on a stable, pelagic submarine rise formed by the drowned reef platform. Main results are as follows:

1. The upper ca. 80 m of the middle Givetian Asbeck Member consist of lagoonal facies with only four alternating MF-types representing sub- to intertidal conditions interrupted by storms. Most common are dendroid stromatoporoids (*Stachyodes*, *Amphipora*); the spectrum of reef builders is restricted. Despite this, the locally significant subsidence was compensated by reef growth.
2. During regression, fenestral microbialites became dominant, which indicate poor living conditions for other reef fauna. But *Stromatactis* and zebra-limestones, as in the final reef phases of the younger (upper Frasnian) Wülfrath (Velbert Anticline, Städter 1989; Nowak 2012; Becker et al. 2016b), Iberg, and Elbingerode reefs (both Harz Mountains, e.g. Gischler and Erkoç 2012; Weller 1991), never developed.
3. Unlike as in western parts of the Hagen-Balve Reef Complex (May and Becker 1996), the global Taghanic Crisis at the middle/upper Givetian boundary has not been recognised in the Hönne Valley. It may occur below the studied interval, where it could be traced by the known strong extinctions in rugose corals (e.g. Birenheide 1989; Schröder 2005).
4. At the top of the Givetian, the lagoonal Asbeck Member is overlain in the studied boreholes by coarse detritus of the reef core and outer reef margin (MF-A5). This indicates a significant reef backstepping in the course of the global Frasnes Events (eustatic Depophase IIb, Johnson et al. 1985; Becker et al. 2020). It enabled the incursion of low-diversity, open shelf polygnathid-ancyrodellid faunas.
5. The deepening correlates in the Beul outcrop with the oldest beds of the Eisborn Member, with five MF-types and various subtypes that mirror a small-scale differentiation of sheltered "coral gardens" in the drowned lagoon. Such a reef phase was previously unknown from the Rhenish Massif. Its fauna is of low diversity, with only few stromatoporoids, brachiopods, trilobites, and subordinate colonial rugose corals (*Disphyllum*, *Haplothecia*, *Hexagonaria*) that are known from other Frasnian reefs.
6. Conodont faunas of the Eisborn Member give precise ages for two phases of increased organic burial in bituminous dark limestones of the Basal Frasnes Event Interval, in the *Ad. rotundiloba pristina* Zone (MN Zone 1) and *Ad. rotundiloba soluta* Subzone (MN Zone 2a). These pulses did not change significantly the local carbon isotope signal (Becker et al. 2016c) but can be correlated with hypoxic event phases elsewhere, e.g. in North Africa (Aboussalam and Becker 2007).
7. The initial drowning of the Hönne Valley Reef resulted in an extreme reduction of the carbonate production rate. The combined sea-level rise and subsidence could not be compensated any more by the growth of reef builders.
8. The basal Frasnian reef drowning in the Hönne Valley region correlates precisely with the sudden change from the last coral limestones to dark, turbiditic Flinz limestones and shales in the Hemer-Apricke region to the west. In other regions of the northern Rhenish Massif, the Basal Frasnes Event suddenly drowned the Neandertal Reef, interrupted the Höfermühle Reef by black shale packages (Ellerkamp et al. 2018), or formed the foundation for the thick Wülfrath Reef Complex (Becker et al. 2016b).
9. The good correlation of Hönne Valley drowning with eustatic sea-level changes suggests that local tectonic movements were not a main extinction factor. Instead, the subsequent low carbonate accumulation recorded in the stable, condensed facies of the overlying Beul Formation suggests that subsidence slowed considerably. Decreasing synsedimentary tectonic activity is also signaled by the end of volcanism in the Balve area.
10. The final Hönne Valley reef phase is a storm-ridden, (auto)parabiostrome dominated by Tabulata (alveolitids, thamnoporids, MF-B5h–i) and with colonial Rugosa, dated as (top-)lower Frasnian. This facies type resembles parts of the lower Givetian initial phase (Löw et al. 2022, this issue).
11. The final extinction was caused by another rapid deepening, in the scale of several tenth of metres, indicated in core HON_1101 by directly overlying pelagic limestones with deep-water (subphotic) palmatolepid faunas. The resulting water depth is estimated as 80–170 m. The transgression

correlates with the global Middlesex Event at the lower/middle Frasnian boundary, defining the base of eustatic Depophase IIc (Johnson et al. 1985; Becker et al. 2020). Further work should try to find the well-established (summarised in Pisarzowska et al. 2020) global isotope signature.

12. The Beul Formation contains partly very rich pelagic conodont assemblages and consists of eight pelagic microfacies types, four of which are restricted to thin specific event levels. Frasnian samples of core HON_1101 support the refined succession around the global *semichatovae* Event established by Saupe and Becker (2022, this issue).
13. The global *semichatovae* Event Interval is developed in the Hönne Valley region as laminated, anoxic black shales, locally (core HON_1101) with four phases. A cyclic development was previously not known from the Rhenish Massif.
14. In the eastern Rhenish Massif, the extremely condensed Usseln Limestone (Gereke 2007) marks a strongly cyclic pre-Lower Kellwasser regressive phase. Only in core HON_1101, much weaker evidence for contemporaneous shallowing comes from the only thin levels of silty limestone (MF-C7) and peloidal packstone (MF-C8).
15. The Lower Kellwasser Event Interval is only in core HON_1101 distinctive. Its dark-grey, ostracod-mollusk pack-grainstones, with indications of bottom currents, differ strongly from the established typical Lower Kellwasser facies (e.g. Schindler 1990; Gereke 2007). The overlying intra-Kellwasser Interval was extremely condensed and characterised by a return to fully oxic, calm, and bioturbated (hemi-)pelagic facies.
16. The Upper Kellwasser Event Interval is characterised in core HON_1101 by recrystallized, polyphase, partly laminated, partly bioturbated, only moderately organic-rich mollusk wacke-packstone. Such an event facies was previously unknown from the Rhenish Massif. It demonstrates that faunal blooms (e.g. ostracods) related to eutrophication reached shallow settings. In core B102, the event interval is more typically developed as a laminated, black calcareous mudstone.
17. Despite the limited sample size from half cores, all Famennian conodont zones were recognisable. The lower/middle Famennian facies differed at short distance and the top of the Beul Formation is strongly diachronous, probably due to variable bottom currents.
18. Pulses of reef drowning and final extinction were caused in the Hönne Valley and other parts of the northern Rhenish Massif by well-known eustatic events that involved in adjacent Flinz basins spreads of hypoxia, recorded by polyphase black shale/limestone deposition. Regional overprint controlled the variable significance of individual events, which were probably linked to global climatic change, but details are still poorly understood. The main phase of the southern Hönne Valley volcanism clearly predates the polyphase reef decline.
19. The identified non-local factors delimiting reef growth and carbonate accumulation make it unlikely that large amounts of upper Givetian to Famennian carbonate can be expected anywhere in the subsurface continuation of the current outcrops. On the other hand, the dominant lagoonal inner platform setting of the thick top-lower/middle Givetian Asbeck Member, with reef margin deposits mostly known from the south and northwest, suggests a continuation in the underground to the north and east.

Taxonomic notes

Ancyrognathus cf. *triangularis* Youngquist, 1945
(Fig. 14c)

Description: In core HON_1101, the top of Bed -29 yielded a distinctive variant of *Ag. triangularis* with rather wide platforms and without free blade.
Discussion: The many previous illustrations of the species suggest considerable variation concerning platform shapes and ornamentation. Typical *Ag. triangularis* possess a short free blade. Our form resembles the specimen figured by Klapper (1990, fig. 11.12). Provisionally, we name such representatives as *Ag.* cf. *triangularis* until formal morphotypes or subspecies are established.
Age: Basal upper Frasnian, *Pa. feisti* Zone (MN Zone 11).

Icriodus cf. *alternatus* Branson and Mehl, 1934
(Fig. 20i)

Description: Juvenile icriodid from Bed -5 of core B102 with very large, asymmetric basal cavity, three, very small nodes in the longitudinal side rows, and five medium-sized nodes in the median denticle row, with the last bigger one not protruding beyond the posterior end of the cusp.
Discussion: Typical *I. alternatus alternatus* are slender, with a very narrow basal cavity, especially in early stages, and a median row of nodes that are smaller and lower than the side row nodes. A second morphotype of the subspecies is characterised in median to adult stages by a wide cavity that extends laterally. The subspecies *I. alternatus helmsi* and *I. alternatus mawsonae* differ in their denticulation. They were recently studied in terms of morphometrics by Girard et al. (2022) but did not include juveniles with very large and asymmetric cavity. The B102 specimen resembles the juvenile *I. alternatus* figured by Matyja (1993, pl. 24, fig. 2). We identify such forms as *I.* cf. *alternatus* until the morphotype nomenclature is further refined.

Age: Lower Famennian, *Pa. minuta minuta* Zone.

Icriodus aff. *expansus* Branson and Mehl, 1938
(Fig. 22l)

Description: Spindle weakly curved, with seven transverse rows of denticles, where median and side row denticles alternate apart from the two posterior rows. Denticles are not connected by longitudinal or transverse ridges; the median row ones are partly larger and as high as the somewhat spinose side row nodes. At the posterior end, the median row continues with two elongate, ascending denticles, the last of which projects as a spine beyond the posterior platform end. The basal cavity is narrow and subsymmetric, without a spur.
Discussion: In typical *I. expansus* (see Narkiewicz and Bultynck 2010), the side and median denticles do not alternate so strongly, and the side denticles are often somewhat elongate in transverse direction. In *I. symmetricus*, the denticles tend to be connected by ridges and typically also do not alter strongly. Preliminarily, we name our form *I.* aff. *expansus*.
Age: Lower Frasnian, *Ad. rotundiloba soluta* Subzone (MN Subzone 2a), Beul outcrop, Bed E1.

Icriodus cf. *tafilaltensis* Narkiewicz and Bultynck, 2010
(Fig. 23b)

Description: Spindle markedly curved (> 10°), especially in the posterior third, with ten transverse rows of elongated nodes or ridges that are mostly connected to the median denticle row (not in the transverse rows 3–5), and with two large middle row denticles at the posterior end, the last one projecting beyond the large, strongly asymmetric basal cavity.
Discussion: Typical *I. tafilaltensis* are characterised by the merging of the two posterior nodes, which are well separated in our specimen; hence the cf. identification. In addition, *I. tafilaltensis* has not yet been described from the middle Frasnian. The number of transverse nodes and shape of the basal cavity differ from *I. symmetricus*.
Age: Middle Frasnian, *Pa. housei* Zone (MN Zone 8), Beul outcrop, Sample top 2.

Mesotaxis guanwushanensis Tian in Hou, 1988 Morphotype 3
(Fig. 22s)

Description: Platform leaf-shaped, subsymmetric, with a short free blade and a straight, long carina. The basal pit is slightly enlarged and elongate.
Discussion: Aboussalam and Becker (2007) regarded *M. falsiovalis* as a senior synonym of the Chinese *Mes. guanwushanensis*. However, there is a small difference that enables a separation of both taxa. In *Mes. falsiovalis,* the minute basal pit is subcircular while it is narrow and elongate in *Mes. guanwushanensis*. Based on this criterion, three morphotypes are separated in the latter. M1, which includes the holotype, lacks a short free blade and the carina does not reach the posterior platform end. In M2, the carina is also short but there is a free blade. Specimens with a free blade and isolated carina nodes at the posterior end are assigned to M3. In the latter, a basal pit that is slightly wider than the aboral carina, as in the Beul specimen, suggests transition towards *Z. ovalis*. The stratigraphic ranges of the three *guanwushanensis* morphotypes are not yet fully established.
Age: Top-lower Frasnian, Beul outcrop, Sample top reef.

"Ozarkodina" aff. *nonaginta* Klapper, Kuz′min and Ovnatanova, 1996
(Fig. 14f)

Description: Specimens from HON_1101, Bed -29, differ from typical "*Oz." nonaginta* by subdued denticles at the rectangular junction of the two blade parts.
Discussion: *"Ozarkodina" nonaginta* was placed by Dzik (2002) in his prioniodinid genus *Pluckidina*. However, the type-species of this genus is a ramiform element, and the supposedly associated Pa element lacks the typical bending of the *"Oz." nonaginta* Group. Most recently, Kotik et al. (2021) used the generic name "*Lagovina*" (not *Lagovidina*, a Famennian prioniodinid genus), which appears to be a nom. nud. Therefore, there is still no valid genus name for the *nonaginta* Group, left here in *"Ozarkodina"* until further revision. The Beul form may represent a new subspecies that is stratigraphically younger than the established upper range of *"Oz." nonaginta* (see Klapper 1997). Open nomenclature is used until the variability of the latter is better documented.
Age: Basal upper Frasnian, *Pa. feisti* Zone (MN Zone 11).

"Ozarkodina" cf. *plana* (Bischoff and Ziegler, 1957)
(Fig. 23h)

Description: Blade with high, alternating large and smaller teeth anterior of the elongated, slightly laterally expanded, shallow basal cavity, a minor incision above the cavity end, and four isolated posterior teeth that gradually become much shorter, with the tips forming a line that arches downwards.
Discussion: The most similar "ozarkodinid" is the Givetian *"Oz." plana* but our top-middle Frasnian specimen may belong to an un-named homeomorphic taxon.
Age: Top-upper Frasnian, *Pa. plana* Zone (MN Zone 10), Beul outcrop, Sample top 3-1.

"Ozarkodina" aff. *sannemanni* (Bischoff and Ziegler, 1957)
(Fig. 23i)

Description: Blade straight and with very narrow, short platforms with one or two small marginal nodes, developed on both sides above the small, elongated basal cavity.

Discussion: The only very incipient development of platforms with few nodes differs from typical *"Oz." sannemanni sannemanni*, which normally does not occur above the lower Frasnian (Klapper 1997). The *"Oz."* aff. *sannemanni* from the Frasnian of Brazil described by Cardoso et al. (2015) is curved and displays a very different type of basal cavity and asymmetric minor platforms.
Age: Top-upper Frasnian, *Pa. plana* Zone (MN Zone 10), Beul outcrop, Sample top 3-1.

Palmatolepis cf. *housei* Klapper, 2007
(Figs. 15a, 19b)

Description: Core HON_1101 yielded a unique *Palmatolepis* with broad, lappet-like side lobe, orientated slightly anteriorly, and with two sini of the posterior platform margin, followed by an incurved posterior apex. The carina is first straight, then sigmoidal, and becomes straight and very fine after the central node. Core B102 produced a very different form with wide platform, subcircular posterior platform margin, and slightly curved carina that terminates with the central node.
Discussion: The HON_1101 specimen is interpreted as an atypical variant of *Pa. housei* that shows morphological trends towards both *Pa. proversa* (side lobe orientation) and *Pa. semichatovae* (lappet shape of side lobe). The B102 specimen differs from *Pa. housei* in the lack of a posterior carina and of a pointed posterior platform tip but the wide platform and fine anterior carina are similar: In the absence of any other similar species, it is also interpreted as an atypical *Pa. housei* variant.
Age: Middle Frasnian, *?Pa. housei* Zone (MN Zone 8), core B102, Sample -24f; basal upper Frasnian, *Pa. feisti* Zone/Subzone (MN Zone 11), core HON_1101, Sample -16c.

Palmatolepis cf. *plana* Ziegler and Sandberg, 1990
(Fig. 19f)

Description: Sample -24e of borehole B102 yielded a palmatolepid with a very fine posterior carina and strongly asymmetric, anteriorly positioned, wide side lobe, which margin runs almost straight towards the posterior tip.
Discussion: We interprete the specimen as transitional from *Pa. housei* towards *Pa. plana* but closer to the latter because of the subrectangular anterior demarcation of the side lobe. Therefore, we record it in open nomenclature as *Pa.* cf. *plana*.
Age: Top-middle Frasnian, *Pa. plana* Zone (MN Zone 10).

Palmatolepis n. sp.
(Fig. 14l)

Description: Several small, narrow palmatolepids with straight carina, and well-defined side lobe differ from named lower to basal middle Frasnian palmatolepids by their chagrin platform.
Discussion: A similar platform shape, but combined with strong platform ornament, characterises the basal middle Frasnian *Pa. maximovae* Kuz´min, 1998. Since we found only small-sized specimens, they may represent juveniles. Therefore, we prefer to use open nomenclature.
Age: Middle Frasnian, *Pa. punctata* to *Ag. primus* zones (MN zones 5/6), core HON_1101, beds -18/-17.

Polygnathus aff. *varcus* Stauffer, 1940
(Fig. 23g)

Description: Free blade very long (ca. 60 % total length), platform short, rather flat, smooth apart from two incipient nodes where it is widest, margins not upturned and without anterior collar, platform carina with four larger merged nodes and small nodes at the posterior end, basal cavity just anterior of the platform.
Discussion: Typical *Po. varcus* have upturned platform margins and deep adcarinal furrows, more platform carina nodes, and the anterior platform margins descend obliquely, forming a slight collar. The Beul specimens may represent a new taxon but are left in open nomenclature until lower Frasnian *Po. varcus* relatives of the Rhenish Massif are described. The Beul form is not conspecific with the two middle Frasnian taxa (*Po.* aff. *varcus* sp. 1 and 2) illustrated by Aboussalam et al. (2020) from the Middle Atlas basement of Morocco.
Age: Middle Frasnian, *Pa. housei* Zone (MN Zone 8), Beul outcrop, Sample top 2.

Polygnathus sp.
(Fig. 23c)

Description: A fragmentary polygnathid from the lower Beul Formation of the Beul outcrop is characterised by a flat, weakly nodose platform and an unusually fine, strongly curved carina that reaches the posterior end.
Discussion: Polygnathids with such platform morphology are uncommon in the middle Frasnian pelagic facies of the Rhenish Massif. Ziegler et al. (2000) included similar forms in *Po. foliatus*, which lectotype, however, is an objective junior synonym of *Po. dubius* (Huddle, 1970) and characterised by very deep adcarinal throughs.
Age: Middle Frasnian, *Pa. housei* Zone (MN Zone 8), Beul outcrop, Sample top 2.

Zieglerina n. sp. B
(Fig. 22h–i)

Description: Platform narrow, elongate, subsymmetric, and with pointed posterior tip (spear-shaped). Ornament with short ribs and minor nodes along the platform margins that is characterised by a net-like microstructure. Free blade with

six merged denticles ascending in height anteriorly, continuing as a straight carina consisting anteriorly of merged denticles, then of six isolated, gradually smaller denticles that reach the posterior end. Basal cavity centred at ca. the middle of the entire length (0.92 mm) and at ca. 1/3 under the anterior platform, very wide (> 60 % platform width), asymmetric, narrowing but extending far towards the posterior end, filled by concentric growth lamellae.

Discussion: The extended, asymmetric basal pit clearly places the new form in *Zieglerina*, which is partly homeomorphic to the upper Givetian genus *Klapperina*. The narrow platform and pit shapes do not resemble that in any named or figured species of both genera. This would justify the introduction of a new species but since re-sampling failed to provide additional representatives and since specimen B9A.14.73 is fractured, we currently apply open nomenclature (with B for Beul). There is no evidence of pathological morphology. The net-like microstructure underlines the good preservation.

Age: Lower Frasnian, *Ad. rotundiloba soluta* Subzone (MN Subzone 2a), Beul outcrop, Bed B11.

Acknowledgements This paper is part of the Ph.D. Thesis of the first author, supervised by the second author. The research was funded by Lhoist Germany Rheinkalk GmbH. There, we are very thankful to Markus Oehmen, Philipp Meissner, and Gabor Lang, who provided drill core material and gave access to the outcrop. Warmest thanks are given to Gerd Schreiber, Rike Zimmermann, and the preparation team at Münster for their help and support during the preparation of thin-sections. We are grateful to Eva Kuropka, Davina Mattijssen, and Lukas Afhüppe (Münster) for their assistance with the conodont samples. Traudel Fährenkemper (Münster) put considerable efforts into our diagrams. We appreciate the careful reviews by Peter Königshof and of an anonymous reviewer.

Funding Open Access funding enabled and organized by Projekt DEAL. The Ph.D. project of the first author was funded by the Lhoist Germany Rheinkalk GmbH.

Data availability All data generated during or analysed during the current study are included in this published article.

Declarations

Conflict of interest The authors declare that they have no conflict of interest.

References

Aboussalam, Z. S. (2003). Das » Taghanic-Event « im höheren Mittel-Devon von West-Europa und Marokko. *Münstersche Forschungen zur Geologie und Paläontologie, 97*, 1–330.

Aboussalam, Z. S., & Becker, R. T. (2007). New upper Givetian to basal Frasnian conodont faunas from the Tafilalt (Anti-Atlas, southern Morocco). *Geological Quarterly, 51*(4), 345–374.

Aboussalam, Z. S., & Becker, R. T. (2009). Aussterben und Radiation bei Conodonten im Zuge der polyphasen, globalen Frasnes-Events (Grenzbereich Mittel-/Ober-Devon). *Terra Nostra, 2009*(3), 15.

Aboussalam, Z. S., & Becker, R. T. (2016). A lower Frasnian reef drowning episode at Walheim (Aachen region, Inde Syncline, NW Rhenish Massif). In R. T. Becker, S. Hartenfels, P. Königshof, & S. Helling (Eds.), *Middle Devonian to Lower Carboniferous stratigraphy, facies, and bioevents in the Rhenish Massif, Germany – an IGCP 596 Guidebook. Münstersche Forschungen zur Geologie und Paläontologie, 108*, 14–28.

Aboussalam, Z. S., & Becker, R. T. (2017). The upper Givetian to lower Frasnian conodont succession and Frasnes Events at Giebringhausen (NE Rhenish Massif, Germany). In J.-C. Liao, & J. I. Valenzuela-Ríos (Eds.), *Fourth International Conodont Symposium. ICOS IV. "Progress on Conodont Investigation". Cuadernos del Museo Geminero, 22*, 339–341.

Aboussalam, Z. S., Becker, R. T., Richter, J., Hartenfels, S., El Hassani, A., & Eichholt, S. (2020). The unique Devonian of Immouzer-du-Kandar (Middle Atlas basement) – biostratigraphy, faunas, and facies development. *Frontiers in Science and Engineering, Earth, Water and Oceans, Environmental Sciences, 10*(1), 127–173.

Aigner, T. (1985). Storm depositional systems. Dynamic stratigraphy in modern and ancient shallow-marine sequences. *Lecture Notes in Earth Sciences, 3*, 1–174.

Bahr, K. (2021). *Geologische Kartierung im Raum Balve-Mellen-Langenholthausen (Nordsauerland, Blatt 4613 Balve)* (pp. 50 + pp. X). Unpublished B.Sc. Mapping Thesis, Cologne: University of Cologne.

Bargatzky, A. (1881). Die Stromatoporen des rheinischen Devons. *Verhandlungen des naturhistorischen Vereins der preußischen Rheinlande und Westfalens, 38*, 233–304.

Bathurst, R. G. C. (1959). The cavernous structure of some Mississippian *Stromatactis* reefs in Lancashire, England. *Journal of Geology, 67*, 506–521.

Bathurst, R. G. C. (1980). *Stromatactis* – Origin related to submarine-cemented crusts in Paleozoic mud mounda. *Geology, 8*, 131–134.

Batruvkova, L. S. (1967). Stratigraphic importance of Devonian Lingulid Brachiopods in the USSR. In D. H. Oswald (Ed.), *International Symposium on the Devonian System, Calgary, 1967, vol. II,* (pp. 525–529). Calgary: Alberta Society of Petroleum Geologists.

Becker, R. T. (1985). Devonische Ammonoideen aus dem Raum Hohenlimburg-Letmathe (Geologisches Blatt 4611 Hohenlimburg). *Dortmunder Beiträge zur Landeskunde, naturwissenschaftliche Mitteilungen*, *19*, 19–34.

Becker, R. T. (1992). Zur Kenntnis von Hemberg-Stufe und *Annulata*-Schiefer im Nordsauerland (Oberdevon, Rheinisches Schiefergebirge, GK 4611 Hohenlimburg). *Berliner geowissenschaftliche Abhandlungen, E*, *3*, 3–41.

Becker, R. T. (1993). Stratigraphische Gliederung und Ammonoideen Faunen im Nehdenium (Oberdevon II) von Europa und Nordafrika. *Courier Forschungsinstitut Senckenberg*, *155*, 1–405.

Becker, R. T. (in press). Devonian and Lower Carboniferous global events in the Central Variscan orogen. In U. Linnemann (Ed.), *Geology of the Central European Variscides and its Avalonian-Cadomian precursors*. Berlin: Springer.

Becker, R. T., & Aboussalam, Z. S. (2004). The Frasne Event – a phased 2nd order global crisis and extinction period around the Middle-

Upper Devonian boundary. In *Devonian neritic-pelagic correlation and events, International Meeting on Stratigraphy, Rabat, Morocco, March 1–10, 2004*, 8–9, Rabat: Institut Scientifique.

Becker, R. T., & Aboussalam, Z. S. (2013a). The global Chotec Event at Jebel Amelane (Western Tafilalt Platform) – Preliminary data. In R. T. Becker, A. El Hassani, & A. Tahiri (Eds.), *International Field Symposium "The Devonian and Lower Carboniferous of northern Gondwana" – Field Guidebook. Document de l'Institut Scientifique, Rabat*, *27*, 129–134.

Becker, R. T., & Aboussalam, Z. S. (2013b). Middle Givetian to middle Frasnian event stratigraphy at Mdoura-East (western Tafilalt). In R. T. Becker, A. El Hassani, & A. Tahiri (Eds.), *International Field Symposium "The Devonian and Lower Carboniferous of northern Gondwana" – Field Guidebook. Document de l'Institut Scientifique, Rabat, 27*, 143–150.

Becker, R. T., & House, M. R. (2009). Devonian ammonoid biostratigraphy of the Canning Basin. *GSWA Bulletin, 145*, 415–438.

Becker, R. T., House, M. R., Kirchgasser, W. T., & Playford, P. E. (1991). Sedimentary and faunal changes across the Frasnian/Famennian boundary in the Canning Basin of Western Australia. *Historical Biology, 5*, 183–196.

Becker, R. T., Königshof, P., & Brett, C. E. (2016a). Devonian Climate, Sea Level and Evolutionary Events: an introduction. In R. T. Becker, P. Königshof, & C. E. Brett (Eds.), *Devonian Climate, Sea Level and Evolutionary Events*. *Geological Society, London, Special Publications, 423*, 1–10.

Becker, R. T., Aboussalam, Z. S., Hartenfels, S., Nowak, H., Juch, D., & Drozdzewski, G. (2016b). Drowning and sedimentary cover of Velbert Anticline reef complexes (northwestern Rhenish Massif). In R. T. Becker, S. Hartenfels, P. Königshof, & S. Helling (Eds.), *Middle Devonian to Lower Carboniferous stratigraphy, facies, and bioevents in the Rhenish Massif, Germany – an IGCP 596 Guidebook*. *Münstersche Forschungen zur Geologie und Paläontologie, 108*, 76–101.

Becker, R. T., Aboussalam, Z. S., Stichling, S., May, A., & Eichholt, S. (2016c). The Givetian-Frasnian Hönne Valley Reef Complex (northern Sauerland) – an outline of stratigraphy and facies development. In R. T. Becker, S. Hartenfels, P. Königshof, & S. Helling (Eds.), *Middle Devonian to Lower Carboniferous stratigraphy, facies, and bioevents in the Rhenish Massif, Germany – an IGCP 596 Guidebook*. *Münstersche Forschungen zur Geologie und Paläontologie, 108*, 126–140.

Becker, R. T., Hartenfels, S., Helling, S., & Schreiber, G. (2016d). The "Nehden Goniate Shale" (lower Famennian, Brilon Reef Complex, NE Rhenish Massif). In R. T. Becker, S. Hartenfels, P. Königshof, & S. Helling (Eds.), *Middle Devonian to Lower Carboniferous stratigraphy, facies, and bioevents in the Rhenish Massif, Germany – an IGCP 596 Guidebook. Münstersche Forschungen zur Geologie und Paläontologie, 108*, 179–195.

Becker, R. T., Piecha, M., Gereke, M., & Spellbrink, K. (2016e). The Frasnian/Famennian boundary in shelf basin facies north of Diemelsee-Adorf. In R. T. Becker, S. Hartenfels, P. Königshof, & S. Helling (Eds.), *Middle Devonian to Lower Carboniferous stratigraphy, facies, and bioevents in the Rhenish Massif, Germany – an IGCP 596 Guidebook*. *Münstersche Forschungen zur Geologie und Paläontologie, 108,* 220–231.

Becker, R. T., Aboussalam, Z. S., & Hartenfels, S. (2018). The Frasnian-Famennian boundary mass extinction – widespread seismic events, the timing of climatic pulses, "pelagic death zones", and opportunistic survivals. In *The Fossil Week, 5th International Paleontological Congress – Paris, 9th-13th July 2018, Abstract Book*, 107; Paris.

Becker, R. T., Marshall, J. E. A., & Da Silva, A.-C., with contributions by Agterberg, F. P., Gradstein, F. M., & Ogg, J. G. (2020). The Devonian Period. In F. M. Gradstein, J. G. Ogg, M. D. Schmitz, & G. M. Ogg (Eds.), *Geologic Time Scale 2020, Chapter 22* (pp. 733–810). Amsterdam: Elsevier.

Beckmann, H. (1950). *Rhenothyra*, eine neue Foraminiferengattung aus dem rheinischen Mitteldevon. *Neues Jahrbuch für Geologie und Paläontologie, Monatshefte, 1950*, 183–187.

Beckmann, H. (1961). *Geologie des Raumes Letmathe-Oestrich.* Letmathe, Festbuch *(*pp. 1–15). Letmathe: Heimatverlag.

Bigey, F., Brice, D., Bultynck, P., Coen, M., Coen-Aubert, M., Drot, J., Jacobs, L., Lethiers, D., Loboziak, S., Mistiaen, B., Mouraviewff, A. N., Paris, F., Sartenaer, P., Streel, M., & Vachard, D. (1982). *Papers on the Frasnian-Givetian boundary* (pp. 1–199). Bruxelles: Geological Survey of Belgium.

Birenheide, R. (1989). Middle/Upper Devonian boundary rugose coral stratigraphy in the Rhenish Mountains of W. Germany. In N. J. McMillan, A. F. Embry, & D. J. Glass (Eds.), *Devonian of the World, Proceedings of the Second International Symposium on the Devonian System, Calgary, Canada*. *Canadian Society of Petroleum Geologists, Memoir, 14*(III), 141–145.

Bischoff, G., & Ziegler, W. (1957). Die Conodontenchronologie des Mitteldevons und destiefsten Oberdevons. *Abhandlungen des Hessischen Landesamtes für Bodenforschung, 22*, 1–136, 21 pls.

Bockwinkel, J., Korn, D., Ebbighausen, V., & Graf, S. (2013). Late Givetian ammonoids from Hagen-Herbeck, Donnerkuhle quarry (Devonian, Rhenish Mountains). *Neues Jahrbuch für Geologie und Paläontologie, Abhandlungen, 270*(3), 257–274.

Böhm, F., & Brachert, T. C. (1993). Deep-water Stromatolites and *Frutexites* Maslov from the Early and Middle Jurassic of S-Germany and Austria. *Facies, 28*, 145–168.

Bohatý, J., & Herbig, H.-G. (2010): Middle Givetian echinoderms from the Schlade Valley (Rhenish Massif, Germany): Habitats, taxonomy and ecostratigraphy. *Paläontologische Zeitschrift, 84*(3), 365–385.

Branson, E. V., & Mehl, M. G. (1934). Conodonts from the Grassy Creek Shale of Missouri. *University of Missouri Studies, 8*, 171–259 [imprint 1933].

Branson, E. V., & Mehl, M. G. (1938). The conodont genus *Icriodus* and its stratigraphic distribution. *Journal of Paleontology, 12*(2), 156–166.

Brett, C. E., & Allison, P. A. (1998). Paleontological approaches to the environmental interpretation of marine mudrocks. In J. Schieber, W. Zimmerle, & P. S. Sethi (Eds.), *Shales and Mudstones. 1*. (pp. 301–349), Stuttgart: Schweizerbart'sche Verlagsbuchhandlung.

Brinkmann, J., & Stoppel, D. (in press). The Geology of the Brilon Reef Complex. *Geologisches Jahrbuch, Sonderheft.*

Bultynck, P. (2003). Devonian Icriodontidae: biostratigraphy, classification and remarks on paleoecology and dispersal. *Revista Española de Micropaleontologia, 35*(3), 295–314.

Burchette, T. P. (1981). European Devonian reefs: a review of current concepts and models. In D. F. Toomey (Ed.), *European fossil reef models*. *SEPM Special Publication*, *30*, 85–142.

Cardoso, C. N., Sanz-López, J., Blanco-Ferrera, S., Lemos, V. B., & Scomazzon, A. K. (2015). Frasnian conodonts at high palaeolatitude (Amazonas Basin, north Brazil). *Palaeogeography, Palaeoclimatology, Palaeoecology, 418*, 57–64.

Carmichael, S. K., Waters, J. A., Königshof, P., Suttner, T. J., & Kido, E, (2019). Paleogeography and paleoenvironments of the Late Devonian Kellwasser event: A review of its sedimentological and geochemical expression. *Global Planetary Change, 183*, 1–17.

Casier, J-G, & Devleeschouwer, X. (1995), Arguments (ostracodes) pour une régression culminant proximité de la limite Frasnien-Famennien Sinsin. *Bulletin de l'Institut royal des Sciences naturelles de Belgique, Sciences de la Terre, 65*, 51–68.

Çinar, C. (1978). Marine Flachwasserfazies in den Honseler Schichten (Givet-Stufe,Lüdenscheider Mulde, Rechtsrheinisches Schiefergebirge). *Göttinger Arbeiten zur Geologie und Paläontologie, 20*, 1–77.

Clausen, C.-D. (1989). Die Goniatiten der Bohrung Balve 1 (Sauerland, östliches Rheinisches Schiefergebirge). *Fortschritte in der Geologie von Rheinland und Westfalen, 35*, 31–56.

Clausen, C.-D, & Ziegler, W. (1989). Die neue Mittel-/Oberdevon-Grenze - ihre Anwendungsmöglichkeiten im Rheinischen Schiefergebirge. *Fortschritte in der Geologie von Rheinland und Westfalen, 35*, 9–30.

Copper, P. (2002a). Silurian and Devonian reefs: 80 million years of global greenhouse between two ice ages. *SEPM Special Publication, 72*, 181–238.

Copper, P. (2002b). Reef development at the Frasnian/Famennian mass extinction boundary. *Palaeogeography, Palaeoclimatology, Palaeoecology, 181*, 27–65.

Copper, P., & Scotese, C. R. (2003). Megareefs in Middle Devonian supergreenhouse climates. In M. A. Chan & A. W. Archer (Eds.), *Extreme depositional environments: Mega end members in geologic time. Geological Society of America, Special Paper, 370*, 209–230.

Day, J., & Witzke, B. F. (2017). Upper Devonian Biostratigraphy, Event Stratigraphy, and Late Frasnian Kellwasser Extinction Bioevents in the Iowa Basin: Western Euramerica. In M. Montenari (Ed.) *Stratigraphy & Timescales, 2*, 243–332, Burlington: Academic Press.

Denayer, J., & Poty, E. (2010). Facies and palaeoecology of the upper member of the Aisemont Formation (Late Frasnian, S. Belgium): an unusual episode within the Late Frasnian crisis. *Geologica Belgica*, *13*, 197–212.

Denckmann, A. (1901a). Ueber das Oberdevon auf Blatt Balve (Sauerland). *Jahrbuch der Königlich preußischen geologischen Landesanstalt und Bergakademie, für 1900, 21*, I–XIX.

Denckmann, A. (1901b). Goniatiten aus dem unteren Oberdevon der Gegend von Iserlohn-Letmathe. *Zeitschrift der deutschen geologischen Gesellschaft, 54*, 16–18.

Denckmann, A. (1902). Über Devon und Carbon des Sauerlandes. *Jahrbuch der Preußischen Geologischen Landesanstalt, 23*, 554–556.

Denckmann, A. (1903). Über die untere Grenze des Oberdevons im Lennetale und im Hönnetale. *Zeitschrift der deutschen geologischen Gesellschaft, 55*, 392–402.

Denckmann, A. (1905). Über Devon und Carbon des Sauerlandes. Bericht über die wissenschaftlichen Ergebnisse der Aufnahmen auf den Blättern Hohenlimburg und Balve. *Jahrbuch der Königlich preußischen geologischen Landesanstalt, 33*, 554–596.

Denckmann, A., & Lotz, H. (1900). Über einige Fortschritte in der Stratigraphie des Sauerlandes. *Zeitschrift der deutschen geologischen Gesellschaft, 52*, 564–567.

De Vleeschouwer, D., Rakociński, M., Racki, G., Bond, D. P. G., Sobień, K., & Claeys, P. (2013). The astronomical rhythm of Late-Devonian climate change (Kowala section, Holy Cross Mountains, Poland). *Earth and Planetary Science Letters, 365*, 25–37.

Devleeschouwer, X., Petitclerc, E., Spassiov, S., Préat, A. (2010). The Givetian-Frasnian boundary at Nismes Parastratotype (Belgium): The magnetic susceptibility signal controlled by ferromagnetic minerals. *Geologica Belgica, 13*(4): 351–366

Dobrzinski, N. (2001). *Geologische Kartierung im Südwesten von Blatt 4613, Balve (Märkischer Kreis/Nordrhein-Westfalen)* (pp. 1–48). Unpublished Diploma Mapping Thesis, Münster: Westfälische Wilhelms-Universität Münster.

Dopieralska, J., Belka, Z., & Walczak, A. (2015). Nd isotope composition of conodonts; An accurate proxy of sea-level fluctuations. *Gondwana Research*, *34*, 284–295.

Dornsiepen, U. (1973). *Die Geologie des Massenkalkes von Balve (Ostrheinisches Schiefergebirge)* (pp. 1–62). Unpublished Diploma Thesis, Braunschweig: Naturwissenschaftliche Fakultät der Technischen Universität Braunschweig.

Dreesen, R., & Dusar, M. (1975). Refinement of conodont biozonation in the Famenne-type. In *Namur 1974, International Symposium in Belgian micropalaeontological limits, from Emsian to Viséan, September 1st to 10th, Publication No. 13*, 1–36, 7 pls.

Dubicka, Z. (2017). Extinction of nanicellid foraminifera during the Frasnian-Famennian biotic crisis: some far-reaching evolutionary consequences. *Lethaia, 51*(2), 112–119.

Dumoulin, V., Bertrand, M., & Preat, A. (1996). Microfacies et cyclicite au sein d´un complexe biostromal de la partie moyenne du Frasnien a cerfontaine “Massif de Phillipeville”, Synclinorium de Dinant (Belgique). *Bulletin de la Société belge de Géologie*, *105*(3/4), 99–118.

Duda, K. (2020). *Der Grenzbereich Unter-/Mittel-Frasnium am Beringhauser Tunnel (Ostsauerland) – Biostratigraphie, Mikrofazies, Isotopengeochemie* (pp. 1–43). Unpublished B.Sc. Thesis, Münster: Westfälische Wilhelms-Universität Münster.

Dunham, R. J. (1962). Classification of carbonate rocks according to depositional texture. *American Association of Petroleum Geologists, Memoir, 1*, 108–121.

Dzik, J. (2002). Emergence and collapse of the Frasnian conodont and ammonoid communities in the Holy Cross Mountains, Poland. *Acta Palaeontologica Polonica, 47*(4), 565–650.

Ebert, J. (1993). Globale Events im Grenz-Bereich Mittel-/Ober-Devon. *Göttinger Arbeiten zur Geologie und Paläontologie, 59*, 1–106.

Eder, W. (1970). Genese Riff-naher Detritus-Kalke bei Balve im Rheinischen Schiefergebirge (Garbecker Kalk). *Verhandlungen der Geologischen Bundesanstalt, 1970*(4), 551–569.

Eder, W. (1971). Riff-nahe detritische Kalke bei Balve im Rheinischen Schiefergebirge (Mittel-Devon, Garbecker Kalk). *Göttinger Arbeiten zur Geologie und Paläontologie*, *10*, 1–66.

Eder, W., & Franke, W. (1982). Death of Devonian reefs. *Neues Jahrbuch zur Geologie und Paläontologie, Abhandlungen, 163*(2), 241–243.

Eichholt, S., & Becker, R. T. (2016). Middle Devonian reef facies and development in the Oued Cherrat Zone and adjacent regions (Moroccan Meseta). *Facies, 62*(2), article 7, 29 pp.

Eiserlo, U. (1987). *Die geologische Gliederung des Steinbruchs Asbeck/ Hönnetal* (pp.1–31). Unpublished Diploma Thesis, Bochum: Ruhr-Universität Bochum.

Ellerkamp, M.-P., Becker, R. T., Schlösser, M., & Aboussalam, Z. S. (2018). Die einzigartige Schneckenfauna aus dem Grenzbereich des Mittel- und Oberdevons von Hofermühle. *Archäologie im Rheinland, 2017*, 33–35.

Embry, A. F., & Klovan, E. J. (1971). A Late Devonian reef tract on Northeastern Banks Island, NWT. *Canadian Society of Petroleum Geologists, 19*, 730–781.

Etter, W. (1995). Benthic diversity patterns in oxygenation gradients: an example from the Middle Jurassic of Switzerland. *Lethaia, 28*, 259–270.

Faber, P. (1980). Fazies-Gliederung und Entwicklung im Mittel-Devon der Eifel. *Mainzer geowissenschaftliche Mitteilungen, 8*, 83–149.

Fåhræus, L. E., Slatt, R. M., & Nowlan, G. S. (1974). Origin of carbonate pseudopellets. *Journal of Sedimentary Petrology, 44*(1), 27–29.

Falahatgar, M., May, A., & Sarfi, M. (2018). First report of the rugose coral *Hexagonaria davidsoni* from the Koshyeilagh Formation (Devonian), Alborz Mountains, Northeastern Iran. *Boletín de la Sociedad Geológica Mexicana, 70*(39), 787–795.

Feist, R., & Schindler, E. (1994). Trilobites during the Frasnian Kellwasser Crisis in European Late Devonian cephalopod limestones. *Courier Forschungsinstutut Senckenberg, 169*, 195–223.

Flick, H., & Schmidt, J. (1987). Eine Vulkaninsel mit Saumriff im Devon des südlichen Rheinischen Schiefergebirges. *Facies, 17*, 67–72.

Flügel, E. (1972). Mikrofazielle Untersuchungen in der Alpinen Trias, Methoden und Probleme. *Mitteilungen der Gesellschaft der Geologie und Bergbaustudenten in Österreich*, *21*, 9–64.

Flügel, E. (1978). *Mikrofazielle Untersuchungsmethoden von Kalken* (pp. 1–454), Berlin: Springer-Verlag.

Flügel, E. (2004). *Microfacies of Carbonate rocks. Analysis Interpretation and Application* (pp. 1–976). Berlin: Springer-Verlag.

Flügel, E., & Hötzl, H. (1976). Palökologische und statistische Untersuchungen im mitteldevonischen Schelf-Kalken (Schwelmer Kalk/Givet/Rheinisches Schiefergebirge). *Bayerische Akademie der Wissenschaften, Mathematisch-Naturwissenschaftliche Klasse, Abhandlungen, 156*, 1–70.

Flügel, E., & Kiessling, W. (2002). Patterns of Phanerozoic reef crisis. In W. Kiessling, E. Flügel, & J. Golonka (Eds.), Phanerozoic reef patterns. *SEPM Special Publication, 72*, 691–733.

Franke, W. (1973). Fazies, Bau und Entwicklungsgeschichte des Iberger Riffes (Mitteldevon bis Unterkarbon III, NW-Harz, W-Deutschland). *Geologisches Jahrbuch, A11*, 3–127.

Frech, F. (1886). Die Cyathophylliden und Zaphrentiden des deutschen Mitteldevon, eingeleitet durch den Versuch einer Gliederung derselben. *Palaeontologische Abhandlungen, 3*(3), 117–234, pls. 13–20.

Fuchs, A. (1990). Charakter und Ende der devonischen Riffentwicklung im Elbingeröder Komplex (Harz.) *Facies, 23*, 97–108.

Garland, J., Tucker, M. E., & Scrutton, C. T. (1996). Microfacies analysis and metre-scale cyclicity in the Givetian back-reef sediments of south-east Devon. *Proceedings of the Ussher Society, 9*, 31–36.

Gereke, M. (2007). Die oberdevonische Kellwasser-Krise in der Beckenfazies von Rhenohercynikum und Saxothuringicum (spätes Frasnium/frühestes Famennium, Deutschland). *Kölner Forum für Geologie und Paläontologie, 17*, 1–228.

Gereke, M., & Schindler, E. (2012). "Time-Specific-Facies" and biological crises – The Kellwasser Event interval near the Frasnian/Famennian boundary (Late Devonian). *Palaeogeography, Palaeoclimatology, Palaeoecology, 367–368*, 19–29.

Gereke, M., Luppold, F. W., Piecha, M., Schindler, E., & Stoppel, D. (2014). Die Typlokalität der Kellwasser-Horizonte im Oberharz, Deutschland. *Zeitschrift der Deutschen Gesellschaft für Geowissenschaften, 165*(2), 145–162.

Ginter, M., & Ivanov, A. (2000). Stratigraphic distribution of chondrichthyans in the Devonian on the East European Platform margin. *Courier Forschungsinstitut Senckenberg, 223*, 325–339.

Girard, C., Klapper, G., & Feist, R. (2005). Subdivision of the terminal Frasnian *linguiformis* conodont Zone, revision of the correlative interval of Montagne Noire Zone 13, and discussion of stratigraphically significant associated trilobites. In D. J. Over, J. R. Morrow., & P. B. Wignall (Eds.), Understanding Late Devonian and Permian-Triassic Biotic and Climatic Events: Towards an Integrated Approach. *Developments in Palaeontology & Stratigraphy, 20*, 181–198.

Girard, C., Charruault, A.-L., Gluck, T., Corradini, C., & Renault, S. (2022). Deciphering the morphological variation and its ontogenetic dynamics in the Late Devonioan conodont *Icriodus alternatus*. *Fossil Record, 25*(1), 25–41.

Gischler, E., & Erkoç, M. M. (2012). Facies of Devonian fore reef limestones: a quantitative study (Iberg Reef, Harz Mts., Germany). *Palaeobiodiversity and Palaeoenvironments, 93*(1), 91–101.

Gouwy, S., Hayduckiewicz, J., & Bultynck, P. (2007). Conodont-based graphic correlation of upper Givetian-Frasnian sections of the Eastern Anti-Atlas (Morocco). *Geological Quarterly, 51*(4), 375–392.

Gutschick, R. C., & Sandberg, C. A. (1983). Mississipian continental margins of the conterminous United States. *SEPM Special Publications, 33*, 79–96.

Hacke, T. (1999). *Die Hangendgrenze des mitteldevonischen Massenkalkes und seine auflagernden Schichten bis in das untere Namur am Nordrand des Remscheid-Altenaer Sattels im Bereich Asbeck und Eisborn (Hönnetal/Sauerland)* (pp.1–53). Unpublished Diploma Mapping Thesis, Clausthal-Zellerfeld: Technische Universität Clausthal.

Ham, W. E. (1952). Algal origin of the "Birdseyes" Limestone in the McLish Formation. *Oklahoma Academy of Sciences, Proceedings, 33*, 200–203.

Hartenfels, S. (2003). *Karbonatmikrofazies und Conodontenbiofazies ausgewählter Profile im Oberdevon und Unterkarbon des Frankenwaldes und des Bayerischen Vogtlandes – Geuser, Kirchgattendorf, Köstenhof (NE-Bayern, Deutschland)* (pp.1–175). Unpublished Diplom Thesis, Cologne: Universität zu Köln.

Hartenfels, S. (2011). Die globalen *Annulata*-Events und die Dasberg-Krise (Famennium, Oberdevon) in Europa und Nord-Afrika – hochauflösende Conodonten-Stratigraphie, Karbonat-Mikrofazies, Paläoökologie und Paläodiversität. *Münstersche Forschungen zur Geologie und Paläontologie*, *105*, 17–527.

Hartenfels, S., & Becker, R. T. (2016a). Famennian sedimentation, faunas, and event stratigraphy at Effenberg Quarry (Remscheid-Altena Anticline, Rhenish Massif). In R. T. Becker, S. Hartenfels, P. Königshof, & S. Helling (Eds.), *Middle Devonian to Lower Carboniferous stratigraphy, facies, and bioevents in the Rhenish Massif, Germany – an IGCP 596 Guidebook. Münstersche Forschungen zur Geologie und Paläontologie, 108*, 141–157.

Hartenfels, S., & Becker, R. T. (2016b online). Age and correlation of the transgressive *Gonioclymenia* Limestone (Famennian, Tafilalt, eastern Anti-Atlas, Morocco). *Geological Magazine, 155*(3), 586–629 [printed 2018].

Hartenfels, S., Becker, R. T., & Aboussalam, Z. S. (2016). Givetian to Famennian stratigraphy, Kellwasser, *Annulata* and other events at the Beringhauser Tunnel (Messinghausen Anticline, eastern Rhenish Massif). In R. T. Becker, S. Hartenfels, P. Königshof, & S. Helling (Eds.), *Middle Devonian to Lower Carboniferous stratigraphy, facies, and bioevents in the Rhenish Massif, Germany – an IGCP 596 Guidebook. Münstersche Forschungen zur Geologie und Paläontologie*, *108*, 196–219.

Hartenfels, S., Becker, R. T., Nowak, H., Aboussalam, Z. S., Juch, D., & Drozdzewski, G. (2017). Das letzte rheinische Riff ertrinkt – neue Erkenntnisse aus dem Oberdevon von Wülfrath. *Archäologie im Rheinland, 2016*, 60–62.

Hartenfels, S., Becker, R. T., Drozdzewski, G., Juch, D., & Aboussalam, Z. S. (2018). "Kommen und Gehen" einer bisher unbekannten Gesteins- und Fossilabfolge beim A44-Neubau bei Hülsbeck. *Archäologie im Rheinland, 2017*, 36–38.

Hartenfels, S., Becker, R. T., Herbig, H.-G., Qie, W.-K., Kumpan, T., De Vleeschouwer, D., Weyer, D., & Kalvoda, J. (2022). The Devonian-Carboniferous transition at Borkewehr near Wocklum (northern Rhenish Massif, Germany) – a potential GSSP section. In S. Hartenfels, C. Hartkopf-Fröder, & P. Königshof (Eds.), T*he Rhenish Massif: More than 150 years of research in a Variscan mountain chain. Palaeobiodiversity and Palaeoenvironments 102*(3). https://doi.org/10.1007/s12549-022-00531-5. [this issue]

Hartkopf-Fröder, C., & Weber, H. M. (2016). From Emsian coastal to Famennian marine environments: palaeogeographic evolution and biofacies in the Bergisch Gladbach-Paffrath Syncline area (Rhenish Massif, Germany). In R. T. Becker, S. Hartenfels, P. Königshof, & S. Helling, (Eds.), *Middle Devonian to Lower Carboniferous stratigraphy, facies, and bioevents in the Rhenish Massif, Germany – an IGCP 596 Guidebook. Münstersche Forschungen zur Geologie und Paläontologie*, *108*, 46–75.

Heinke, H.-J. (1978). *Stratigraphische und fazielle Untersuchungen im Devon und Unterkarbon am Nordrand des Remscheid-Altenaer-Sattels zwischen Iserlohn und dem Hönnetal (Mbl. 4612 Iserlohn, Mbl. 4512 Menden und Mbl. 4613 Balve).* Unpublished Diplom Thesis, Phillips-University Marburg, 132 pp., 3 pls, 1 map.

Helling, S., & Becker, R. T. (2022). Two new species of *Gondwanaspis* (Trilobita, Odontopleurida) from around the Givetian-Frasnian boundary of the northern Rhenish Massif. In S. Hartenfels, C. Hartkopf-Fröder, & P. Königshof (Eds.), *The Rhenish Massif: More than 150 years of research in a Variscan mountain chain. Palaeobiodiversity and Palaeonenvironments 102*(3). https://doi.org/10.1007/s12549-022-00525-3. [this issue]

Hering, G. (1995). Milankovitch-Zyklen in mitteldevonischen Schelf-Carbonaten des Rheinischen Schiefergebirges. *Göttinger Arbeiten zur Geologie und Paläontologie, 65*, 1–63.

Hewitt, R. A. (1996). Architecture and Strength of the Ammonoid Shell. In N. H. Landman, K. Tanabe, K., & R. A. Davis (Eds.), Ammonoid Paleoniology. *Topics in Geobiology, 13*, 297–339.

Hladil, J. (1986). Trends in the development and cyclic patterns of middle and upper Devonian buildups. *Facies, 15*, 1–34.

Holzapfel, E. (1910). Die Geologie des Nordabfallens der Eifel mit besonderer Berücksichtigung der Gegend von Aachen. Mit einer geologischen Exkursionskarte für die Umgebung von Aachen von W. Wunstorf. *Abhandlungen der Königlichen Preußischen Geologische Landesanstalt, Neue Folge, 66*, 1–218.

Hou, H.-F. (Ed., 1988). *Devonian stratigraphy, paleontology and sedimentary facies of Longmenshan, Sichuan.* Beijing: Geological Publishing House.

House, M. R. (1985) Correlation of mid-Palaeozoic ammonoid evolutionary events with global sedimentary perturbations. *Nature, 313*, 17–22.

House, M. R., Menner, V. V., Becker, R. T., Klapper, G., Ovnatanova, N. S., & Kuz´min, A. V. (2000). Reef episodes, anoxia and sea-level changes in the Frasnian of the southern Timan (NE Russian platform). In E. Insalaco, P. W. Skelton, & T. J. Palmer (Eds.), *Carbonate Platform Systems: components and interactions*. *Geological Society, London, Special Publication, 178*, 147–176.

Huddle, J. W. (1970). Revised descriptions of some Late Devonian conodont genera andspecies proposed by Ulrich and Bassler in 1926. *United States Geological Survey, Professional Paper, 578*, 1–55.

Ivanov, A. O. (2021). A New Phoebodontid Shark from the Devonian of the Urals and the Distribution of *Phoebodus* Species. *Paleontological Journal, 55*(3), 301–310.

Jakubowicz, M., Belka, Z., & Berkowski, B. (2014). *Frutexites* encrustations on rugose corals (Middle Devonian, southern Morocco): complex growth of microbial microstromatolites. *Facies, 60*, 631–650.

Joachimski, M. M., Breisig, S., Buggisch, W., Talent, J. A., Mawson, R., Gereke, M., Morrow, J. R., Day, J. & Weddige, K. (2009): Devonian climate and reef evolution: Insights from oxygen isotopes in apatite. *Earth and Planetary Science Letters, 284*, 599–609.

Johnson, J. G., Klapper, G., & Sandberg, C. A. (1985). Devonian eustatic fluctuations in Euramerica. *Geological Survey of America, Bulletin, 96*, 567–587.

Jux, U. (1960a). Die devonischen Riffe im Rheinischen Schiefergebirge, Teil I. *Neues Jahrbuch für Geologie und Paläontologie, Abhandlungen, 110*(2), 186–258.

Jux U (1960b) Die devonischen Riffe im Rheinischen Schiefergebirge, Teil II. *Neues Jahrbuch für Geologie und Paläontologie, Abhandlungen, 110*(3), 259–392.

Jux, U. (1964). Zur stratigraphischen Gliederung des Devonprofils von Bergisch Gladbach (Rheinisches Schiefergebirge). *Decheniana, 117*(2), 159–174.

Kamp, H. von (1972). *Erläuterungen zu Blatt 4611 Hohenlimburg, 2. völlig neu bearbeitete Auflage.* Geologische Karte von Nordrhein-Westfalen 1:25000 (pp. 1–182). Krefeld: Geologisches Landesamt Nordrhein-Westfalen.

Kershaw, S. (1994). Classification and Geological Significance of Biostromes. *Facies, 31*, 81–92.

Kiessling, W. (2008). Sampling-standardized expansion and collaps of reef building in the Phanerozoic. *Fossil Record, 11*(1), 7–18.

Kiessling, W., & Simpson, C. (2011). On the potential for ocean acidification to be a general cause of ancient reef crises. *Global Change Biology, 17*, 56–67.

Kiessling, W., Flügel, E., & Golonka, J. (1999). Paleoreef maps: evaluation of a comprehensive database on Phanerozoic reefs. *The American Association of Petroleum Geologists, Bulletin, 83*(10), 1552–1587.

Klapper, G. (1989). The Montagne Noire Frasnian (Upper Devonian) conodont succession. In N. J. McMillan, A. Embry, & D. J. Glass (Eds.), Devonian of the world. *Canadian Society of Petroleum Geologists Memoir, 14*(III), 449–468 [imprint 1988].

Klapper, G. (1990). Frasnian species of the Late Devonian conodont genus *Ancyrognathus*. *Journal of Paleontology, 64*(6), 998-1025.

Klapper, G. (1997). Graphic correlation of Frasnian (Upper Devonian) sequences in Montagne Noire, France, and western Cabada. *Geological Society of America, Special Paper, 321*, 113–128.

Klapper, G. (2007). Frasnian (Upper Devonian) conodont succession at Horse Spring and correlative sections, Canning Basin, Western Australia. *Journal of Paleontology, 81*(3), 513–537.

Klapper, G. (2021). Revision of the Frasnian Late Devonian conodont genus *Ancyrodella. Bulletin of Geosciences, 96*(3), 295–325.

Klapper, G., & Kirchgasser, W. T. (2016). Frasnian Late Devonian conodont biostratigraphy in New York: graphic correlation and taxonomy. *Journal of Paleontology, 90*(3), 525–554.

Klapper, G., Feist, R., Becker, R. T., & House, M. R. (1993). Definition of the Frasnian/Famennian Stage boundary. *Episodes, 16*(4), 433–441.

Klapper, G., Kuz´min, A. V., & Ovnatanova, N. S. (1996). Upper Devonian conodonts from the Timan-Pechora region, Russia, and correlation with a Frasnian composite standard. *Journal of Paleontology, 70*(1), 131–152.

Klapper, G., Uyeno, T. T., Armstrong, D. K., & Telford, P. G. (2004). Conodonts of theWilliams Island and Long Rapids formations (Upper Devonian), Frasnian-Famennian) of the Onakawana B Drillhole, Moose River Basin, northern Ontario, with a revision of lower Famennian species. *Journal of Paleontology, 78*(2), 371–387.

Koch-Früchtl, U., & Früchtl, M. (1993). Stratigraphie und Faziesanalyse einer mitteldevonischen Karbonatabfolge im Remscheid-Altenaer Sattel (Sauerland). *Geologie und Paläontologie in Westfalen, 26*, 47–75.

Koptíková, L., Bábek, O., Hladil, J., Kalvoda, J., & Slavík, L. (2010). Stratigraphic significance and resolution of spectral reflectance logs in Lower Devonian carbonates of the Barrandian area, Czech Republic; correlation with magnetic susceptibility and gamma-ray logs. *Sedimentary Geology, 225*, 83–89.

Kotik, I. S., Zhuravlev, A. V., Maydl, T. V., Bushnev, D. A., & Smoleva, I. V. (2021). Early-Middle Frasnian (Late Devonian) carbon isotope Event in the Timan-Pechora Basin (Chernyshev Swell, Pymvashor River section, North Cis-Urals, Russia). *Geologica Acta, 19*(3), 1–17.

Kralick, J. A. (1994). The conodont genus *Ancyrodella* in the middle Genesee Formation (lower Upper Devonian, Frasnian), Western New York. *Journal of Paleontology, 68*(6), 1384–1395.

Krebs, W. (1967). Reef development in the Devonian of the eastern Rhenish Slate Mountains, Germany. In D. H. Oswald (Ed.), *International Symposium on the Devonian System, Calgary, 1967, II,* (pp. 295–306). Calgary: Alberta Society of Petroleum Geologists.

Krebs, W. (1971). Die devonischen Riffe in Mitteleuropa. *Mitteilungen der Technischen Universität Carolo-Wilhelmina zu Braunschweig, 6*(2/3), 22–33.

Krebs, W. (1974). Devonian carbonate complexes of Central Europe. In L. F. Laporte (Ed.), Reefs in time and space. *SEPM, Special Publication, 18*, 155–208.

Krebs, W. (1979). Devonian basinal facies. *Special Papers in Palaeontology, 23*, 125–139.

Kruse, M. (2013). *Geologische Diplomkartierung Oberrödinghausen – Asbeck – Eisborn* (pp. 1–93). Unpublished Diplom Mapping Thesis. Münster: Westfälische Wilhelms-Universität Münster.

Kürschner, W., Rieck, T., & Stritzke, R. (1999). Zur Geologie des Paläozoikum-Gebietes um Altenbüren und Brilon (östliches Rheinisches Schiefergebirge). *Münstersche Forschungen zur Geologie und Paläontologie, 86*, 11–24.

Kuz´min, A. V. (1998). New species of Early Frasnian *Palmatolepis* (Conodonta) from southern Timan. *Paleontologicheskiy Zhurnal, 1998*(2), 70–76. [in Russian]

Lamarck, J.-B. P. A. de (1801). *Système des animaux sans vertèbres, ou Tableau général des classes, des ordres et des genres de ces animaux présentant leurs caractères essentiels et leur distribution, d'après la considération de leurs rapports naturels et de leur organisation, et suivant l'arrangement établi dans les galeries du Muséum d'Histoire Naturelle, parmi leurs dépouilles conservées.* VIII + 432 pp., Paris.

Lange, W. (1929). Zur Kenntnis des Oberdevons am Enkeberg und bei Balve (Sauerland). *Abhandlungen der Preußischen Geologischen Landesanstalt, neue Folge, 119*, 1–132 + 3 pls.

Lecompte, M. (1939). Les tabulés du Dévonien moyen et supérieur du bord du bassin de Dinant. *Memoires du Musée royal d´Histoire naturelle de Belgique, 90*, 1–229, pls. 1–23.

Lecompte, M. (1951). Les stromatoporoides du Dévonien moyen et superiéur du bassin de Dinant. Part 1. *Mémoires de l'Institut Royal des Sciences Naturelles de Belgique, 116*, 1–225, pls. 1–35.

Lecompte, M. (1952). Les stromatoporoides du Dévonien moyen et supérieur du bassin de Dinant. Deuxième Partie. *Mémoires de l'Institut Royal des Sciences Naturelles de Belgique, 117*, 217–359, pls. 36–70.

Lecompte, M. (1970). Die Riffe im Devon der Ardennen und ihre Bildungsbedingungen. *Geologica et Palaeontologica, 4*, 25–71.

Löw, M., Söte, T., Becker, R. T., May, A., Stichling, S. (2022). Microfauna and Microfacies from the initial reef stadium of Binolen in the Hönne Valley (Sauerland, Middle Devonian). In S. Hartenfels, C. Hartkopf-Fröder, & P. Königshof (Eds.), *The Rhenish Massif: More than 150 years of research in a Variscan mountain chain*. *Palaeobiodiversity and Palaeoenvironments 102*(3). https://doi.org/10.1007/s12549-022-00540-4. [this issue]

Lüddecke, F., Hartenfels, S., & Becker, R. T. (2017). Conodont biofacies of a monotonous middle Famennian pelagic carbonate succession (Upper Ballberg Quarry, northern Rhenish Massif). In B. Mottequin, L. Slavík, & P. Königshof (Eds.), *Climate change and biodiversity patterns in the mid-Palaeozoic*. *Palaeobiodiversity and Palaeoenvironments, 97*(3), 591–613.

Machel, H. G., & Hunter, G. (1994). Facies Models for Middle to Late Devonian Shallow-marine Carbonates, with Comparisons to Modern Reefs: a Guide for Facies Analysis. *Facies, 30*, 155–176.

Malmsheimer, K. W., Mensink, H., & Stritzke, R. (1991). Gesteinsvielfalt im Riffgebiet um Brilon. *Geologie und Paläontologie in Westfalen, 18*, 67–83.

Matyja, H. (1993). Upper Devonian of Western Pommerania. *Acta Geologica Polonica, 43*(1/2), 27–94.

May, A. (1983). Ein Korallenriff im Oberen Mittel-Devon von Werdohl (Sauerland). *Dortmunder Beiträge zur Landeskunde, naturwissenschaftliche Mitteilungen, 17*, 35–46

May, A. (1987). Der Massenkalk (Devon) nördlich von Brilon (Sauerland). *Geologie und Paläontologie in Westfalen, 10*, 51–84.

May, A. (1992). Paleoecology of Upper Eifelian and Lower Givetian Coral Limestones in the Northwestern Sauerland (Devonian, Rhenish Massif). *Facies, 26*, 103–116.

May, A. (1993a). Korallen aus dem höheren Eifelium und unteren Givetium (Devon) des nordwestlichen Sauerlandes (Rheinisches Schiefergebirge). Teil I: Tabulate Korallen. *Palaeontographica, Abt. A, 227*, 87–224, pls. 5–19.

May, A. (1993b). Stratigraphie, Stromatoporen-Fauna und Palökologie von Korallenkalken aus dem Ober-Eifelium und Unter-Givetium des nordwestlichen Sauerlandes (Rheinisches Schiefergebirge). *Geologie und Paläontologie von Westfalen, 24*, 3–93, pls. 1–12.

May, A. (1994a). Foraminiferen, Kalkalgen und andere Mikrofossilien aus dem Givetium und Frasnium (Devon) des Sauerlandes (Rheinisches Schiefergebirge). *Dortmunder Beiträge zur Landeskunde, naturwissenschatliche Mitteilungen, 28*, 7–31.

May, A. (1994b). Paleoecology and paleobiogeography of corals and reef-builders from the Middle Devonian of the Sauerland (Germany). *Courier Forschungsinstitut Senckenberg, 172*, 147–159.

May, A. (2003). Die Fossilführung des Mitteldevons im Raum Attendorn-Olpe (West-Sauerland; Rechtsrheinisches Schiefergebirge). *Geologie und Paläontologie in Westfalen, 60*, 47–79.

May, A. (2005). Die Stromatoporen des Devons und Silurs von Zentral-Böhmen (Tschechische Republik) und ihre Kommensalen. *Zitteliana, B25*, 117–250.

May, A., & Becker, R. T. (1996). Ein Korallenhorizont im Unteren Bänderschiefer (höchstes Mittel-Devon) von Hohenlimburg-Elsey im Sauerland (MTB 4611 Hohenlimburg; Rheinisches Schiefergebirge). *Berliner Geowissenschaftliche Abhandlungen, E18*, 209–241.

May, A., & Marks J. (2014). Eine Korallen-Fauna aus der Oberhonsel-Formation (Givetium; Devon) von Garbeck (West-Sauerland). *Dortmunder Beiträge zur Landeskunde, naturwissenschaftliche Mitteilungen, 45*, 69–80.

McLean, R. A. (2010). *Frasnian (Upper Devonian) Colonial Disphyllid Corals from Western Canada: Taxonomy and Biostratigraphic Significance* (pp. 1–189, 44 pls), Ottawa: NRC Research Press.

Mestermann, B. (1995). Fenstergefüge im südlichen Briloner Massenkalk. *Geologie und Paläontologie in Westfalen, 41*, 55–67.

Milne-Edwards, H., & Haime, J. (1851). Monographie des Polypiers fossils des terrains paleozoiques, précedée d´un tableau general de la classification polypes. *Archives du Muséum d´Histoire Naturelle, 5*, 1–502, pls. 1–20.

Mottequin, B., & Poty, E. (2016). Kellwasser horizons, sea-level changes and brachiopod-coral crises during the late Frasnian in the Namur-Dinant Basin (southern Belgium): a synopsis. In R. T. Becker, P. Königshof, & C. E. Brett (Eds.), *Devonian Climate, Sea Level and Evolutionary Events*. *Geological Society, London, Special Publications, 423*, 235–250.

Mottequin, B., Denayer, J., Poty, E., & Devleeschouwer, X. (2015). Middle to Upper Frasnian succession, Kellwasser events and the Frasnian–Famennian Boundary in the Namur–Dinant Basin. In J. Denayer, B. Mottequin, & C. Prestianni (Eds.), *IGCP 596 - SDS Symposium, Climate change and Biodiversity patterns in the Mid-Palaeozoic, Field Guidebooks*. *Strata, Travaux de Géologie sédimentaire et Paléontologie, Serié 1: communications, 17*, 24–45.

Murphy, A. E., Sageman, B. B., & Hollander, D. J. (2000). Eutrophication by decoupling of the marine biogeochemical cycles od C, N. and P: A mechanism for the Late Devonian mass extinction. *Geology, 28*(5), 427–430.

Narkiewicz, K., & Bultynck, P. (2010). The Upper Givetian (Middle Devonian) *subterminus* conodont zone in North America, Europe, and North Africa. *Journal of Paleontology, 84*(4), 588–625.

Narkiewicz, K., Narkiewicz, M., & Bultynck, P. (2016). Conodont biofacies of the Taghanic transgressive interval (middle Givetian): Polish record and global comparisons. In R. T. Becker, P. Königshof, & C. E. Brett (Eds.), *Devonian Climate, Sea Level and Evolutionary Events*. *Geological Society, London, Special Publications, 423*, 201–222.

Nicholson, H. A. (1886–1892): A monograph of the British stromatoporoids. *Palaeontographical Society, 39–46*, 1–234, pls. 1–29.

Nowak, H. (2012). *Paläoökologie und Faziesanalyse des devonischen Riffkomplexes von Wülfrath (Rheinl.)* (pp. 1–49). Unpublished M.Sc. Thesis. Münster: Westfälische Wilhelms-Universität, Münster.

Nowak, M. (2010). *Ein oberdevonisches Korallen-Biostrom am Beul bei Eisborn – Stratigraphie und Fazies* (pp.1–28). Unpublished B.Sc. Thesis. Münster: Westfälische Wilhelms-Universität Münster.

Nowinski, A. (1993). Tabulate corals from the Givetian and Frasnian of the Holy Cross Mountains and Silesian Upland. *Acta Palaeontologica Polonica, 37*(2/4), 183–216.

Nyhuis, C. J., & Amler, M. R. W. (2013). Rafting versus benthic colonization: Invasion of oxygen-depleted muds? – An example from the late Mississippian of the Rhenish Massif. In J. Reitner, Y. Qun, W. Yongdong, & M. Reich (Eds.), *Palaeobiology and Geobiology of Fossil Lagerstätten through Earth History* (pp.120–121), Göttingen: Universitätsverlag Göttingen.

Nyhuis, C. J., Rippen, D., & Denayer, J. (2014). Facies characterization of organic-rich mudstones from the Chokier Formation (lower Namurian), south Belgium. *Geologica Belgica, 17*(3–4), 311–322.

Oetken, S. (1997). Faziesausbildung und Conodonten-Biofazies mittel-/oberdevonischer Riffgesteine in der mittleren Lahnmulde (Rheinisches Schiefergebirge). *Wissenschaft in Dissertationen, 207*, 1–161.

Özkan, R., Nazik, A., Munnecke, A., Daysam Demiray, G., Schindler, E., Aydin Özbek, T., Şeker Zor, E., Yilmaz, I., Brocke, R., Sancay, R. H., Wilde, V., & Yal in, M. N. (2019). Givetian/Frasnian (Middle/Upper Devonian) transition in the eastern Taurides, Turkey. *Turkish Journal of Earth Sciences, 28*, 207–231.

Oleneva, N. V. (2019). New Spriferids (Brachiopoda) from the Upper Devonian of the Central Devonian Field and Southern Timan. *Paleontologicheskiy Zhurnal, 2019*(4), 43–55.

Ovnatanova, N. S., & Kononova, L. I. (2008). Frasnian Conodonts from the Eastern Russian Platform. *Paleontological Journal, 42*(10), 997–1166.

Pacton, M., Gorin, G. E., & Vasconcelos, C. (2011) Amorphous organic matter – Experimental data on formation and the role of microbes. *Review of Palaeobotany and Palynology, 166*, 253–267.

Paeckelmann, W. (1913). Das Oberdevon des Bergischen Landes. *Abhandlungen der Königlichen Preußischen Geologischen Landesanstalt, neue Folge, 70*, 3–356.

Paeckelmann, W. (1924). Das Devon und Carbon der Umgebung von Balve i. Westf. *Jahrbuch der Preußischen Geologischen Landesanstalt zu Berlin, 44*, 51–97.

Paeckelmann, W., with a contribution by Pfeffer, P. (1938). Erläuterungen zu Blatt Balve. *Geologische Karte von Preussen und benachbarten deutschen Ländern, Lieferung 349*, 1–70.

Paproth, E. (1986). An introduction to a field trip to the Late Devonian outcrops in the northern Rheinisches Schiefergebirge (Federal Republic of Germany). *Annales de la Société géologique de Belgique, 109*, 275–284.

Pickett, J. (1967). Untersuchungen zur Familie Phillipsastreidae (Zoantharia rugosa). *Senckenbergiana lethaea, 48*(1), 1–89, pls. 1–7.

Piecha, M. (1993). Stratigraphie, Fazies und Sedimentpetrographie der rhythmisch und zyklisch abgelagerten, tiefobedevonischen Beckensedimente im Rechtsrheinischen Schiefergebirge (Adorf-Bänderschiefer). *Courier Forschungsinstitut Senckenberg, 163,* 1–151.

Piper, D. J. W., & Stow, D. A. V. (1991). Fine-grained turbidites. In G. Einsele, W. Ricken, & A. Seilacher (Eds.), *Cycles and events in stratigraphy* (pp. 360–376). Berlin: Springer.

Pisarzowska, A., Becker, R. T., Aboussalam, Z. S., Szczerba, M., Sobień, K., Kremer, B., Owocki, K., & Racki, G. (2020). Middlesex/*punctata* event in the Rhenish Basin (Padberg section, Sauerland, Germany) – Geochemical clues to the early-middle Frasnian perturbation of global carbon cycle. *Global and Planetary Change, 191*, 103211.

Playford, P. E. (1980). Devonian "Great Barrier Reef" of Canning Basin, Western Australia. *American Association of Petroleum Geologists Bulletin, 64*(6), 814–839.

Polenz, H. (2008). *Eulenköpfe, Seelilien und Flugsaurier. Ein Geo-Reiseführer zum Kalkstein, Kalk-Abbau und zu den Fossilien des Hönnetales* (pp. 1–135), Essen: Klartext Verlag.

Préat, A., El Hassani, A., & Mamet, B. (2008). Iron bacteria in Devonian carbonates (Tafilalt, Anti-Atlas, Morocco). *Facies, 54*, 107–120.

Price, J. D. (1982). *Some Famennian (Upper Devonian) ammonoids from north western Europe* (pp.1-555). Unpublished Ph.D. Thesis. Hull: University of Hull.

Racki, G. (1993). Evolution of the bank to reef complex in the Devonian of the Holy Cross Mountains. *Acta Palaeontologica Polonica, 37*(2/4), 87–182

Racki, G. (1999). Frasnian-Famennian biotic crisis: undervalued tectonic control? *Palaeogeography, Palaeoclimatology, Palaeoecology, 141*, 177–198.

Racki, G. (2005). Towards understanding Late Devonian global events: few answers, many questions. *Developments in Palaeontology & Stratigraphy, 20*, 5–36.

Racki, G., & Soboń-Podgórska, J. (1993). Givetian and Frasnian calcareous microbiotas of the Holy Cross Mountains. *Acta Palaeontologica Polonica, 37*, 255–289.

Ribbert, K.-H., & Lange, F.-G. (1993). *Klastika und Carbonate im Mittel- und Oberdevon des Velberter Sattels.* Deutsche Geologische Gesellschaft, 145. Hauptversammlung, 28.9. bis 1.10.1993, Krefeld, Exkursionsführer, 5–16, Krefeld: Geologisches Landesamt Nordrhein-Westfalen.

Ribbert, K.-H., Wrede, L., Oesterreich, B., Baumgarten, H., Gawlik, A., Heuser, H., Piecha, M., Roth, R., Thünker, M., Baales, M., Cichy, E. & Zeiler, M. (2017). *Geologie im Rheinischen Schiefergebirge. Teil 3: Sauer- und Siegerland. 243*, 1 map; Krefeld: Geologischer Dienst NRW.

Richter, J. (2013). *Geologische Kartierung im Raum Beckum-Hövel (Nordsauerland, Blatt 4613 Balve)* (pp.1–55). Unpublished B.Sc. Mapping Thesis. Münster: Westfälische Wilhelms-Universität Münster.

Rieck, T., & Stritzke, R. (1999). Zur Fazies und Paläogeographie der Givet-Stufe (Mitteldevon) im Gebiet des Messinghäuser Sattels (östliches Rheinisches Schiefergebirge). *Münstersche Forschungen zur Geologie und Paläontologie, 86*, 25–38.

Rytina, M.-K., Becker, R. T., Aboussalam, Z. S., Hartenfels, S., Helling, S., Stichling, S., & Ward, D. (2013). The allochthonous Silurian-Devonian in olistostromes at the "Southern Variscan Front" (Tinerhir region, SE Morocco). – preliminary data. In R. T. Becker, A. El Hassani, & A. Tahiri, (Eds.), *International Field Symposium "The Devonian and Lower Carboniferous of northern Gondwana", Field Guidebook. Documents de l'Institut Scientifique, Rabat, 27*, 11–21

Sageman, B. B., Murphy, A. E., Werne, J. P., Ver Straeten, C. A., Hollander, D. J., & Lyons, T. W. (2003). A tale of shales: the relative role of production, decomposition, and dilution in the accumulation of organic-rich strata, Middle–Upper Devonian, Appalachian basin. *Chemical Geology, 195*, 229–273.

Sandberg, C. A., & Dreesen, R. (1984). Late Devonian icriodid biofacies models and alternate shallow-water conodont zonation. *Geological Society of America, Special Paper, 196*, 143–177.

Sandberg, C. A., Ziegler, W., & Bultynck, P. (1989). New standard conodont zones and early *Ancyrodella* phylogeny across Middle-Upper Devonian Boundary. *Courier Forschungsinstitut Senckenberg, 110*, 195–230.

Sandberg, C. A., Ziegler, W., Dreesen, R., & Butler, J. L. (1992). Conodont Biochronology, Biofacies, Taxonomy, and Event Stratigraphy around Middle Frasnian (F2h), Frasnes, Belgium. *Courier Forschungsinstitut Senckenberg, 150*, 1–87.

Saupe, F., & Becker, R. T. (2022). Refined conodont stratigraphy at Martenberg (Germany) as base for a formal middle/upper Frasnian substage boundary. In S. Hartenfels, C. Hartkopf-Fröder, & P. Königshof (Eds.) *The Rhenish Massif: More than 150 years of research in a Variscan mountain chain. Palaeobiodiversity and Palaeoenvironments 102*(3), https://doi.org/10.1007/s12549-022-00537-z. [this issue]

Schäfer, W. (1978). *Stratigraphie, Fazies und Paläogeographie in Oberdevon und Unterkarbon im Bereich des Balver Riffgebietes (Rheinisches Schiefergebirge)* (pp. 1–122 + 2 pls. + 1 map). Ph.D. Thesis, Marburg: Philips-University Marburg.

Schindler, E. (1990). Die Kellwasser-Krise (hohe Frasne-Stufe, Ober-Devon). *Göttinger Arbeiten zur Geologie und Paläontologie, 46*, 1–115 + 5 pls.

Schindler, E. (1993). Event-stratigraphic markers within the Kellwasser Crisis near the Frasnian/Famennian boundary (Upper Devonian) in Germany. *Palaeogeography, Palaeoclimatology, Palaeoecology, 104*, 115–125.

Schlotheim, E. F. Baron von (1820). *Die Petrefactenkunde auf ihrem jetzigen Standpunkte durch die Beschreibung seiner Sammlung versteinerter und fossiler Überreste des Thier- und Pflanzenreichs der Vorwelt erläutert* (pp. 1–437, pls. 15–29). Gotha.

Schmidt, W. (1951). Die stratigraphische Entwicklung des Famennien in der Gegend von Aachen. *Geologisches Jahrbuch, 65*, 451-462.

Schröder, S. (2005). Stratigraphie und Systematik rugoser Korallen aus dem Givetium und Unter-Frasnium des Rheinischen Schiefergebirges (Sauerland/Bergisches Land). *Zitteliana, B25*, 39–116.

Schudack, M. E. (1993). Karbonatzyklen in Riff- und Lagunenbereichen des devonischen Massenkalkkomplexes von Asbeck (Hönnetal, Rheinisches Schiefergebirge). *Geologie und Paläontologie in Westfalen*, *26*, 77–106.

Schülke, I. (1995). Evolutive Prozesse bei *Palmatolepis* in der frühen Famenne-Stufe (Conodonta, Ober-Devon). *Göttinger Arbeiten zur Geologie und Paläontologie, 67*, 1–108, 14 pls.

Schülke, I., & Popp, A. (2005). Microfacies development, sea-level change, and conodont stratigraphy of Famennian mid- to deep platform deposits of the Beringhauser Tunnel section (Rheinisches Schiefergebirge, Germany). *Facies, 50*, 647–664.

Scoffin, T. P. (1993). The geological effects of hurricanes on coral reefs and the interpretation of storm deposits. *Coral Reefs, 12*, 203–221.

Söte, T., Hartenfels, S., & Becker, R. T. (2017). Uppermost Famennian stratigraphy and facies development of the Reigern Quarry near Hachen (northern Rhenish Massif, Germany). In B. Mottequin, L. Slavík, P. Königshof (Eds.) *Climate change and biodiversity patterns in the mid-Palaeozoic. Palaeobiodiversity and Palaeoenvironments, 97*(3), 633–654.

Spalletta, C., Perri, M. C., Over, D. J., & Corradini, C. (2017). Famennian (Upper Devonian) conodont zonation: revised global standard. *Bulletin of Geosciences*, *92*(1), 31–57.

Spiske, M. (2003). *Geologische Neukartierung des Blattes 4612 Iserlohn, Deilinghofen – Apricke – Riemke* (pp. 1–47, 2 appendices, 1 map). Unpublished Diplom Mapping Thesis. Münster: Westfälische Wilhelms-Universität Münster.

Städter, T. (1989). Mikrofazies, Strukturverhältnisse und Diagenese der Wülfrather Kalksteinlagerstätte (Devon, Rheinisches Schiefergebirge). *Facies, 21*, 57–98.

Stauffer, C. R. (1940). Conodonts from the Devonian and associated clays of Minnesota. *Journal of Paleontology, 14*, 417–435.

Stichling, S. (2011). *Stratigraphie und Fazies der Bohrung B102 im Raum Hönnetal (Nord-Sauerland)* (pp. 1–67). Unpublished B.Sc. Thesis. Münster: Westfälische Wilhelms-Universität Münster.

Stichling, S., Aboussalam, Z. S., Becker, R. T., Eichholt, S., & Hartenfels, S. (2015). Event controlled reef drowning and extinction in the Hönne Valley (northern Rhenish Massif, Hagen-Balve reef complex). In B. Mottequin, J. Denayer, P. Königshof, C. Prestianni, & S. Olive (Eds.), *IGCP 596 – SDS Symposium "Climate change and Biodiversity patterns in the mid-Palaeozoic. Strata, Travaux de Géologie sédimentaire et Paléontologie, Série 1: communications, 16*, 138–139.

Stichling, S., Becker, R. T., Hartenfels, S., & Aboussalam, Z. S. (2016). New data on the extinction of the Hagen-Balve reef complex (based on bore hole HON_1101). In P. Gurdebecke, J. De Weirdt, T. R. A. Vandenbroucke, & B. D. Cramer (Eds.), *IGCP 591, The Early to Middle Paleozoic Revolution, Closing Meeting, Ghent University, Belgium, 6-9 July 2016, Abstracts*, 130–131.

Stichling, S., Becker, R. T., Hartenfels, S. & Aboussalam, Z.S. (2017). Conodont dating of reef drowning and extinction in the Hönne Valley (northern Rhenish Massif, Germany). In J.-C. Liao, & J. I. Valenzuela-Ríos (Eds.), *Fourth International Conodont Symposium, ICOS IV, "Progress on Conodont Investigation". Cuadernos del Museo Geominero, 22*, 163–165.

Strutz, C. (2004). *Petrographisch/fazielle Untersuchungen an einer Bohrung im devonischen Massenkalk von Asbeck/Hönnetal* (pp.1–55). Unpublished B.Sc. Thesis. Bochum: Ruhr-Universität Bochum.

Stritzke, R. (1989). Stratigraphie, Faziesanalyse und Paläogeographie im Oberdevon des Briloner Vorriffgebietes (Ostsauerland). *Fortschritte in der Geologie von Rheinland und Westfalen, 35*, 75–106.

Stritzke, R. (1990). Die Karbonatsedimentation im Briloner Vorriffbereich. *Geologisches Jahrbuch, Reihe D*, *95*, 253–315.

Szrek, P., & Salwa, S. (2020 online). High-energy events in the Frasnian-Famennian boundary interval of the Płucki section in the Holy Cross Mountains. *Facies, 66*(9). https://doi.org/10.1007/s10347-020-0593-0.

Termier, H., Termier, G., & Vachard, D. (1975). Recherches micropaléontologiques dans le Paléozoique supérieur du Maroc central. *Cahiers de Micropaléontologie, 4*, 5–99, 10 pls.

Torley, K. (1908). Die Fauna des Schleddenhofes bei Iserlohn. *Abhandlungen der Preußischen Geologischen Landesanstalt, Neue Folge, 53*, 1–56, 10 pls.

Torley, K. (1934). Die Brachiopoden des Massenkalkes der Oberen Givet-Stufe von Bilveringsen bei Iserlohn. *Abhandlungen der senckenbergischen naturforschenden Gesellschaft, 4*(3), 67–148, pls. 1–9.

Vandercammen, A. (1955). Quelques Spiriferidae nouveaux du Dévonien de la Belgique. *Bulletin de l´Institut royal des Sciences naturelles de Belgique, 1955*(90), 1–4.

Vandercammen, A. (1957). Révision du genre *Gürichella* W. Paeckelmann, 1913. *Bulletin de l´Institut royal des Sciences naturelles de Belgique, 1957*(1389), 1–50.

Walliser, O. H., & Franke, W. (1983). "Pelagic" carbonates in the Variscan Belt – their sedimentary and tectonic environments. In H. Martin, & F. W. Eder (Eds.), *Intracontinental Fold Belts* (pp. 77–92). Berlin: Springer.

Ward, P. D., Becker, R. T., Aboussalam, Z. S., Rytina, M.-K., & Stichling, S. (2013). The Devonian at Oued Ferkla (Tinejdad region, SE Morocco). In R. T. Becker, A. El Hassani, & A. Tahiri (Eds.), *International Field Symposium "The Devonian and Lower Carboniferous of northern Gondwana". Field Guidebook. Document de l'Institut Scientifique, Rabat, 27*, 23–29.

Wedekind, R. (1913a). Die Goniatitenkalke des unteren Oberdevon von Martenberg bei Adorf. *Sitzungsberichte der Gesellschaft für naturforschende Freunde, Berlin, 1913*(1), 23–77.

Wedekind, R. (1913b). Beiträge zur Kenntnis des Oberdevons am Nordrande des Rheinischen Schiefergebirge. 2. Zur Kenntnis der Prolobitiden. *Neues Jahrbuch für Mineralogie, Geologie und Paläontologie, 1913*(1), 78–95.

Wedekind, R. (1922). Zur Kenntnis der Stringophyllen des oberen Mitteldevon. *Sitzungsberichte der Gesellschaft zur Beförderung der gesamten Naturwissenschaften zu Marburg, 1921*(1), 1–16.

Weller, H. (1989). Das Rübeländer Mud Mound im Riffkomplex von Elbingerode (Harz) und seine sedimentologischen Eigenschaften. *Hercynia, Neue Folge, 26*(4), 321–337.

Weller, H. (1991). Facies and Development of the Devonian (Givetian/Frasnian) Elbingerode Reef Complex in the Harz Area (Germany). *Facies, 25*, 1–50.

Wendt, J., & Aigner, T. (1985). Facies patterns and depositional environments of Palaeozoic cephalopod limestones. *Sedimentary Geology, 44*, 263–300.

Wendt, J., & Belka, Z. (1991). Age and depositional environment of Upper Devonian (early Frasnian to early Famennian) black shales and limestones (Kellwasser facies) in the eastern Anti-Atlas, Morocco. *Facies, 25*, 51–89.

Wetzel, A., & Uchmann, A. (1998). Biogenic sedimentary structures in mudstones – an overview. In J. Schieber, W. Zimmerle, & P. S. Sethi (Eds.), *Shales and Mudstones, 1*, 351–369.

Weyer, D. (2016). Review of some Frasnian ahermatypic coral localities from Germany and description of a new genus *Spinaxon* (Anthozoa, Rugosa, Upper Devonian). *Geologica Belgica, 19*(1–2), 147–163.

Wilder, H. (1989). Neue Ergebnisse zum oberdevonischen Riffsterben am Nordrand des mitteleuropäischen Variszikums. *Fortschritte in der Geologie von Heinland und Westfalen, 35*, 57–74.

Wilson, J. L. (1975). *Carbonate facies in geologic history* (pp. 1–471), New York: Springer.

Wray, J. L. (1967). Upper Devonian calcareous algae from the Canning Basin, Western Australia. *Colorado School of Mines, Professional Contributions, 3*, 1–76, pls. 1–11.

Youngquist, W. (1945). Upper Devonian conodonts from the Independence Shale (?) of Iowa. *Journal of Paleontology 19*, 355–367.

Zatoń, M., Borszcz, T., Berkowski, B., Rakociński, M., Zapalsi, M. K., & Zhuravlev, A. V. (2015). Paleoecology and sedimentary environment of the Late Devonian coral biostrome from the Central Devonian Field, Russia. *Palaeogeography, Palaeoclimatology, Palaeoecology, 424*, 61–75.

Zhou, X.-Y. (1980). Tabulata. In S.-Y. Xian, S.-D. Wang, X.-Y. Zhou, J.-F. Xiong, & T.-R. Zhou (Eds.), *Nandan typical stratigraphy and palaeontology of Devonian, in South China* (pp. 117–135, 158–161, pls. 40–48), Guizhou: Peoples Press.

Zhou, K., & Pratt, B. R. (2019). Upper Devonian (Frasnian) *Stromatactis*-bearing mud mounds, western Alberta, Canada: reef framework dominated by peloidal microcrystalline calcite. *Journal of Sedimentary Research, 89*, 833–848.

Ziegler, W., & Sandberg, C. A. (1984). *Palmatolepis*-based revision of upper part of standard Late Devonian conodont zonation. *Geological Society of America, Special Paper, 196*, 179–194.

Ziegler, W., & Sandberg, C. A. (1990). The Late Devonian Standard Conodont Zonation. *Courier Forschungsinstitut Senckenberg, 121*, 1–115.

Ziegler, W., Ovnatanova, N. S. & Kononova, L. (2000). Devonian Polygnathids from the Frasnian of the Rhenisches Schiefergebirge, Germany, and the Russian Platform. *Senckenbergiana lethaea, 80*(2), 593–645.